

PROTON SPIN RELAXATION IN LIQUID  $\text{CHCl}_3$  AND IN

$\text{H}_2\text{O}-\text{D}_2\text{O}$  SOLUTIONS OF CHROMIUM (III)

By

BILLY FRANK MELTON

Bachelor of Science

Oklahoma State University

Stillwater, Oklahoma

1964

Submitted to the Faculty of the Graduate College  
of the Oklahoma State University  
in partial fulfillment of the requirements  
for the degree of  
DOCTOR OF PHILOSOPHY  
May, 1970

CALIFORNIA  
STATE UNIVERSITY  
LIBRARY


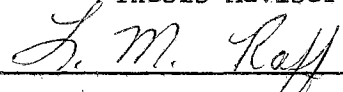
OCT 12 1970

PROTON SPIN RELAXATION IN LIQUID  $\text{CHCl}_3$  AND IN  
 $\text{H}_2\text{O}-\text{D}_2\text{O}$  SOLUTIONS OF CHROMIUM (III)

Thesis Approved:



Thesis Adviser



Dean of the Graduate College

762472

## ACKNOWLEDGEMENT

For inspiration, guidance, and an education, credit is due Dr. V. L. Pollak. Special thanks goes to Dr. E. E. Kohnke and the other committee members, Dr. L. M. Raff and Dr. H. A. Pohl, for their timely and willing assistance.

The author is indebted to Dr. Eli Namanworth of the Chemistry Department of Case Western Reserve University for allowing him the use of the 60 MHz pulsed NMR spectrometer. He wishes to thank Mr. Israel Mayk, Summer NSF Undergraduate Research Participant at CWRU, for his assistance in carrying out the high frequency measurements.

Acknowledgement is made to the National Science Foundation and the National Aeronautics and Space Administration for fellowship support during the conduct of this research.

## TABLE OF CONTENTS

Chapter	Page
I. INTRODUCTION. . . . .	1
II. THEORY. . . . .	3
Definitions and General Remarks. . . . .	3
Relaxation Time Equations. . . . .	5
Exchange Phenomena . . . . .	9
III. EARTH'S FIELD NMR TECHNIQUE . . . . .	13
IV. INSTRUMENTATION . . . . .	17
Introduction . . . . .	17
Current Control. . . . .	17
Detection Circuit. . . . .	21
Relay Multivibrators . . . . .	24
Timing Circuits. . . . .	24
SCR Trigger Circuits . . . . .	27
Pulse and Timing Circuit . . . . .	29
V. PROTON SPIN RELAXATION AND SELF-DIFFUSION IN LIQUID $\text{CHCl}_3$ . . . . .	34
Introduction . . . . .	34
Experimental . . . . .	37
Results and Discussion . . . . .	38
VI. PROTON SPIN RELAXATION AND EXCHANGE PROPERTIES OF HYDRATED CHROMIC IONS IN $\text{H}_2\text{O}$ AND $\text{H}_2\text{O}-\text{D}_2\text{O}$ MIXTURES . . . . .	48
Introduction . . . . .	48
Experimental . . . . .	52
Results and Discussion . . . . .	54
VII. SUMMARY AND CONCLUSIONS . . . . .	89
Instrumentation. . . . .	89
Chloroform . . . . .	89
Solutions of Chromium (III). . . . .	90
BIBLIOGRAPHY. . . . .	92
APPENDIX A - NON-LINEAR LEAST SQUARES CURVE FITTING PROCEDURE . . . . .	94

TABLE OF CONTENTS (Continued)

Chapter	Page
APPENDIX B - THEORETICAL EXPRESSIONS FOR PROTON SPIN RELAXATION TIMES IN CHROMIC SOLUTIONS. . . . .	97
APPENDIX C - SOLUTION OF THE BLOCH-McCONNELL EQUATIONS FOR THE $\text{Cr}(\text{H}_2\text{O})_6^{3+}$ - $\text{Cr}(\text{H}_2\text{O})_5(\text{H}_3\text{O})^{4+}$ - $\text{H}_2\text{O}$ SYSTEM . . . . .	102

LIST OF TABLES

Table	Page
I. Activation Energies for Relaxation, Rotation, Translation, Self-Diffusion, and Viscosity in Benzene and Chloroform.	44
II. Parameters Obtained From the Least Squares Fit of the Equations in the Text to the Data in Figures 17-19 . . .	59
III. Rate Constants for Reaction (16a) Obtained From the Data in Figure 20 . . . . .	65

LIST OF FIGURES

Figure	Page
1. Energy Levels for a Spin $I = 1/2$ in a Magnetic Field $B_0$ . . .	3
2. Longitudinal and Transverse Components of $\vec{M}$ After Application of an External Field in the z-Direction . . . . .	5
3. Representation of Magnetic Fields in the Earth's Field NMR Technique. . . . .	14
4. Magnetic Field and Sample Magnetization Versus Time for the Earth's Field NMR Technique. . . . .	14
5. Magnetic Field Versus Time for Measuring $T_1$ in the Earth's Field of 0.54 Gauss. . . . .	15
6. Current Control Circuitry. . . . .	18
7. Coil Current and Coil Voltage Measured at Point Y of Figure 6. . . . .	19
8. Signal Detection Circuit. . . . .	22
9. Current Relay Multivibrator. . . . .	25
10. Signal Relay Multivibrator . . . . .	25
11. Monostable Multivibrator Timing Circuit. . . . .	26
12. Firing Circuit for 2N1777 SCR. . . . .	28
13. Firing Circuit for 2N1848 SCR. . . . .	28
14. Pulse and Timing Circuit . . . . .	30
15. Field Dependence of Proton $T_1$ in Deoxygenated $CHCl_3$ . . . . .	39
16. Temperature Dependence of High-Field Proton $T_1$ in Deoxygenated $CHCl_3$ . . . . .	40
17. Field Dependence of $pT_1^{cor}$ in 0.10 M $HClO_4$ Solutions of $Cr(NO_3)_3$ . . . . .	55

LIST OF FIGURES (Continued)

Figure	Page
18. Temperature Dependence of $pT_1^{cor}$ at Various Fields and Acid Concentrations. . . . .	56
19. Temperature Dependence of $pT_1^{cor}$ and $pT_2^{cor}$ at 14 kG in 0.10 M $HClO_4$ Solutions of $Cr(NO_3)_3$ . . . . .	57
20. Temperature Dependence of $pT_1^{cor}$ in Highly Acidified Solutions of $Cr(NO_3)_3$ . . . . .	62
21. Proton Relaxation Times $pT_{1,2}^{cor}$ at 14 kG in 0.10 M $HClO_4$ Solutions of $Cr(NO_3)_3$ of Varying Proton Fraction $\beta$ . . . . .	71
22. Temperature Dependence of Proton Relaxation Times $pT_{1,2}^{cor}$ at 14 kG in 0.10 M $HClO_4$ Solutions of $Cr(NO_3)_3$ Containing 80% $D_2O$ -20% $H_2O$ ( $\beta = 0.2$ ) . . . . .	72
23. Temperature Dependence of Proton Relaxation Times $pT_{1,2}^{cor}$ at 14 kG in 4.0 M $HClO_4$ Solutions of $Cr(NO_3)_3$ of Varying Proton Fraction $\beta$ . . . . .	82



## CHAPTER I

### INTRODUCTION

The field of nuclear magnetic resonance has grown at an enormous rate since the first experiments were performed in 1946 by Purcell, Pound, and Torrey at Harvard, and by Bloch, Hansen, and Packard at Stanford. Although high resolution NMR has become an important research tool, rivaled only by infrared spectroscopy in structure determination of complex organic molecules, most of the research has been related to chemical shifts and the correlation of these shifts to chemical binding and structure. By comparison, studies of the field dependence of nuclear spin relaxation times has found relatively little application. One finds that most of the commonly used apparatuses are limited to the range  $10^3$  to  $10^4$  gauss, and operate in low field only at the expense of signal-to-noise ratio. The earth's field technique is shown to be uniquely suited to such field dependence studies. The range of accessible fields is over three orders of magnitude, extending from the earth's field of 0.5 gauss to 500 gauss. The ease of measuring this field dependence gives a dimension to this method which is lacking in the more standard NMR techniques. Nevertheless, the method has been relatively little exploited as a research tool. The main reasons for this are probably (1) a suitable instrument is not available commercially, (2) the circuitry required has not been published in the open literature, and (3) the sensing head of the device must be located where the earth's

field is sufficiently homogeneous, which means out-of-doors or in a non-magnetic building.

Herein, the required instrumentation is developed and described in some detail, and experimental results are presented on proton spin relaxation in two different chemical systems which show strong field dependence in the range of fields accessible to the earth's field technique. The first, liquid  $\text{CHCl}_3$ , provides an interesting example of the application of NMR to the study of molecular motion in pure liquids. The second, aqueous solutions of chromium (III), provides an example of the application of nuclear magnetic resonance to the study of chemical equilibria and proton exchange kinetics.

## CHAPTER II

### THEORY

#### Definitions and General Remarks

Consider an ensemble of particles of spin  $1/2$  located in an external magnetic field  $\vec{B}_0$  directed along the  $z$ -axis. In the absence of interactions among the particles there are two discrete energy levels for each spin, corresponding to  $I_z = \pm 1/2$  and having energies  $E = -\vec{\mu} \cdot \vec{B}_0 = -\gamma\hbar \vec{I} \cdot \vec{B}_0 = -\gamma\hbar I_z B_0$ . The constant  $\gamma$  is the gyromagnetic ratio for the particle in question, and for protons has the value 4.26 kHz/gauss. The energy separation between the two levels is  $\Delta E = \gamma\hbar B_0 = \hbar \omega_0$ , where  $\omega_0 = \gamma B_0$  is the classical Larmor precession frequency of the spins in the external field  $B_0$ .

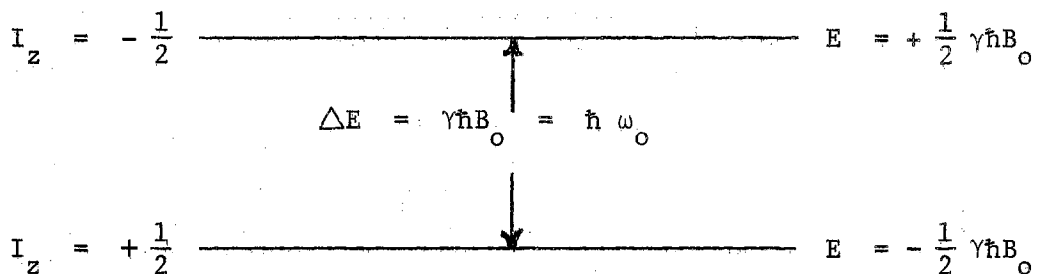


Figure 1. Energy Levels for a Spin  $I = 1/2$  in a Magnetic Field  $B_0$

Superimposed on the external field is a small field  $\Delta\vec{B}(t)$  which fluctuates rapidly in time due to interaction with spins on the same or neighboring molecules, which are undergoing rapid Brownian motion within the liquid. Fourier components of the fluctuating field at zero frequency cause a broadening of the energy levels in Figure 1, whereas the Fourier components at the resonant frequency  $\omega_0 = \gamma B_0$  cause spins to make transitions between the energy levels of the system. When equilibrium is reached there is an excess of spins in the lower energy level, which gives rise to a net magnetization within the sample along the z-direction, whose magnitude is given by the Curie law

$$M_0 = \frac{N \gamma^2 \hbar^2 I(I+1)}{3kT} B_0.$$

A plot of sample magnetization versus time after application of  $\vec{B}_0$  is given in Figure 2. The z-component of magnetization  $M_z$  grows exponentially toward the equilibrium Curie value with a time constant  $T_1$ , the spin-lattice or longitudinal relaxation time in the field  $B_0$ . Any component of magnetization  $M_{xy}$  perpendicular to  $\vec{B}_0$  decays exponentially toward zero with a time constant  $T_2$ , the spin-spin or transverse relaxation time. Classically speaking, the transverse component of  $\vec{M}$  decays because there is a distribution of Larmor precession frequencies  $\omega = \gamma (B_0 + \Delta B)$  for the spins in the sample due to interactions of the spins among themselves. The distribution of frequencies causes the transverse component of  $\vec{M}$  to smear out as the spins lose phase coherence with each other. After several time constants  $T_2$  the spins have lost phase coherence altogether, and the transverse component of  $\vec{M}$  is zero.

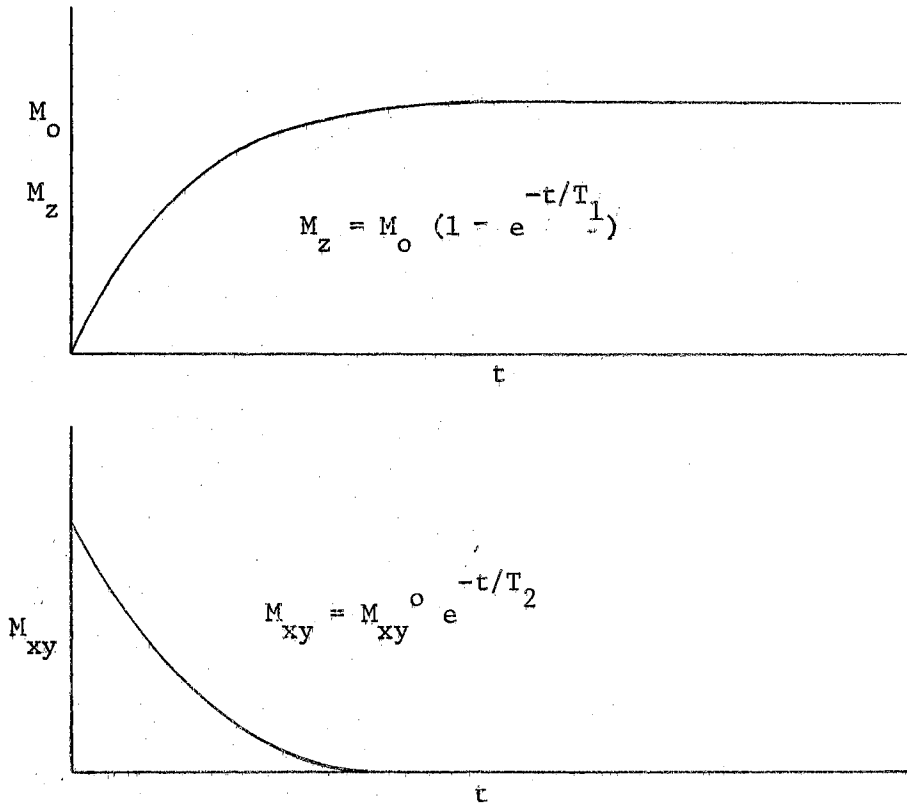


Figure 2. Longitudinal and Transverse Components of  $\vec{M}$  After Application of an External Field in the z-Direction

#### Relaxation Time Equations

In the simple theory, the relaxation time  $T_1$  is related to the transition probability per unit time between the two energy levels of the spin system by the equation  $1/T_1 = 2W_{\alpha\beta}$ , where  $\alpha$  refers to  $I_z = +1/2$  and  $\beta$  to  $I_z = -1/2$ .

The Hamiltonian of a nuclear spin  $\vec{I}$  in an external magnetic field  $\vec{B}_0$  along the z-direction and interacting with other spins  $\vec{S}_j$  within the sample has the form

$$H = -\gamma_I \hbar I_z B_0 + H'$$

The first term is the Zeeman energy of the spin in the constant magnetic field  $B_0$ , and  $H'$  is the spin-spin interaction term considered as a perturbation. It has the form<sup>1</sup>

$$H' = -\gamma_I \hbar^2 \sum_j \gamma_{S_j} \left[ \frac{3(\vec{I} \cdot \vec{r}_j)(\vec{S}_j \cdot \vec{r}_j)}{r_j^5} - \frac{\vec{I} \cdot \vec{S}_j}{r_j^3} \right] + \sum_j A_j \vec{I} \cdot \vec{S}_j \quad (1)$$

The first term is the dipole-dipole interaction between  $\vec{I}$  and the spins  $\vec{S}_j$ ,  $\vec{r}_j$  being the position vector of spin  $\vec{S}_j$  with respect to  $\vec{I}$  in the laboratory frame. The second term is the Fermi hyperfine interaction if  $\vec{S}_j$  is an electron spin, or the electron-coupled scalar interaction if  $\vec{S}_j$  is a nuclear spin. Only particles of spin  $I = 1/2$  are considered, so there is no quadrupole interaction.

The Hamiltonian  $H'$  is, in the case of non-viscous liquids, a rapidly varying function of time. If  $\vec{I}$  and  $\vec{S}_j$  are on the same molecule  $\vec{r}_j$  varies randomly in time due to tumbling or internal rotation of the molecules of the liquid. If  $\vec{I}$  and  $\vec{S}_j$  are on different molecules  $\vec{r}_j$  varies due to rotation or translation of the two molecules relative to one another. The scalar coupling constant  $A_j$  can fluctuate rapidly between zero and  $A_j$  due to chemical exchange of the spins from one molecule to another, since  $A_j$  is zero unless  $\vec{I}$  and  $\vec{S}_j$  are on the same molecule. The scalar term can also fluctuate rapidly in time due to rapid transitions of  $\vec{S}_j$  between its various energy levels. This can occur if spin  $\vec{S}_j$  is coupled strongly to the lattice, as would be the case for particles having spin greater than  $1/2$  and having electric quadrupole moments.

Given the perturbation Hamiltonian  $H'$ , the transition probability

per unit time between the states  $\alpha$  and  $\beta$  can be calculated from the formula of time dependent perturbation theory<sup>2</sup>

$$w_{\alpha\beta} = \frac{1}{\hbar^2} \int_0^t \overline{(\beta|H_1(t)|\alpha) * (\beta|H_1(t')|\alpha)} e^{i\omega_{\beta\alpha}(t'-t)} dt' + \text{complex conjugate} \quad (2)$$

where  $\omega_{\beta\alpha}$  is defined by

$$\omega_{\beta\alpha} = (E_{\beta} - E_{\alpha})/\hbar = \gamma_I B_0,$$

and the bar denotes an ensemble average. It is assumed that  $H_1(t)$  is a stationary perturbation so that

$$\overline{(\beta|H_1(t)|\alpha) * (\beta|H_1(t')|\alpha)} \quad (3)$$

depends on  $t$  and  $t'$  only through their difference  $t - t' = \tau$ . After one makes this substitution Equation (3) becomes

$$\overline{(\beta|H_1(t - \tau)|\alpha) (\beta|H_1(t)|\alpha) * } = G_{\beta\alpha}(\tau) \quad (4)$$

where  $G_{\beta\alpha}(\tau)$  is called the correlation function of  $H_1(t)$  and depends on the states  $\alpha$  and  $\beta$  and the time  $\tau$ . Substituting Equation (4) into Equation (2) one obtains

$$W_{\alpha\beta} = \frac{1}{\hbar^2} \int_{-t}^t G_{\beta\alpha}(\tau) e^{-i\omega_{\beta\alpha}\tau} d\tau. \quad (5)$$

Several useful properties of  $G_{\beta\alpha}(\tau)$  result from the fact that  $H_1(t)$  is a random function of time. For a typical perturbation

$$\overline{(\beta | H_1(t) | \alpha)} = 0,$$

so if  $H_1(t - \tau)$  and  $H_1(t)$  were unrelated one could write

$$G_{\beta\alpha}(\tau) = \overline{(\beta | H_1(t - \tau) | \alpha) (\beta | H_1(t) | \alpha)^*} = 0.$$

However, for  $\tau = 0$

$$G_{\beta\alpha}(0) = \overline{|(\beta | H_1(t) | \alpha)|^2} \geq 0.$$

For typical physical systems,  $H_1(t)$  varies in time due to some physical movement. For values of  $\tau$  less than some critical time  $\tau_c$  the movement may be considered negligible, and  $H_1(t - \tau) \approx H_1(t)$ . For times long compared to  $\tau_c$ ,  $H_1(t)$  and  $H_1(t - \tau)$  become progressively less correlated, and  $G_{\beta\alpha}(\tau)$  approaches zero. For times long compared to  $\tau_c$  the limits of integration in Equation (5) may be taken as  $\pm \infty$ , and the transition probability  $W_{\alpha\beta}$  becomes independent of time. Thus, Equation (5) becomes

$$W_{\alpha\beta} = \frac{1}{h^2} J_{\beta\alpha}(\omega_{\beta\alpha}) \quad (6)$$

where

$$J_{\beta\alpha}(\omega) = \int_{-\infty}^{+\infty} G_{\beta\alpha}(\tau) e^{-i\omega\tau} d\tau \quad (7)$$

is called the spectral density of the correlation function  $G_{\beta\alpha}$  at the frequency  $\omega$ . It is generally assumed, and can be proved in special cases<sup>3</sup>, that  $G_{\beta\alpha}(\tau)$  is related to  $\tau_c$  by the simple exponential relation

$$G_{\beta\alpha}(\tau) = \overline{|(\beta | H_1(t) | \alpha)|^2} e^{-|\tau|/\tau_c}.$$



Substituting this into Equation (7) and performing the integration one obtains

$$J_{\beta\alpha}(\omega) = \frac{2 |(\beta|H_1(t)|\alpha)|^2}{1 + \omega^2 \tau_c^2} \cdot$$

Then

$$\frac{1}{T_1} = 2W_{\alpha\beta} = \frac{2}{\hbar^2} J_{\beta\alpha}(\omega_{\beta\alpha}) = \frac{4}{\hbar^2} \frac{|(\beta|H_1(t)|\alpha)|^2}{1 + \omega_{\beta\alpha}^2 \tau_c^2} \cdot \quad (8)$$

Thus, the spin-lattice relaxation time depends on the strength of the coupling between the spin  $\vec{I}$  and the neighboring spins  $\vec{S}_j$ , which enters the equation via the term  $|(\beta|H_1(t)|\alpha)|^2$ . It depends on the temperature through the correlation time  $\tau_c$ , and it depends on the strength of the external applied magnetic field through the term  $\omega_{\beta\alpha} = \gamma_I B_0$ . More complete formulas for  $T_1$ , as well as formulas for  $T_2$  may be found in Appendix B. The general form of all the equations is very similar to Equation (8).

#### Exchange Phenomena

Now consider the case in which spins, assumed to be protons, can exist in two environments A and B having different relaxation times  $T_{1A}$  and  $T_{1B}$ . The probability that a proton is in environment A is  $p_A$ , and the probability that a proton is in environment B is  $p_B$ . In the limit of rapid exchange of protons between the two environments the observed

proton relaxation rate is just the weighted average of the relaxation rates in the separate environments, i.e.,

$$\frac{1}{T_1} = \frac{P_A}{T_{1A}} + \frac{P_B}{T_{1B}} \quad (9)$$

An example of such a system is water which contains dissolved paramagnetic salts. Environment A is water molecules in the solvent, and environment B is water molecules in the primary hydration sphere of the paramagnetic ion. In this case  $T_{1B} \ll T_{1A}$  due to interaction of the proton spin with the electron spin of the paramagnetic ion. From Equations (1) and (8) the dipolar contribution to the relaxation rate of the spin  $\vec{I}$  is proportional to  $\gamma_S^2$ . Therefore, since  $\gamma$  for an electron is of the order of a thousand times that of a proton, electrons are of the order of  $10^6$  times more effective in producing relaxation. Whereas relaxation times of protons in the solvent water are of the order of seconds, relaxation times in the primary hydration sphere of paramagnetic ions are of the order of microseconds.

When the limit of rapid exchange is not quite reached, the relaxation behavior of the two environment system can still be described by a single relaxation time  $T_1$ , but now  $T_1$  depends not only on the relaxation times  $T_{1A}$  and  $T_{1B}$  but also on how fast protons exchange between the two environments. The corrected expression is<sup>4</sup>

$$\frac{1}{T_1} = \frac{1}{T_{1A}} + \frac{P_B}{T_{1B} + \tau_{BA}} \quad (10)$$

where  $\tau_{BA}$  is the average lifetime of a proton in environment B before transfer to environment A. The approximation  $p_A \approx 1$  valid for dilute

solutions has been made in going from Equation (9) to Equation (10). The relaxation behavior of systems in which protons can exist in more than two environments can also be handled, and in the limit of very rapid exchange the expressions are analogous to Equation (9). When the exchange is slow the expressions become quite complicated, as exemplified by the equation describing the  $\text{Cr}(\text{H}_2\text{O})_6^{3+} - \text{Cr}(\text{H}_2\text{O})_5\text{OH}^{2+} - \text{H}_2\text{O}$  system, which is given in Appendix B.

FOOTNOTES

<sup>1</sup>C. P. Slichter, Principles of Magnetic Resonance (Harper and Row, New York, 1963), pp. 46, 84, 102.

<sup>2</sup>Ibid, pp. 135-142.

<sup>3</sup>Ibid, p. 230.

<sup>4</sup>Z. Luz and S. Meiboom, J. Chem. Phys., 40, 2686 (1964).

## CHAPTER III

### EARTH'S FIELD NMR TECHNIQUE

To measure the proton spin-lattice relaxation time of liquids using the earth's field NMR technique<sup>1,2,3</sup>, the sample, approximately 400 ml in volume, is placed inside a coil whose axis is oriented perpendicular to the earth's magnetic field  $\vec{B}_e$  of 0.54 gauss (Figure 3). At time  $t = 0$  the current is turned on in the coil, establishing a polarizing field of the order of 500 gauss along the axis of the coil. The magnetization within the sample grows exponentially toward its equilibrium value with a time constant  $T_{1p}$ , the spin-lattice relaxation time in  $B_p$ . After a time  $t = t_p$  which is long compared to  $T_{1p}$ , the polarizing field is reduced to some intermediate value  $B_i$  (Figure 4). At time  $t = t_p + t_i$  the intermediate field is reduced suddenly<sup>4</sup> to zero, leaving the magnetization at right angles to the earth's magnetic field. The magnetization then precesses about the earth's magnetic field at the Larmor frequency, which for protons is  $f = \gamma B_e / 2\pi = 2310$  Hz. The changing magnetic flux induces a sinusoidal voltage in the coil, which is amplified and displayed on an oscilloscope screen. The signal dies out with a time constant  $T_{2e}$ , the spin-spin relaxation time of the sample in the earth's field  $B_e$ . The initial amplitude of the free precession signal is a measure of the amount of relaxation that took place in

the interval  $t_i$ . Variation  $t_i$  in successive measurements allows calculation of the relaxation time  $T_{1i}$  in the intermediate field. To measure  $T_1$  in the field  $B_p$ , the magnetic field is reduced to zero at time  $t = t_p$ , i.e.,  $t_i = 0$ . By varying  $t_p$  the relaxation time  $T_{1p}$  can be determined.

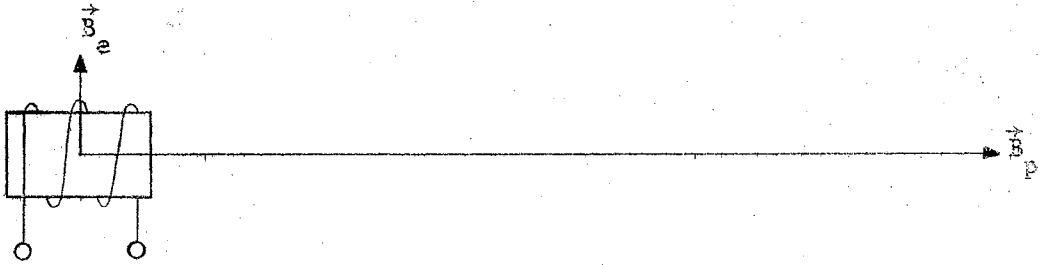


Figure 3. Representation of Magnetic Fields in the Earth's Field NMR Technique

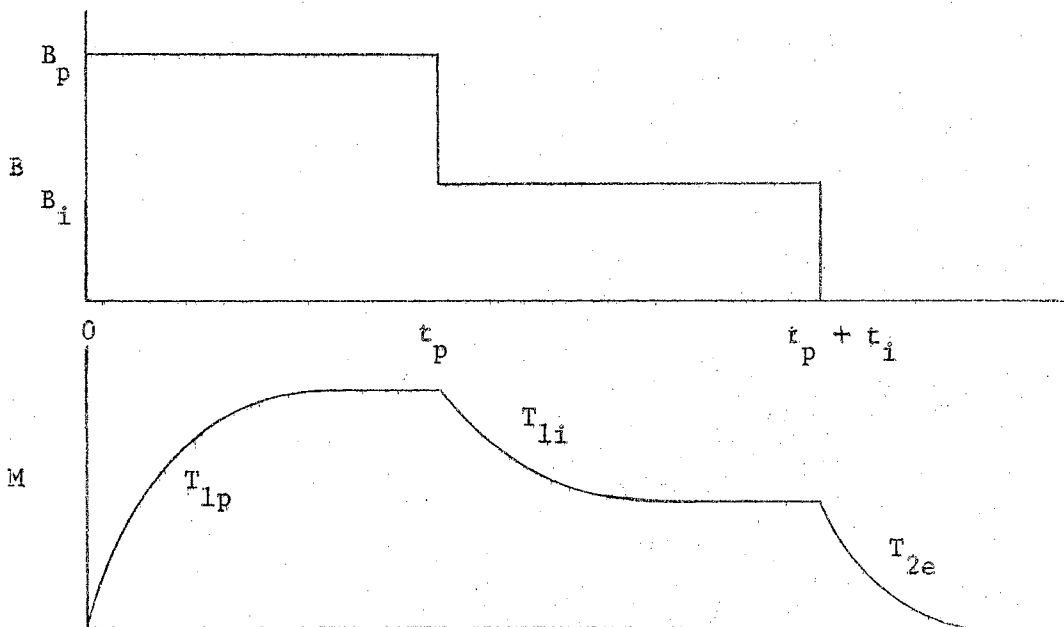


Figure 4. Magnetic Field and Sample Magnetization Versus Time for the Earth's Field NMR Technique

To measure  $T_1$  in the earth's field of 0.54 gauss, the polarizing field  $B_p$  is applied for a time long compared to  $T_{1p}$ . Now  $B_p$  is reduced to zero adiabatically<sup>4</sup> rather than suddenly, which leaves the nuclear magnetization parallel to the earth's field  $\vec{B}_e$ . After a time  $t_e$  an "inspection pulse" is applied, whose function is to rotate the remanent magnetization so as to be perpendicular to  $\vec{B}_e$ . The inspection pulse is generated by turning on the coil current adiabatically to give a field of a few gauss, and then removing it suddenly. The amplitude of the ensuing precession signal is again a measure of how much relaxation took place in the interval  $t_e$ .

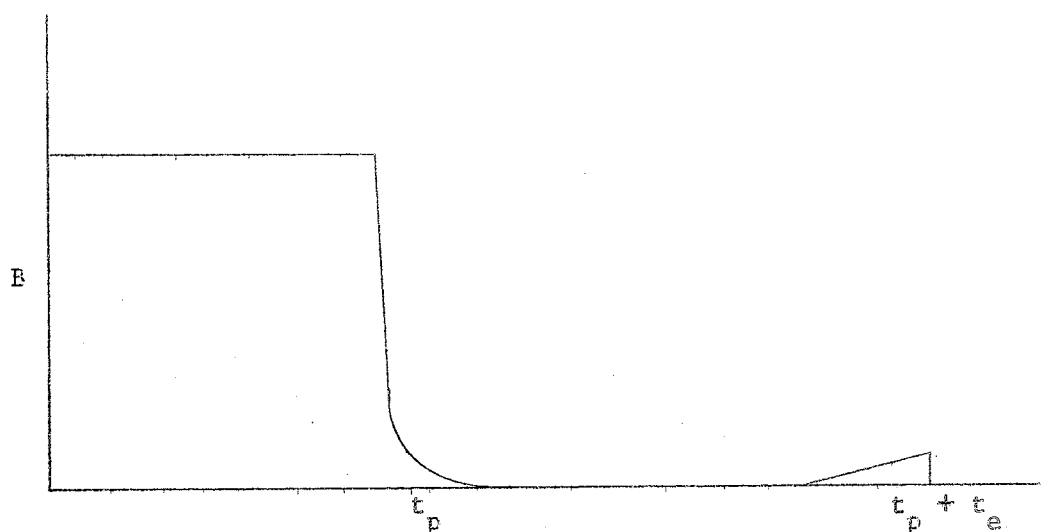


Figure 5. Magnetic Field Versus Time for Measuring  $T_1$  in the Earth's Field of 0.54 Gauss

#### FOOTNOTES

<sup>1</sup>M. Packard and R. Varian, Phys. Rev., 93, 941 (1954).

<sup>2</sup>A. Abragam, The Principles of Nuclear Magnetism (Oxford University Press, London, 1961), p. 64.

<sup>3</sup>D. E. Mitchell, M.S. Thesis, Oklahoma State University, 1964 (unpublished).

<sup>4</sup>The conditions for sudden and adiabatic passage are discussed in references 2 and 3.



## CHAPTER IV

### INSTRUMENTATION

#### Introduction

To measure the field dependence of proton spin-lattice relaxation times using the earth's field NMR technique, instrumentation is required which will maintain a polarizing field  $B_p$  in an air core coil for a time  $t_p$ , reduce the field suddenly to an intermediate value  $B_i$  for a time  $t_i$ , and then reduce the field suddenly to zero. The coil must then be disconnected from the polarizing circuitry and connected across a capacitor, forming a series resonant LC circuit tuned to the Larmor precession frequency of the spins. The signal must then be amplified and displayed on an oscilloscope screen. Thus four components are required: (1) a switching circuit for rapid changing of currents in an inductive load, (2) a power supply for maintaining regulated current in the load, (3) detection circuitry for observing the free precession signal, and (4) timing circuits for control of polarizing and switching times.

#### Current Control

The current control circuit is shown in Figure 6. A plot of the coil current and coil voltage is given in Figure 7. The operation of the silicon controlled rectifier current switching circuit is very much like the one described by Mitchell<sup>1</sup>, except series regulating power

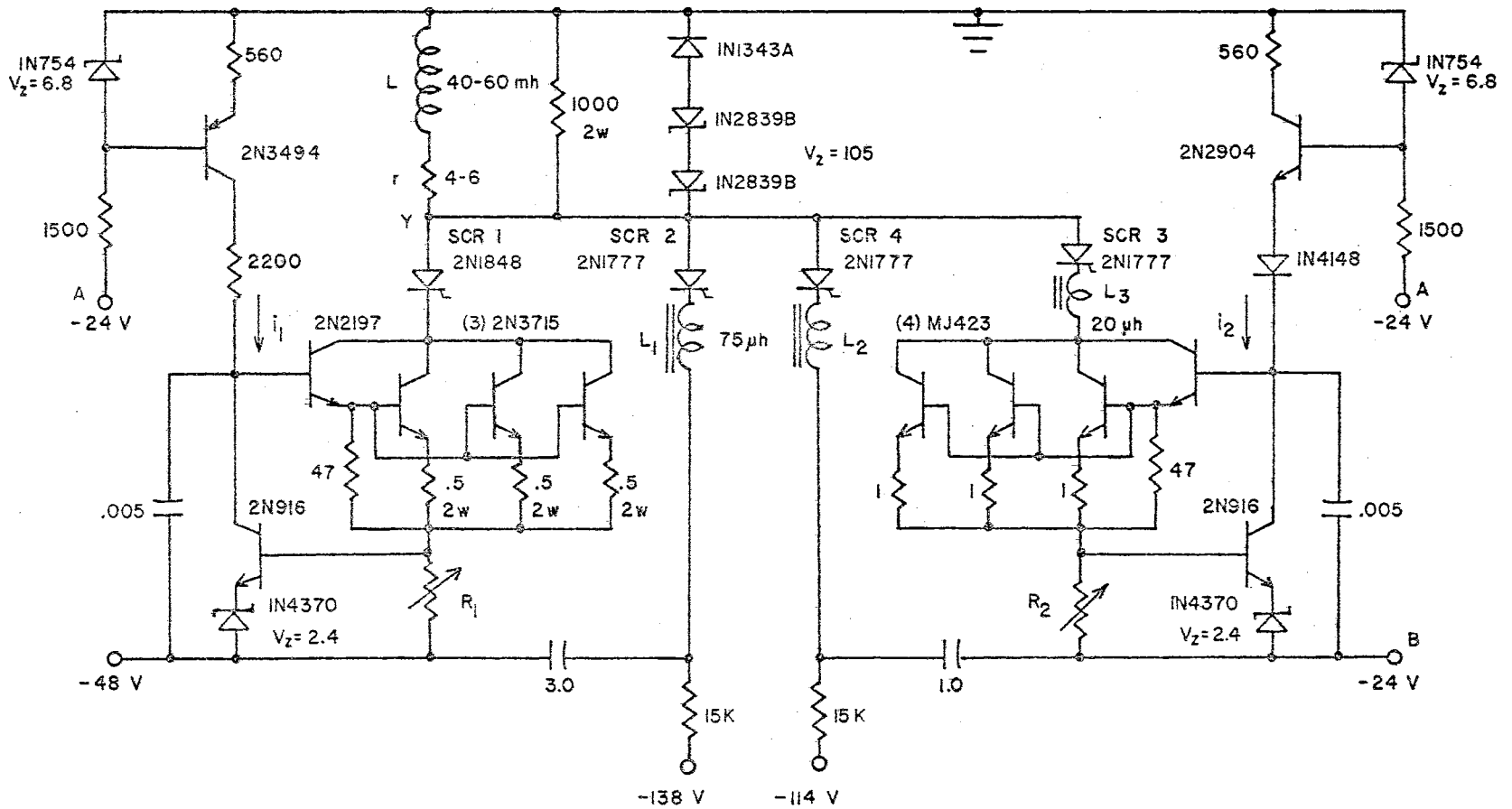


Figure 6. Current Control Circuitry

transistors have been added to provide constant current in the load.

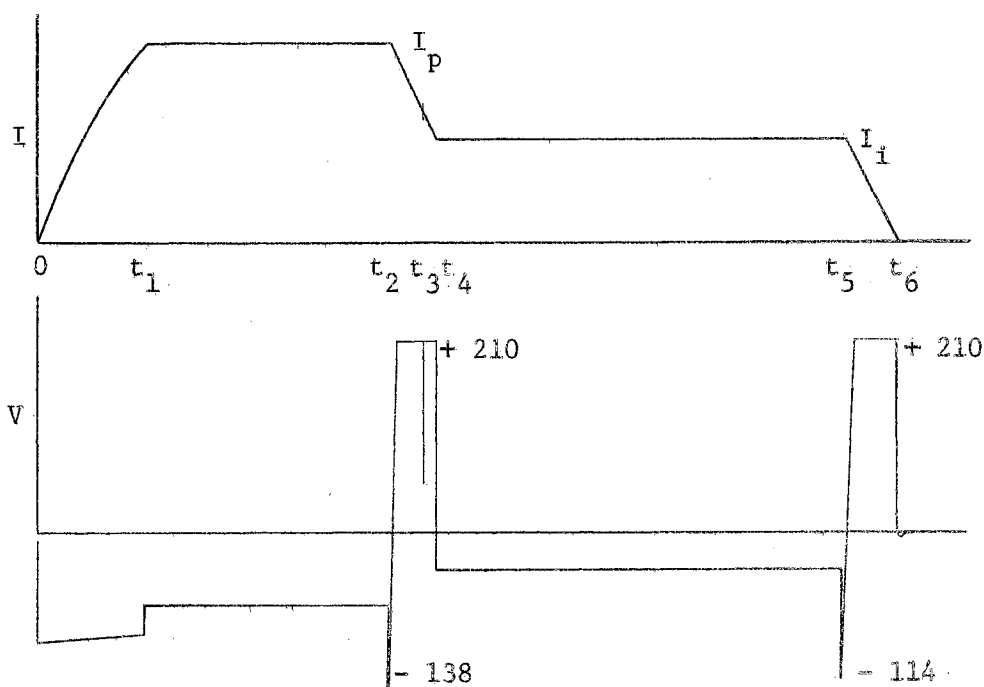


Figure 7. Coil Current and Coil Voltage Measured at Point Y of Figure 6

SCR #1 is triggered at time  $t = 0$ , and the voltage at point Y in Figure 6 drops to nearly -48 volts (Figure 7). The current rises exponentially with a time constant  $L/r$ . At time  $t_1$  the current has increased to a level such that the voltage across  $R_1$  is greater than the 2.4 volt zener reference voltage, and the 2N916 conducts. This diverts some of the current  $i_1$  that was formerly available as base current for the series regulating transistors. They come out of saturation and prevent further current increase. The negative feedback signal to the base of the three 2N3715 series regulating transistors maintains the load current constant until time  $t_2$  when SCR #2 is fired. The voltage at point Y drops to -138 volts, reverse biasing SCR #1 and shutting it

off. The voltage at Y rises sinusoidally as the energy in the coil is dumped into the 3.0  $\mu\text{f}$  commutating capacitor. When the voltage reaches +210 volts the two 1N2839B zener diodes begin conducting, and the current in the coil decreases linearly at a rate  $di/dt = V_z/L$ . At time  $t_3$  when the current has decreased to just above 2.0 amperes SCR #3 is fired. A current  $I_1$  determined by the value of  $R_2$  and the 1N4370 zener voltage passes through the MJ423 series regulating power transistors. The remaining coil current passes through the 1N2839B zener diodes, which maintains the potential at Y equal to +210 volts. This remanent current continues to decrease at a rate  $di/dt = V_z/L$ . When the zener current reaches zero at time  $t_4$  the potential at Y drops to the value  $-I_1 r$ . The coil current is kept constant by the negative feedback provided by sampling resistor  $R_2$  and the 2N916 error detector and amplifier. The intermediate field is cut off at time  $t_5$  by triggering SCR #4. The cut off sequence is similar to that for SCR #1.

The chokes  $L_1$ ,  $L_2$ , and  $L_3$  in Figure 6 limit transients which occur when the SCR's are triggered from the non-conducting into the conducting state. Chokes  $L_1$  and  $L_2$  are 75  $\mu\text{h}$  and are made up of 22 turns of #20 wire on an Arnold A-930157-2 molybdenum permalloy core. Choke  $L_3$  is 20  $\mu\text{h}$  and consists of 5 turns of #16 wire on a Ferroxcube 203F250-3C ferrite core.

The 0.005  $\mu\text{f}$  capacitors across the 2N916 transistors prevent high frequency instability of the high gain feedback network. The 1000 ohm resistor in parallel with the coil serves to damp oscillations which occur on switching current in the inductive load.

The 2N3494 and 2N2904 transistors act as constant current sources and provide regulation against changes in power supply voltage. The 1N4148 diode at the collector of the 2N2904 transistor prevents current from being drawn from the base to collector of the 2N916 when the 24-volt power supply at point B is turned off.

The 48-volt supply is designed for loads of from 4 to 6 ohms and for polarizing currents of from 4 to 6 amperes. The 24-volt intermediate field supply is designed for currents from 2 amperes to 30 milliamperes. Regulation for both is  $\pm 1\%$ , the principal limitation being temperature drift. The negative temperature coefficient of the 1N4370 reference zener diode and the base-emitter voltage of the 2N916, plus the positive temperature coefficient of the sampling resistors  $R_1$  and  $R_2$  couple to make the current decrease as the temperature is increased. Regulation could be improved at the expense of increased power loss in the sampling resistors by using higher reference voltages. Zener diodes with breakdown voltages greater than 5.5 volts have positive temperature coefficients which could serve to cancel the negative temperature coefficient of the base-emitter junction of the reference amplifier. The present system is, however, sufficient for most purposes.

#### Detection Circuit

After the current in the coil has been reduced to zero the magnetization within the sample precesses freely about the earth's magnetic field and induces a voltage in the coil. The circuitry necessary to detect and amplify this signal is shown in Figure 8 along with the relays for switching from the polarizing to the detection mode.

The coil L is the sample coil. The coil L' is the "bucking coil"

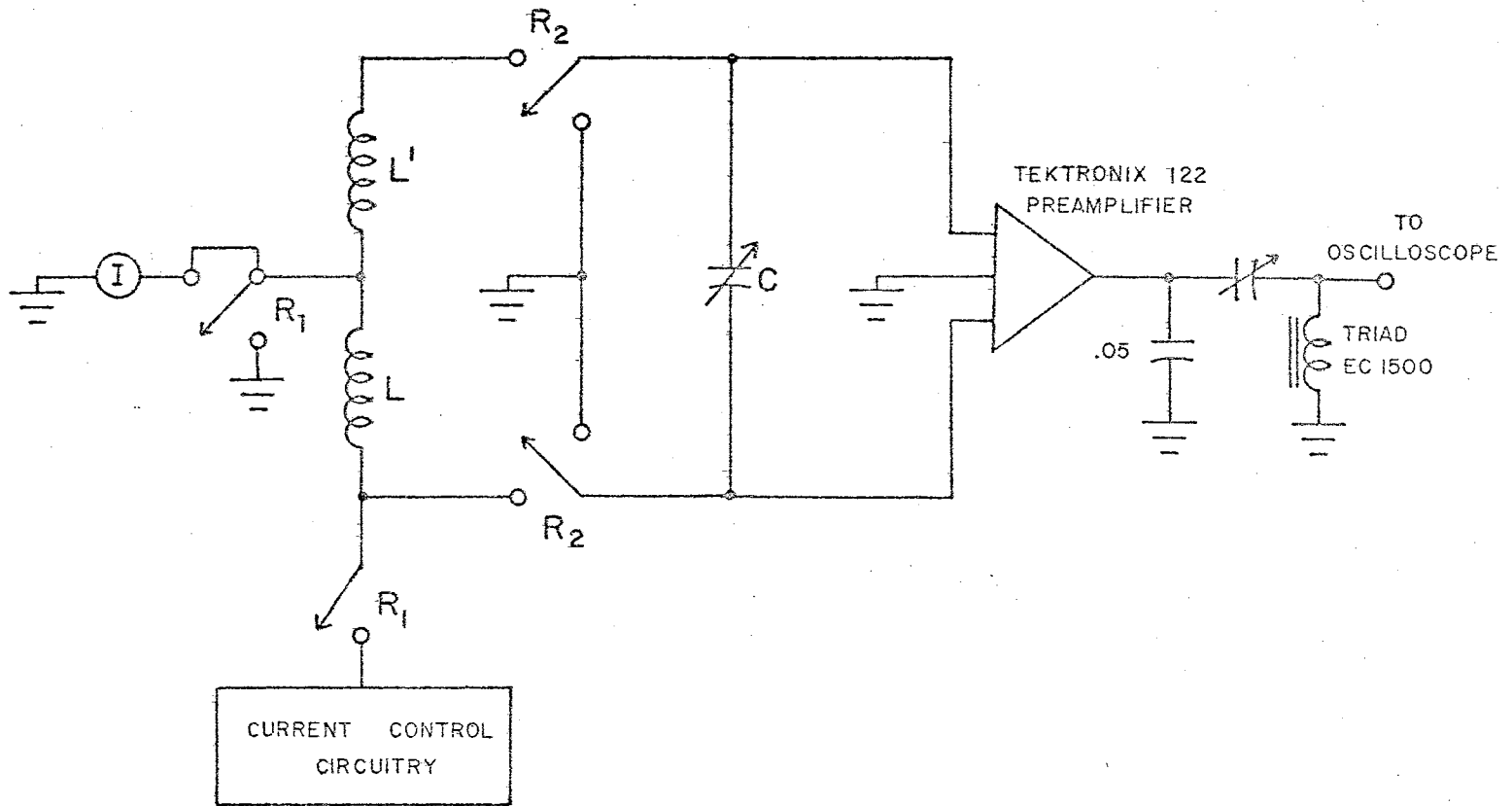


Figure 8. Signal Detection Circuit

which is, to a close approximation, an exact duplicate of the sample coil<sup>1,2</sup>. It is connected so that any stray voltage induced in the sample coil will be cancelled by an equal and opposite voltage induced in the "bucking coil." Relay  $R_1$  is a double pole double throw Potter and Brumfield mercury-wetted contact relay, and  $R_2$  is a Potter and Brumfield HC11DB half-size non-polarized relay. The relays are activated in the polarizing mode and deactivated in the detection mode to minimize the possibility of stray pickup that may exist in the relay activating coils.

When the relays are activated in the polarizing mode, relay  $R_2$  grounds the detection circuitry, and  $R_1$  connects the sample coil to the polarizing circuitry and to a meter for measuring the current through the coil. In the detection mode relay  $R_1$  disconnects the polarizing circuitry from the coil and grounds the center tap of  $L$  and  $L'$ . Relay  $R_2$  connects the sample and bucking coils to the capacitor  $C$ , forming a series resonant LC circuit tuned to the Larmor precession frequency of the spins. Low dissipation factor polystyrene capacitors are used in the tuned circuit in order to prevent dropping the circuit  $Q$ . The output tuner may be treated as a band-pass filter with a bandwidth of about  $180 \text{ Hz}^1$ .

At a bandwidth of 75 Hz, corresponding to a circuit  $Q$  of 31, the signal-to-noise ratio is approximately 150 to 1 for a 450 ml water sample in a field of 350 gauss. The signal-to-noise ratio can be improved by winding coils of higher  $Q^2$  and thereby narrowing the bandwidth, at the expense of transient response of the detection system.

## Relay Multivibrators

The current and signal relays are controlled by bistable multivibrators shown in Figures 9 and 10. In the detection mode transistor  $Q_1$  is on,  $Q_2$  is off, and the relays are deactivated. They are activated in the polarizing mode by the leading or trailing edge of a square pulse, which is differentiated by the 0.01  $\mu$ f capacitor and 470 K voltage divider. The negative spike of the differentiated pulse turns  $Q_1$  off,  $Q_2$  on, and activates the relay. The relays are deactivated in a similar fashion by a negative pulse at the base of  $Q_2$ . The zener diode, in parallel with  $Q_2$  keeps the collector-emitter voltage below the transistor breakdown voltage when the relay is deactivated.

## Timing Circuits

The basic timing circuit (Figure 11) is a monostable multivibrator with a unijunction transistor used as the timing element. In the quiescent state  $Q_1$  is on,  $Q_2$  is off, and the potential at Z is near -23 volts. The emitter of the unijunction transistor is clamped to a potential well below the firing voltage through diode  $D_1$ . A positive pulse at the base of  $Q_1$ , or pushing switch  $S_1$ , turns  $Q_1$  off and  $Q_2$  on. The potential at point Z moves to within a few volts of ground, and the timing capacitor  $C_1$  charges through  $R_1$ . When the unijunction fires, the negative pulse generated at the emitter of  $Q_2$  turns it off, and the circuit resumes the initial state. Capacitor  $C_1$  rapidly discharges through  $D_1$ , providing for fast recovery. The time delay is approximate-



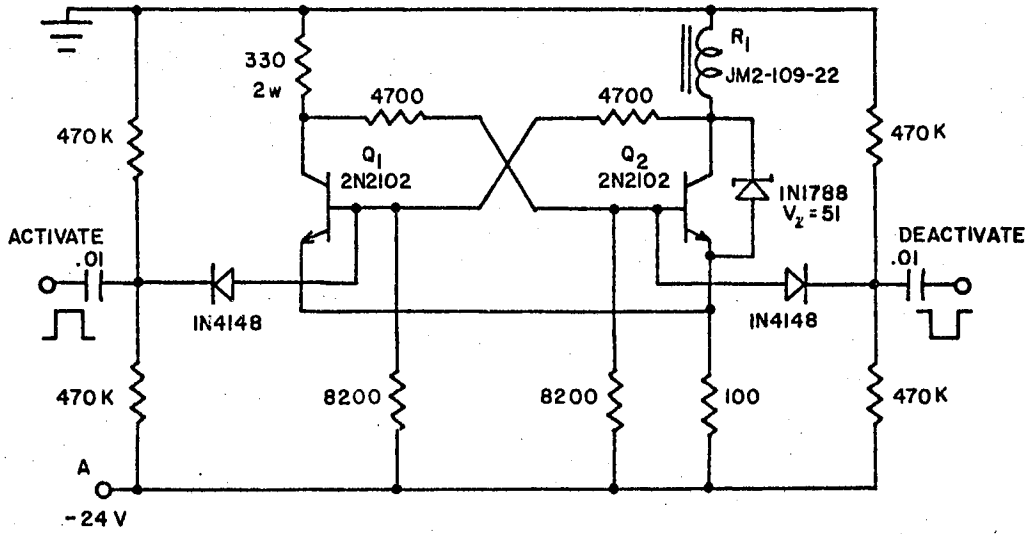


Figure 9. Current Relay Multivibrator

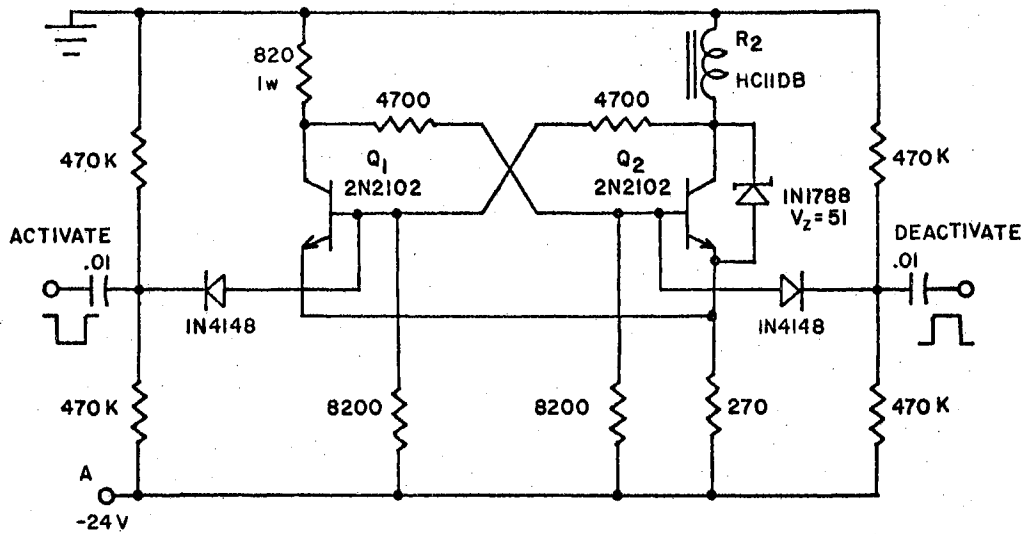


Figure 10. Signal Relay Multivibrator



ly  $R_1(C_1 + C_2)$ , the exact value depending on the unijunction firing voltage. The square pulse at the collector of  $Q_1$  is differentiated by the RC network and triggers a second stage at the end of the time delay of the first.

Capacitor  $C_2$  is kept small since when the unijunction fires it charges through the external power supply, which can cause transients unless the supply is a low impedance source. Capacitor  $C_1$  may be any value, and  $R_1$  can be any value between 3.3 K and 3.3 Meg, the limitations being the minimum valley current and the maximum peak point emitter current of the unijunction<sup>3</sup>. The 100 ohm resistor in series with  $C_1$  limits the emitter current when  $C_1$  discharges through the unijunction. High currents heat the unijunction, plus reduce the pulse amplitude at the emitter of  $Q_2$  when the unijunction fires.

The 2N1671C was chosen for its low leakage current and low peak point emitter current, which are necessary for long timing intervals<sup>3</sup>. The design objective was for polarizing times between 2 ms and 20 sec, which are easily obtainable with this circuit. Accuracy is better than  $\pm 0.5\%$ . For short timing intervals, 2N2646 unijunction transistors operate satisfactorily, and at reduced cost.

#### SCR Trigger Circuits

The SCR trigger circuits are shown in Figures 12 and 13, one type for the high current 2N1848, and one type for all of the 2N1777 SCR's. The operation for both is the same. The emitter of the unijunction is kept in the quiescent state at -12 volts, which is just below the emitter

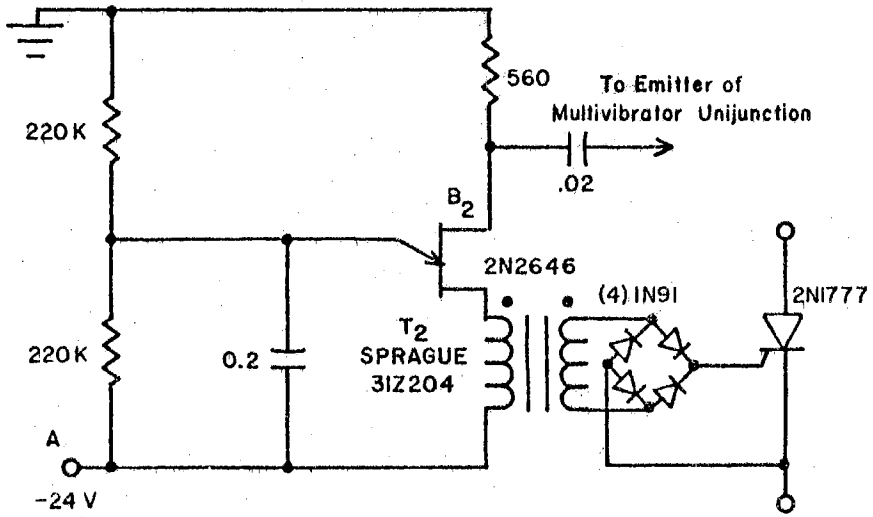


Figure 12. Firing Circuit for 2N1777 SCR

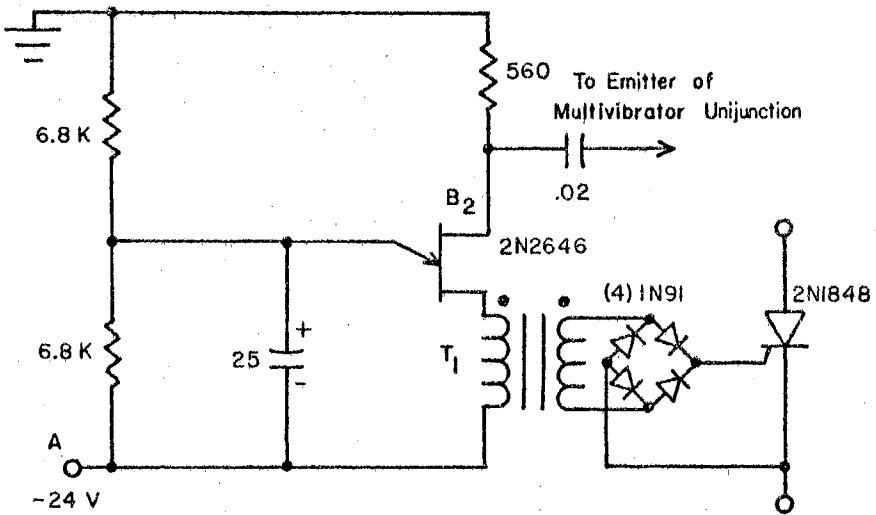


Figure 13. Firing Circuit for 2N1848 SCR

firing voltage of the unijunction. A negative pulse at  $B_2$  causes the peak point voltage of the unijunction to drop below the emitter voltage. The capacitor discharges through the unijunction and transformer, firing the SCR.

Transformer  $T_1$  consists of a primary and secondary of 400 turns of #29 wire wound on an Arnold A-213192-2 molybdenum permalloy core. The 25  $\mu$ f capacitor discharging through this transformer generates a pulse greater than 300  $\mu$ sec wide, which is sufficient to insure that the SCR holding current has built up in the inductive load before the gate drive is reduced to zero. The bridge rectifier network prevents transients in the SCR gate circuit from being fed back into the trigger circuit. Further isolation is provided by using separate unijunction transistors for firing the SCR's and triggering the multivibrators. Placing the SCR trigger transformer in series with  $C_1$  or in base one of the unijunction in Figure 11 caused instability of the multivibrators.

#### Pulse and Timing Circuit

The complete pulse and timing circuit which controls the firing of the SCR's and the switching of the relays is shown in Figure 14. It consists of a string of six essentially identical monostable multivibrators like the one in Figure 11. Multivibrator #1 is triggered into the unstable state by pushing switch  $S_1$ , and each succeeding multivibrator is automatically triggered into its unstable state at the end of the time delay of the preceding stage. When  $S_1$  is pushed, MV #1 flips into its unstable state, which triggers the multivibrator in Figure 10 and activates the signal relay  $R_2$ , grounding the detection circuitry.

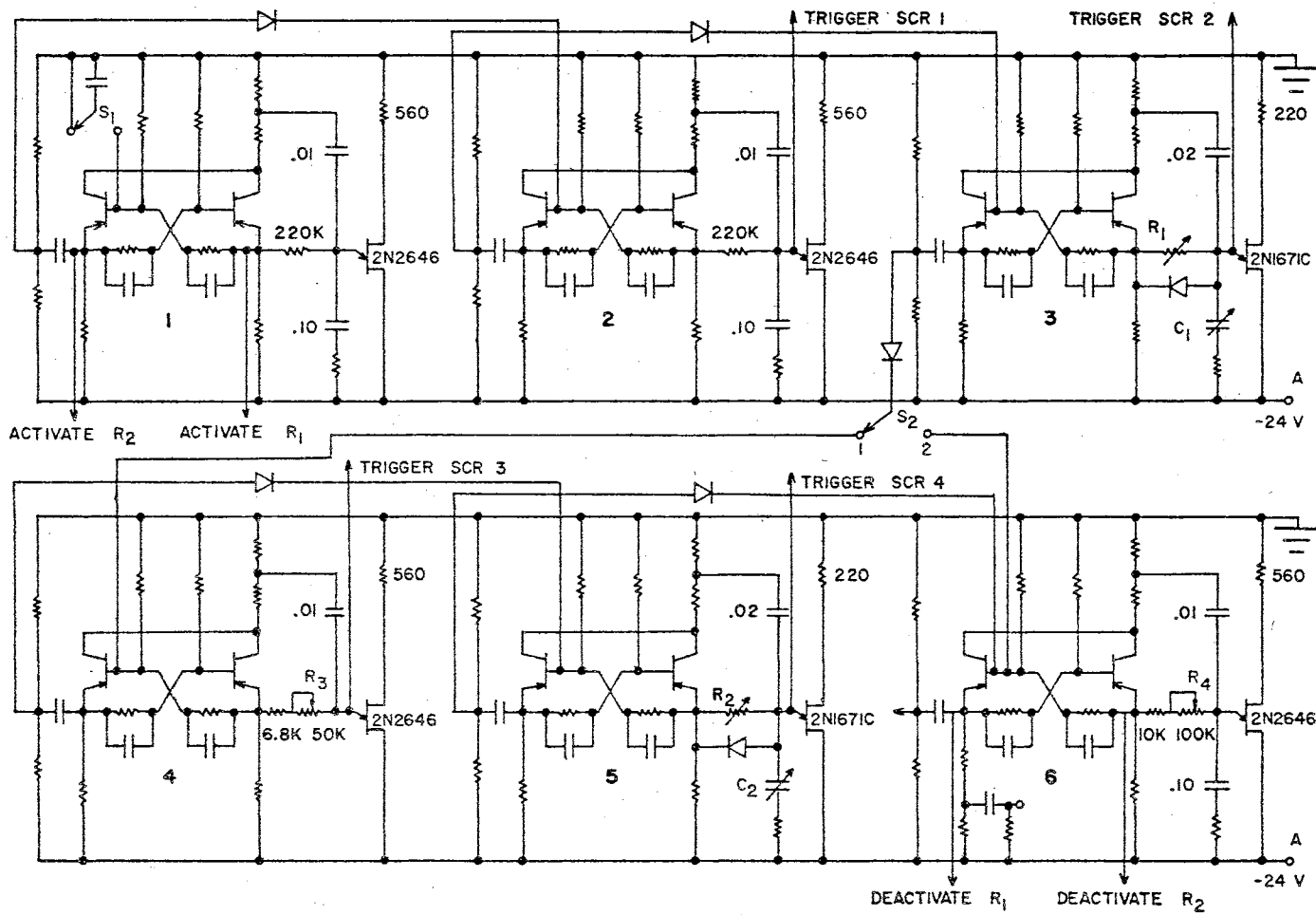


Figure 14. Pulse and Timing Circuit

Approximately 20 ms later MV #1 reverts back to its stable state, which triggers the current relay multivibrator (Figure 9) and connects the coils to the polarizing circuitry. At the same time MV #1 triggers MV #2, which returns to its quiescent state 20 ms later and triggers the circuit in Figure 13. This circuit fires SCR #1 and turns the current on in the coil. At a time between 20 ms and 20 sec later, depending on the values of  $R_1$  and  $C_1$ , MV #3 reverts back to its quiescent state. This triggers SCR #2 which causes the current to begin decreasing in the coil (point  $t_2$  in Figure 7). After a time depending on the setting of  $R_3$ , MV #4 reverts and fires SCR #3. The three MJ423 transistors in Figure 1 can carry 2 amperes for only a few hundred microseconds while the voltage at Y is +210 volts with respect to ground. Therefore,  $R_3$  in Figure 14 must be set so that SCR #3 is fired when the coil current is just above 2 amperes. After a time between 2 ms and 20 sec later, depending on the values of  $R_2$  and  $C_2$ , MV #5 runs down, which fires SCR #4 and turns off the current in the coil. At the same time MV #6 is triggered into its unstable state, which sends a pulse to the current relay multivibrator (Figure 9) to deactivate the current relay. Although SCR #4 is triggered at the same time as the current relay multivibrator, the current is reduced to zero within 1.5 ms, whereas it requires approximately 3 ms for the current relay to actually break contact. When MV #6 runs down the signal relay multivibrator is triggered (Figure 10), which deactivates relay  $R_2$  and connects the coil to the detection circuit. The time between deactivation of the current relay and signal relay is variable from 1 to 10 ms by means of  $R_4$ . This time is made as

short as possible, subject to the requirement that the signal relay not make contact with the coils until after the current relay has disconnected the polarizing circuitry. When the signal relay connects the coil to the detection circuit, a transient due to ringing of the coil masks the free precession signal for 30-80 ms, depending on the  $Q$  of the coil, which places a lower limit on the  $T_2$  of samples which can be studied by this method.

The oscilloscope sweep may be triggered at the end of the time delay of MV #6, or another stage may be added to delay the sweep until after the switching transient has died out. If desired, a pulse from the last multivibrator can be fed back to MV #1 to make the circuit cycle continuously.

To measure  $T_1$  in the high field, switch  $S_2$  is placed in position 2, which bypasses the multivibrators which turn the intermediate field on and off. The current is reduced to zero at the end of the polarizing time, and MV #6 is triggered, which deactivates the current and signal relays for observing the precession signal.

Some experiments have been done using the inspection pulse technique (Figure 5) to measure  $T_1$  in the earth's field of 0.54 gauss. However, the circuitry required for this technique is still in the developmental stage and has not been included.



FOOTNOTES

<sup>1</sup>D. E. Mitchell, M.S. Thesis, Oklahoma State University, 1964 (unpublished).

<sup>2</sup>T. R. Ligon, M.S. Thesis, Oklahoma State University, 1967 (unpublished).

<sup>3</sup>J. F. Cleary, ed., G. E. Transistor Manual (General Electric Company, Syracuse, 1964), pp. 300-347.

## CHAPTER V

### PROTON SPIN RELAXATION AND SELF- DIFFUSION IN LIQUID $\text{CHCl}_3$

#### Introduction

The study of nuclear spin relaxation in pure liquids is of considerable interest from the point of view of liquid kinetics and liquid structure. Since the intramolecular contribution to proton spin relaxation times depends on the tumbling motion of the molecules, while the intermolecular contribution depends on their relative translations, valuable information about these two motions can be obtained only if the inter- and intramolecular contributions to  $T_1$  can be separated from one another. Ordinarily such separation cannot be obtained directly from the experimental data. One case in which the separation has been experimentally obtained is the work of Bonera and Rigamonti<sup>1</sup>, who studied proton relaxation in mixtures of benzene and its perdeuterated analog at various concentrations. By repeating the measurements at different temperatures, they obtained activation energies for rotation and translation which could be compared with the predictions of the BPP model<sup>2</sup>.

Proton relaxation measurements on chloroform have been reported previously in the literature<sup>3-6</sup>. In the case of this liquid the rotational and translational motions of  $\text{CHCl}_3$  molecules can be deduced from a study of the field and temperature dependence of proton spin-lattice

relaxation times alone. Proton relaxation in high fields is dominated by the proton-proton dipolar interaction, whereas in low fields the scalar coupling  $\hbar J \vec{I} \cdot \vec{S}$  between the proton and the three chlorine nuclei on the same molecule is responsible for relaxation. The relaxation time of the  $i$ th proton is given by<sup>6</sup>

$$\frac{1}{T_1} = \frac{1}{T_{1DD}} + \sum_k^* J_k^2 S_k (S_k + 1) \frac{\tau_k}{1 + (\omega_i - \omega_k)^2 \tau_k^2} \quad (11)$$

where the summation  $\sum_k^*$  extends over all three chlorine nuclei on the same molecule. In Equation (11)  $S$  is the nuclear spin;  $\omega$  is the Larmor precession frequency;  $J$ , the scalar coupling constant; and  $\tau$ , the correlation time for the scalar interaction, equal in this case to the chlorine relaxation time. The chlorine nuclei relax very rapidly due to the interaction of their quadrupole moments with electric field gradients within the sample, which vary randomly in time due to tumbling of the  $\text{CHCl}_3$  molecule<sup>7</sup>. The chlorine relaxation times are given by

$\tau_k^{-1} = C_k \tau_{\text{rot}}$ , where  $C_k$  is a constant for a particular nucleus and chemical environment, and  $\tau_{\text{rot}}$  is the rotational correlation time<sup>7</sup>. According to the Debye model<sup>1</sup>,  $\tau_{\text{rot}}$  is related to the bulk viscosity of the solvent by the relation

$$\tau_{\text{rot}} = 4\pi \eta a^3 / 3kT = \eta V_m / kT \quad (12)$$

where  $a$  is the molecular radius, and  $V_m$  is the molecular volume. The failure of the Debye expression to correctly predict rotational correlation times for all except the most highly associated liquids is well documented<sup>8</sup>. O'Reilly<sup>9</sup> has recently used the large-step random-walk

theory of rotational diffusion and the quasilattice theory of liquids to derive an expression for  $\tau_{rot}$  which provides better agreement with experiment. Completely a priori calculations with his model are not possible, however, without a knowledge of the energy required to create a vacancy in the liquid lattice.

The quantity  $(T_1^{DD})^{-1}$  in Equation (11) is the field-independent dipolar contribution to the observed relaxation rate. Its rotational and translational contributions may be estimated using the theoretical formulas of Bloembergen, Purcell, and Pound<sup>2</sup> as corrected by Kubo and Tomita<sup>10</sup> and extended by Gutowsky and Woessner<sup>11</sup> to systems of many nuclei. They are

$$(T_1^{DD})^{-1} = (T_1^{rot})^{-1} + (T_1^{tr})^{-1} \quad (13a)$$

$$(T_1^{rot})^{-1} = \hbar^2 \gamma_i^2 \left[ \frac{3}{2} \gamma_i^2 \sum_j r_{ij}^{-6} + \frac{4}{3} \sum_k^* S_k (S_k + 1) \gamma_k^2 r_{ik}^{-6} \right] \tau_{rot} \quad (13b)$$

$$(T_1^{tr})^{-1} = \hbar^2 \gamma_i^2 N \pi D^{-1} \left[ \frac{1}{2} \gamma_i^2 \sum_j (r_{ij}^{-1})^0 + \frac{4}{9} \sum_k^* S_k (S_k + 1) \gamma_k^2 (r_{ik}^{-1})^0 \right] \quad (13c)$$

In the above equations  $\gamma$  is the gyromagnetic ratio of the nucleus;  $r$  is the internuclear distance;  $D$  is the self-diffusion coefficient for the molecules of the liquid; and  $N$  is the number of molecules per unit volume. In these formulas,  $\sum_j$  are summations over nuclei of the same type as the  $i$ th, and  $\sum_k^*$  are over all others. In Equation (13b) the summations are over nuclei in the same molecule, while in Equation (13c) they are over nuclei of a neighboring molecule,  $(r_{ik}^{-1})^0$  being the mean value of  $r_{ik}^{-1}$  for two molecules in contact. For  $\text{CHCl}_3$  the first term

in Equation (13b) is absent.

In the present study the earth's field NMR technique is used to measure the field and temperature dependence of proton spin-lattice relaxation times in a solution of  $\text{CHCl}_3$ . Measurements in low fields are shown to yield the scalar coupling constants and the chlorine quadrupole relaxation times, whose temperature dependence is determined by the rotational motion of the  $\text{CHCl}_3$  molecules. Relaxation times in high fields will be shown to be determined mainly by the dipolar interaction between protons on neighboring molecules. Hence the temperature dependence of high-field  $T_1$  reflects the temperature dependence of the translational motion of the  $\text{CHCl}_3$  molecules. The activation energies for translation and rotation are obtained and are compared with activation energies for self-diffusion and viscosity. Measurements on proton self-diffusion coefficients in  $\text{CHCl}_3$  at various temperatures are also carried out, and used to test the validity of the Stokes-Einstein equation  $D = kT/6\pi a \eta$  relating self-diffusion and liquid viscosity.

### Experimental

The chloroform sample for relaxation measurements was prepared from commercial reagent grade chloroform and was deoxygenated by scrubbing with purified nitrogen for approximately 24 hours. The apparatus is similar to the one described by Arthur<sup>12</sup>. After deoxygenation the sample was evacuated and sealed. For comparison, a test sample was sealed in a nitrogen atmosphere and irradiated for approximately 24 hours with ultraviolet light. The uv light speeds up the reaction of dissolved oxygen with a few tenths percent alcohol usually present as a stabilizer.

in commercial chloroform. This sample had a relaxation time as long as one which was first deoxygenated and then sealed; both were 85 sec at 30 °C. This demonstrates the effectiveness of the uv irradiation method as a means of deoxygenating samples for which alcohol is not an objectionable impurity.

Self-diffusion coefficients for chloroform were measured using standard spin-echo techniques.<sup>18</sup> Sample temperature was controlled over the range of 210 to 300 °K by means of a gas flow cryostat. A wide-line magnet was used, together with an NMR Specialties pulsed NMR spectrometer operating at 60 MHz. To obtain the required field gradient, the cylindrical sample tube was moved in a direction parallel to its own axis, away from the center of the magnet gap. A field region was reached at which the shape of the free-precession signal conformed reasonably well to the theoretical shape for a region of constant field gradient<sup>13</sup>. From the shape of the signal, the field gradient was calculated to be 0.41 G/cm. As a check on this and other aspects of experimental technique, the self-diffusion coefficient of acetone was measured over the same range of temperatures as chloroform. The results were in good agreement with values found in the literature<sup>14</sup>. Also, the self-diffusion constant of water was measured at room temperature and at 1.5 °C, with similar good results. None of the samples used in self-diffusion measurements were deoxygenated.

### Results and Discussion

Typical field dependence curves at several temperatures are shown in Figure 15. The temperature dependence of the high-field  $T_1$  ( $= T_1^{DD}$ ) is given in Figure 16 along with the results of Blicharski, et al.<sup>6</sup> The

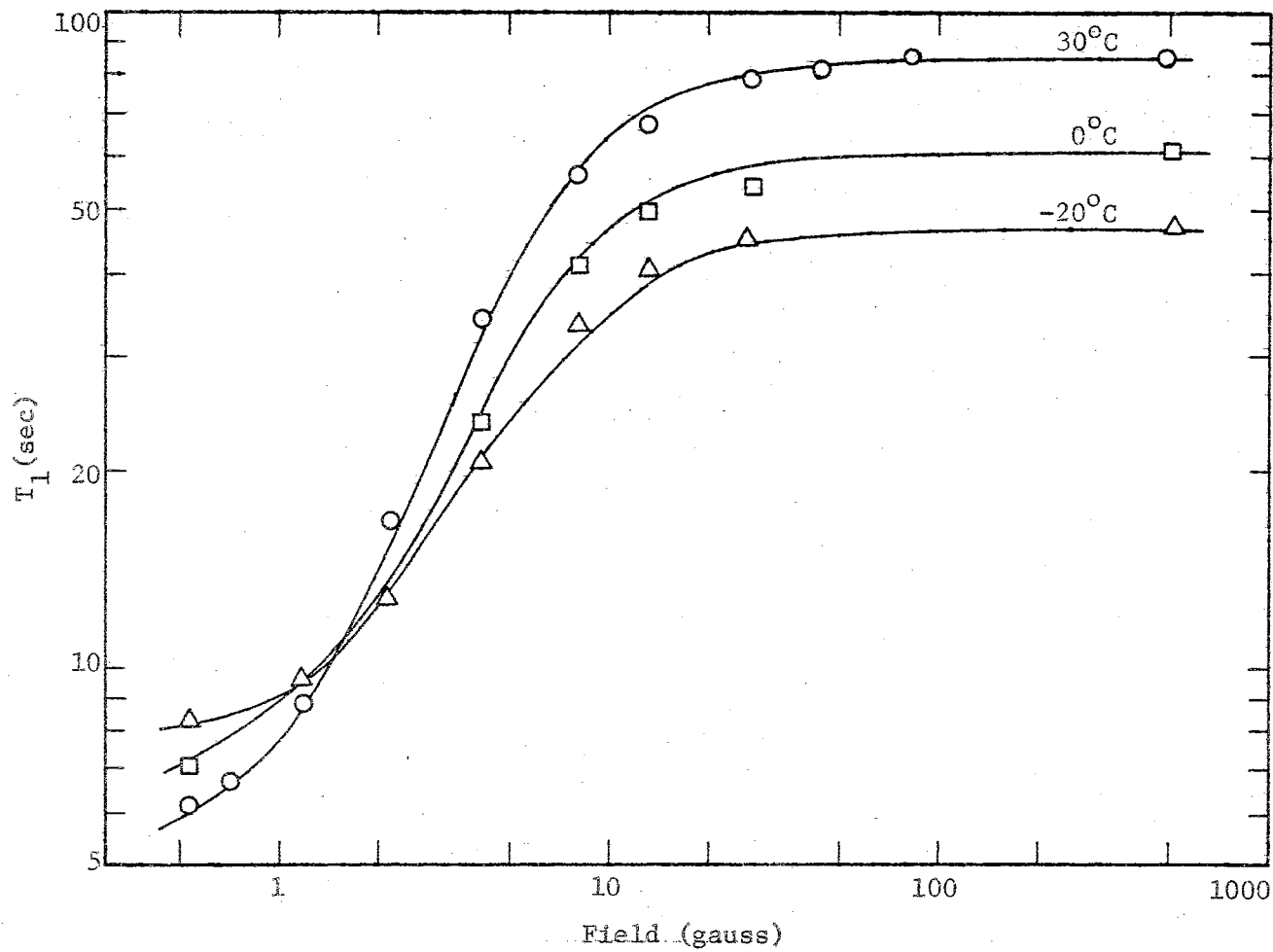


Figure 15. Field Dependence of Proton  $T_1$  in Deoxygenated  $\text{CHCl}_3$

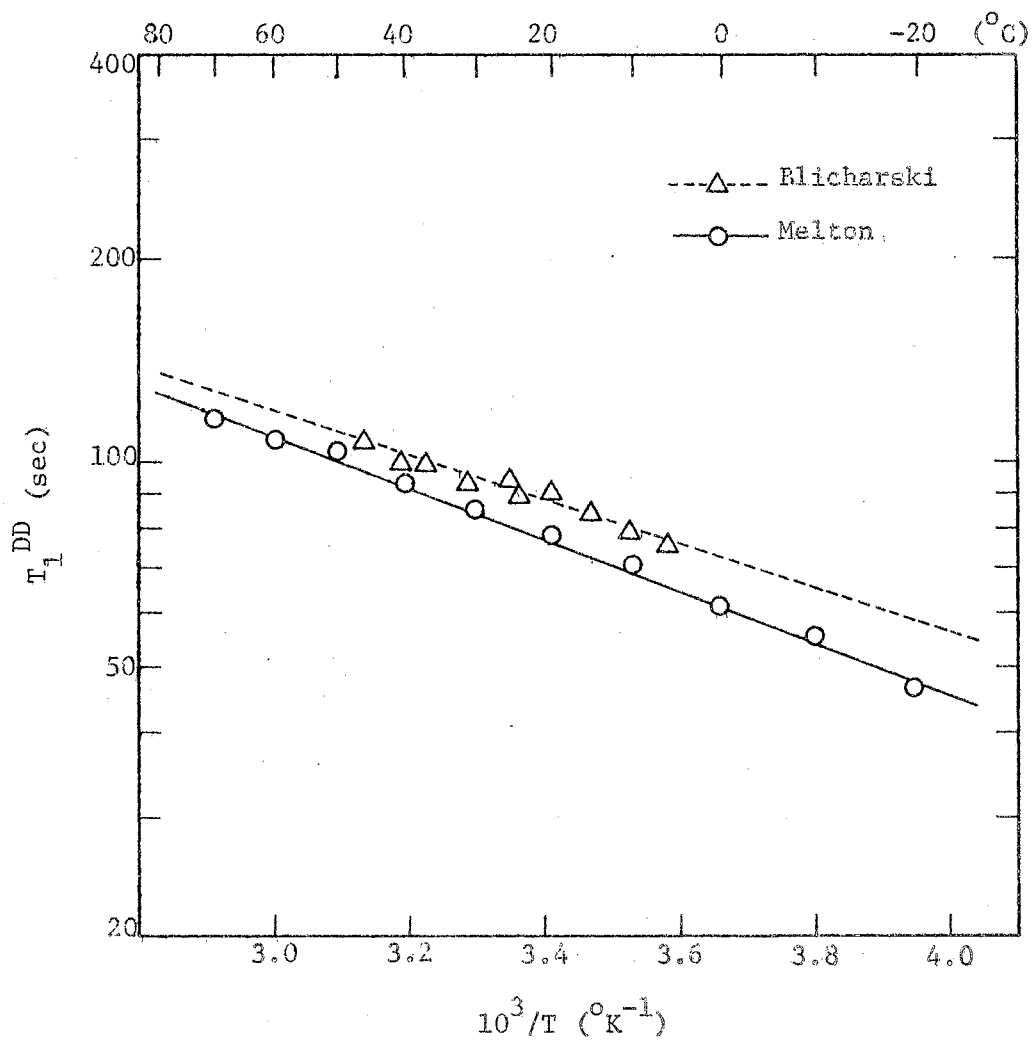


Figure 16. Temperature Dependence of High-Field Proton  $T_1$  in Deoxygenated  $\text{CHCl}_3$ .



solid curves through the data points represent least squares fits of Equation (11) to the experimental data. In the summations it was necessary to take into account the two chlorine isotopes  $\text{Cl}^{35}$  and  $\text{Cl}^{37}$ , which have a naturally occurring isotopic ratio of approximately three to one. Both isotopes have spin 3/2, but possess slightly different gyromagnetic ratios and quadrupole moments and therefore different  $J$  and  $\tau$ . It was assumed that  $J_{37}/J_{35} = \gamma_{37}/\gamma_{35}$  and  $\tau_{37}/\tau_{35} = (Q_{35}/Q_{37})^2$ , where  $Q$  is the nuclear quadrupole moment<sup>15</sup>. For the temperature dependences of  $\tau$  and  $T_1^{\text{DD}}$  relations of the form  $\tau_{35} = \tau_{35}^{\circ} \exp(\Delta E_{\text{rot}}/RT)$  and  $T_1^{\text{DD}} = (T_1^{\text{DD}})^{\circ} \exp(\Delta E_{\text{rel}}/RT)$  were assumed, and the unknown quantities  $\tau_{35}^{\circ}$ ,  $\Delta E_{\text{rot}}$ ,  $(T_1^{\text{DD}})^{\circ}$ ,  $\Delta E_{\text{rel}}$ , and  $J_{35}$  were used as adjustable parameters to fit the data. The non-linear least squares curve fitting procedure is outlined in Appendix A. The results were  $\Delta E_{\text{rot}} = 1.6 \pm 0.1$  kcal/mole,  $\Delta E_{\text{rel}} = 1.76 \pm 0.05$  kcal/mole, and  $J_{35}/2\pi = 4.7 \pm 0.1$  Hz. At 20 °C  $\tau_{35}$  was found to be 24  $\mu\text{sec}$ , which agrees well with a value of 23  $\mu\text{sec}$  from the data of O'Reilly and Schacher<sup>7</sup>, who measured the  $\text{Cl}^{35}$  relaxation time in  $\text{CHCl}_3$  directly. They report a value of  $1.4 \pm 0.1$  kcal/mole for  $\Delta E_{\text{rot}}$ , which is smaller than the result found herein but within the range of experimental error. Winter's estimate<sup>3</sup> of 5.5 Hz for  $J_{35}/2\pi$  was based on  $\tau_{35} = 17.4$   $\mu\text{sec}$  at room temperature. Repeating his calculations using  $\tau_{35} = 24$   $\mu\text{sec}$  gives  $J_{35}/2\pi = 4.7$  Hz, which is the same as found herein. Ottavi<sup>4</sup> has reported results which lead to  $J_{35}/2\pi = 3.7$  Hz and, in a later publication<sup>5</sup>, 5.2 Hz. No explanation for the difference was given. Blicharski's data<sup>6</sup> lead to  $\Delta E_{\text{rel}} = 1.5 \pm 0.2$  kcal/mole.

The fact that  $\Delta E_{\text{rot}}$  differs from the activation energy  $\Delta E_{\text{rel}}$  for relaxation in high fields suggests that  $T_1^{\text{tr}}$  contributes significantly to  $T_1^{\text{DD}}$ . This is born out by calculation of  $T_1^{\text{rot}}$  using Equation (13b). Using accepted values for the general physical constants and the value  $\tau_{\text{rot}} = 1.9 \times 10^{-12}$  sec, which was obtained by O'Reilly and Schacher<sup>7</sup> from the  $\text{Cl}^{35}$  relaxation data, one obtains  $(T_1^{\text{rot}})^{-1} = 0.88 \times 10^{-3} \text{ sec}^{-1}$  at 20 °C. Using this result and the observed value  $T_1^{\text{DD}} = 78 \text{ sec}$  (Figure 16), one calculates with the aid of Equation (13a),  $(T_1^{\text{tr}})^{-1} = 11.9 \times 10^{-3}/\text{sec}$ . Hence, the rotational contribution to  $T_1^{\text{DD}}$  is expected to be less than 10% of the translational contribution, and  $\Delta E_{\text{rel}}$  represents the activation energy for translation. The nonequality of the activation energies for translation and rotation has been discussed before<sup>7,9,16</sup>,

By using Equation (13c), assuming  $(r_{ij}^{-1})^0 = (r_{ik}^{-1})^0 = (2a)^{-1}$  and calculating  $a$  assuming a filling factor of 0.74 for hexagonal close packing of hard spheres, one calculates  $(T_1^{\text{tr}})^{-1} = 5.4 \times 10^{-3}/\text{sec}$  at 20 °C. Due to the small gyromagnetic ratios of  $\text{Cl}^{35}$  and  $\text{Cl}^{37}$ , the second term inside the brackets of Equation (13c) is less than 10% of the first, and  $T_1^{\text{tr}}$  is determined mainly by the dipolar interaction between protons on neighboring molecules. The calculated  $(T_1^{\text{tr}})^{-1}$  is about a factor of two smaller than the experimental rate. But this is reasonable agreement considering the crudeness of the model and the approximations involved in calculating quantities like  $(r_{ij}^{-1})^0$  which could easily be off by a factor of two for a molecule like  $\text{CHCl}_3$ , in which the proton is not

at the center of a molecule of spherical symmetry. Similar discrepancies occur when the Debye formula is used to calculate rotational correlation times. Equation (12) gives  $\tau_{\text{rot}} = 14 \times 10^{-12}$  sec for  $\text{CHCl}_3$  at 20 °C, which is about a factor of seven too large. Such poor agreement is not unusual, as the Debye formula quite often predicts rotational correlation times which are too large by a factor of ten or more.

As indicated in Table I, the self-diffusion constant of liquid chloroform was found to be  $2.5 \times 10^{-5}$  cm<sup>2</sup>/sec at 25 °C, with an activation energy  $\Delta E_D = 2.1 \pm 0.2$  kcal/mole. The room temperature value is in agreement with the value  $2.6 \times 10^{-5}$  cm<sup>2</sup>/sec obtained by McCall<sup>17</sup>. Recent measurements by O'Reilly<sup>9</sup> gave  $D = 3.3 \times 10^{-5}$  cm<sup>2</sup>/sec at 300 °K, and  $D = 0.50 \times 10^{-5}$  cm<sup>2</sup>/sec at 200 °K, with  $\Delta E_D = 2.2$  kcal/mole. The discrepancy between  $\Delta E_D$  and  $\Delta E_{\text{tr}}$ , confirmed by the work of others<sup>6,9</sup>, appears to be real, and raises a question about the adequacy of the theory of relaxation by intermolecular dipolar interaction.

The results of Bonera and Rigamonti<sup>1</sup> on benzene are also given in Table I, since they allow similar comparisons to be made for that liquid. It is seen that  $\Delta E_D = \Delta E_{\text{tr}}/T$ , in agreement with the Stokes-Einstein relation. Again,  $\Delta E_{\text{rot}}$  is much smaller than  $\Delta E_D$ , as appears to be the case for all but the most highly associated liquids. As in chloroform,  $\Delta E_{\text{tr}}$  appears to be significantly smaller than  $\Delta E_D$ . Taking into account the temperature dependence of  $N$  in Equation (13c) only increases this discrepancy. It has been suggested that the difference between these two activation energies may be due to modulation of the intermolecular dipolar interaction by molecular rotations as well as by translations<sup>1</sup>.

TABLE I

ACTIVATION ENERGIES FOR RELAXATION, ROTATION, TRANSLATION,  
SELF-DIFFUSION, AND VISCOSITY IN BENZENE AND CHLOROFORM

Molecule	$\Delta E_{rel}$ (kcal/mole)	$\Delta E_{rot}$ (kcal/mole)	$\Delta E_{tr}$ (kcal/mole)	$\Delta E_D$ (kcal/mole)	$\Delta E_{\eta/T}$ (kcal/mole)
$\text{CHCl}_3$	$1.76 \pm 0.05$	$1.5 \pm 0.1$	$1.76 \pm 0.05$	$2.1 \pm 0.2^b$	$2.3 \pm 0.1^a$
$\text{C}_6\text{H}_6$	$1.9 \pm 0.2^c$	$1.2 \pm 0.3^c$	$2.5 \pm 0.2^c$	$3.1 \pm 0.2^d$	$3.1 \pm 0.1^a$

<sup>a</sup>E. W. Washburn, ed., International Critical Tables (McGraw-Hill Book Co., New York, 1926).

<sup>b</sup>At 25 °C  $10^5 D = 2.5 \pm 0.1 \text{ cm}^2/\text{sec}$ .

<sup>c</sup>G. Bonera and A. Rigamonti, *J. Chem. Phys.* 42, 171 (1965).

<sup>d</sup>R. Hausser, G. Maier, and F. Noack, *Z. Naturforsch.*, 21a, 1410 (1966).

This seems reasonable for a molecule like  $\text{CHCl}_3$ , in which the proton is not at the center of a molecule of spherical symmetry, and would lead to an activation energy  $\Delta E_{\text{inter}} < \Delta E_{\text{D}}$ . However, since  $\tau_{\text{rot}}$  is so short, it is unlikely that such a mechanism could account satisfactorily for the observed relaxation rate.

#### FOOTNOTES

- <sup>1</sup>G. Bonera and A. Rigamonti, *J. Chem. Phys.*, 42, 171 (1965).
- <sup>2</sup>N. Bloembergen, E. M. Purcell, and R. V. Pound, *Phys. Rev.*, 73, 679 (1948).
- <sup>3</sup>J. M. Winter, *Compt. Rend.*, 249, 1346 (1959).
- <sup>4</sup>H. Ottavi, *Compt. Rend.*, 252, 1439 (1961).
- <sup>5</sup>H. Benoit, J. Hennequin, and H. Ottavi, *Chim. Anal. (Paris)*, 44, 471 (1962).
- <sup>6</sup>J. Blicharski, J. W. Hennel, K. Krynicki, J. Mikulski, T. Waluga, and G. Zapalski, *Arch. Sci. (Geneva)* 13, 452 (1960).
- <sup>7</sup>D. E. O'Reilly and G. E. Schacher, *J. Chem. Phys.*, 39, 1768 (1963).
- <sup>8</sup>W. B. Moniz, W. A. Steele, and J. A. Dixon, *J. Chem. Phys.*, 38, 2418 (1963).
- <sup>9</sup>D. E. O'Reilly, *J. Chem. Phys.*, 49, 5416 (1968).
- <sup>10</sup>R. Kubo and K. Tomita, *J. Phys. Soc. Japan*, 9, 888 (1954).
- <sup>11</sup>H. S. Gutowsky and D. E. Woessner, *Phys. Rev.*, 104, 843 (1956).
- <sup>12</sup>P. Arthur, *Anal. Chem.*, 36, 701 (1964).
- <sup>13</sup>H. Y. Carr and E. M. Purcell, *Phys. Rev.*, 94, 630 (1954).
- <sup>14</sup>D. W. McCall, D. C. Douglass, and E. W. Anderson, *J. Chem. Phys.*, 31, 1555 (1959).
- <sup>15</sup>A. Abragam, *The Principles of Nuclear Magnetism* (Oxford University Press, London, 1961), p. 332.

- <sup>16</sup>G. B. Benedek and E. M. Purcell, J. Chem. Phys., 22, 2003 (1954).
- <sup>17</sup>D. W. McCall and D. C. Douglass, J. Phys. Chem., 71, 987 (1967).
- <sup>18</sup>V. L. Pollak, private communication.

## CHAPTER VI

### PROTON SPIN RELAXATION AND EXCHANGE PROPERTIES OF HYDRATED CHROMIC IONS IN $H_2O$ AND $H_2O-D_2O$ MIXTURES

#### Introduction

Although the basic mechanism for proton spin relaxation in aqueous chromium (III) solutions is well understood<sup>1</sup>, relaxation times reported by different observers for apparently identical systems do not agree<sup>2-7</sup>. Thermal hysteresis<sup>3,6</sup>, solution aging<sup>2</sup>, specific anion effects<sup>7</sup>, and pH dependence<sup>8,9,10</sup> have all been noted. Some of these effects appear to be a result of the unusual features of chromium (III) chemistry. In aqueous solution  $Cr^{3+}$  hydrolyzes readily, forming  $CrOH^{2+}$  and higher hydrolysis products, which have been shown<sup>8</sup> to have a pronounced effect on proton relaxation times in the solution. Chromium (III) also forms stable coordination compounds with a large number of other ligands, and at high temperatures long-lasting hydrolytic polymers are easily formed<sup>11</sup>. Once formed, these polymers break down very slowly, even in highly acid media, giving rise to the thermal hysteresis effects which have been reported<sup>6</sup>.

Chromium is one, among several paramagnetic ions, in which the lifetime for protons in the primary hydration sphere at low temperatures is relatively long, so that the observed relaxation rate of the solution is limited by the rate of proton exchange between the hydration sphere of



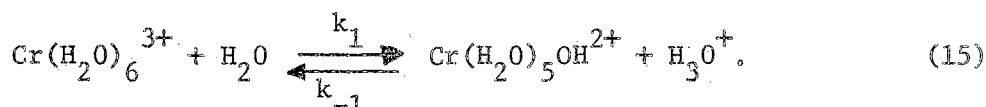
the ion and the bulk water. At high temperatures exchange is fast, and the solution relaxation rate is limited by the rate of relaxation in the ion hydration sphere. The observed proton relaxation time in a solution containing only  $\text{Cr}(\text{H}_2\text{O})_6^{3+}$  is given by the expression

$$(T_1^{\text{obs}})^{-1} = (T_{1w}^{\text{o}})^{-1} + (T_{1w}^{\text{s}})^{-1} + p(T_{1x} + \tau_{xw})^{-1} \quad (14)$$

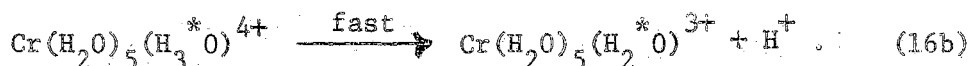
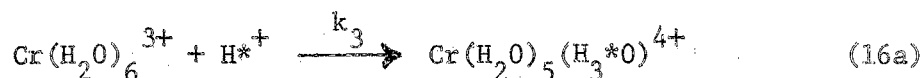
where the subscripts x and w refer to water of hydration in  $\text{Cr}(\text{H}_2\text{O})_6^{3+}$  and bulk water respectively. The quantity  $T_{1w}^{\text{s}}$  is the proton relaxation time in the bulk water due to dipolar interaction with the  $\text{Cr}^{3+}$  spins, and  $T_{1w}^{\text{o}}$  is the relaxation time due to other mechanisms in the solvent.

The latter quantity can be equated to the relaxation time in the solvent not containing paramagnetic ions, but otherwise under conditions identical to those of the studied solution. The time  $\tau_{xw}$  is the average lifetime of a proton in the hydration sphere of  $\text{Cr}(\text{H}_2\text{O})_6^{3+}$ , and p is the probability of finding a particular proton in  $\text{Cr}(\text{H}_2\text{O})_6^{3+}$ . A relation similar to Equation (14) is assumed to hold for  $T_2^{\text{obs}}$ , although in general there will also be transverse relaxation by the so-called "Δω-effect"<sup>12</sup>. However, on the basis of the parameters derived herein, one can show that this relaxation mechanism is negligible in the case of  $\text{Cr}(\text{H}_2\text{O})_6^{3+}$  solutions up to 14 kG, which was the highest field studied. A more general expression for  $T_1^{\text{obs}}$ , valid for solutions containing  $\text{Cr}(\text{H}_2\text{O})_5\text{OH}^{2+}$  in addition to  $\text{Cr}(\text{H}_2\text{O})_6^{3+}$ , is given in Appendix B. Also reproduced there are theoretical expressions for  $T_{1x}$  and  $T_{1w}^{\text{s}}$  which will be used later in interpreting the experimental data.

Protons in  $\text{Cr}(\text{H}_2\text{O})_6^{3+}$  are known to exchange with the bulk water by transfer across hydrogen bonds rather than by exchange of whole water molecules. The latter have hydration lifetimes of the order of hours<sup>13</sup>. In intermediate acid concentrations the dominant exchange mechanism is believed to be the first acid hydrolysis reaction<sup>8,14</sup>



In highly acidified solutions there is an additional acid-catalyzed proton exchange reaction<sup>9,10</sup>, which is believed to occur via the mechanism



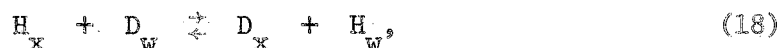
Reaction (16a) involves the protonation of one of the six coordinated water molecules of  $\text{Cr}(\text{H}_2\text{O})_6^{3+}$ , forming a coordinated  $\text{H}_3\text{O}^+$  in which the three protons are equivalent. This is assumed to be the rate determining step of the acid-catalyzed proton exchange reaction, and is followed by a rapid deprotonation with a probability of 2/3 that the proton transferred is not the proton originally accepted by the ion. In weakly acidified or non-acidified solutions complications arise due to formation of  $\text{Cr}(\text{H}_2\text{O})_5\text{OH}^{2+}$ , which is believed to have a pronounced effect on the observed relaxation rate due to its rapid rate of proton exchange with the bulk water<sup>8</sup>.

The effects of isotopic substitution of deuterons on the proton

relaxation times in aqueous solutions of  $\text{Cr}(\text{NO}_3)_3$  have been studied by Mazitov<sup>15</sup>. The observed increase in the proton relaxation times with deuteration was interpreted on the basis of an increase in the lifetime of protons in the primary hydration sphere of  $\text{Cr}^{3+}$ . It has been recently suggested that changes in proton relaxation times as the solvent is changed from  $\text{H}_2\text{O}$  to  $\text{D}_2\text{O}$  can also be expected on the basis of a change in the probability of finding a proton in the ion hydration sphere<sup>16</sup>. This arises due to the difference in vibrational zero-point energies of protons and deuterons, which can give rise to a proton fraction in the hydration sphere which differs from that in the bulk. In this case the observed relaxation time would be given by the equation

$$(T_1^{\text{obs}})^{-1} = (T_{1w}^{\text{o}})^{-1} + (T_{1w}^{\text{s}})^{-1} + p(T_{1x} + \tau_{xw})^{-1} [(1-K)\beta + K]^{-1} \quad (17)$$

where  $\beta$  is the fraction of protons in the solution. The constant  $K$  is the equilibrium constant for the exchange reaction



where  $K$  is assumed to be independent of  $\beta$ . Its temperature dependence is given by the relation  $K = \exp(\Delta S^\circ/R) \exp(-\Delta H^\circ/RT)$ , where  $\Delta S^\circ$  and  $\Delta H^\circ$  are the differences in entropy and enthalpy between the products and reactants in their standard states. Although not stated explicitly in the derivation in reference 16, Equation (17) holds only if the concentrations of the species  $\text{AH}_m\text{D}_{n-m}$ , where  $m = 0, 1, 2, \dots, n$ , are related by statistical factors alone<sup>17</sup>. This is a very good approximation for solvent water and should be expected to hold for coordinated water as well. This theory was in partial agreement with published experimental results,

but definitive conclusions were not possible on the basis of available data.

In the present study, measurements of the field and temperature dependence of proton spin relaxation times were undertaken on a 0.10 M  $\text{HClO}_4$  solution of  $\text{Cr}(\text{NO}_3)_3$  for the purpose of determining the rate constants of Reaction (15) and the relaxation parameters of the hexaquo species  $\text{Cr}(\text{H}_2\text{O})_6^{3+}$ . Proton spin relaxation times were measured in solutions containing up to 8.0 M  $\text{HClO}_4$  in order to determine the rate constant  $k_3$  of Reaction (16a). Measurements were made as a function of mole fraction of  $\text{D}_2\text{O}$  in order to determine the quantity  $K$  in Equation (17) and to study the effect of deuteration on the other parameters influencing proton spin relaxation. Measurements were also made on weakly acidified solutions of  $\text{H}_2\text{O}$  which contained appreciable quantities of the first hydrolysis product  $\text{Cr}(\text{H}_2\text{O})_5\text{OH}^{2+}$ . Its relaxation and exchange properties were examined and compared with those for  $\text{Cr}(\text{H}_2\text{O})_6^{3+}$ .

### Experimental

Measurements of proton  $T_1$  in the range from 1.1 to 520 gauss were made using the earth's field free precession technique. Measurements at 14 kG (60 MHz) were made using standard spin-echo NMR techniques<sup>18,19</sup>.

The sample temperature was controlled, in the earth's field technique, by pumping heated or cooled water around the sealed glass sample bottle. The tempering liquid was doped with  $\text{Mn}^{2+}$  ions so as to suppress its contribution to the NMR signal. At 14 kG the sample temperature was controlled by a regulated gas flow cryostat. Temperature stability

was approximately  $\pm 0.5$  C<sup>o</sup> with both systems.

The chromium solutions were prepared from reagent grade  $\text{Cr}(\text{NO}_3)_3$  and were acidified with  $\text{HClO}_4$ . All were prepared by dilution of the same master solution, which was 0.10 M in  $\text{HClO}_4$ . No measurable change could be detected between a freshly prepared master solution and one stored for over a year at room temperature.

Values of the viscosity of  $\text{H}_2\text{O}$  used in calculating rotational correlation times were taken from standard tables<sup>20</sup>; those for  $\text{D}_2\text{O}$  were calculated from  $\eta(\text{D}_2\text{O})/\eta(\text{H}_2\text{O})$  ratios taken from the data of Hardy and Cottingham<sup>21</sup> and Lewis and MacDonald<sup>22</sup>. Viscosities for mixtures of  $\text{H}_2\text{O}$  and  $\text{D}_2\text{O}$  were estimated by assuming a linear variation of viscosity with proton fraction<sup>22</sup>. For the calculation of  $T_{1w}^s$ , self-diffusion coefficients for  $\text{H}_2\text{O}$  were taken from the data of Simpson and Carr<sup>23</sup>. Self-diffusion coefficients for  $\text{Cr}^{3+}$  do not appear to have been measured and were approximated by the values for  $\text{La}^{3+}$ , which were calculated from conductivity data using the Nernst equation<sup>24</sup>. Errors introduced by this approximation are not serious since diffusion coefficients for the ions are less than 25% of those for water, and only the sum appears in the calculations. Self-diffusion coefficients for protons in mixtures of  $\text{H}_2\text{O}$  and  $\text{D}_2\text{O}$  have been measured by Douglass and McCall<sup>25</sup> at 25 C<sup>o</sup>. Values at other temperatures were calculated using the Stokes-Einstein equation

$$D(\beta, T) = kT/6\pi r(\beta) \eta(\beta, T).$$

Values of  $\eta(\beta, T)$  were known experimentally, and the  $\beta$ -dependence of the

Stokes-Einstein radius  $r$  could be calculated from the known variation of  $D$  and  $\eta$  with proton fraction at 25 °C. Self-diffusion coefficients for  $\text{Cr}^{3+}$  in deuterated solutions were calculated from the Stokes-Einstein equation by assuming that the ratios  $r(\beta)/r(\beta=1)$  were the same for  $\text{Cr}^{3+}$  as for  $\text{H}_2\text{O}$ .

## Results and Discussion

### Solutions of Moderate Acidity

The experimental field and temperature results for chromic ions in 0.10 M perchloric acid solution of water are shown in Figures 17-19. The observed proton relaxation times in the solution have been corrected for relaxation in water not containing paramagnetic ions using the relation

$$(T_1^{\text{cor}})^{-1} = (T_1^{\text{obs}})^{-1} - (T_{1w}^{\text{o}})^{-1} \quad (19)$$

with a similar definition for  $T_2^{\text{cor}}$ . According to Equation (14),  $pT_1^{\text{cor}}$  should be independent of the concentration of paramagnetic ions, which was indeed found to be the case.

The experimental curves can be accounted for satisfactorily by using Equation (14) along with the standard theoretical expressions for  $T_{1x}$  and  $T_{1w}^s$  which are given in Appendix B. In all, the equations contain five unknown quantities which are to be determined by fitting the theoretical expressions to the experimental data. They are the proton lifetime  $\tau_{xw}$ , the rotational correlation time  $\tau_r$  of the  $\text{Cr}(\text{H}_2\text{O})_6^{3+}$  complex, the correlation time for electron relaxation  $\tau_v$ , the scalar coupling constant  $A$ , and the constant  $C$  appearing in the Bloembergen-

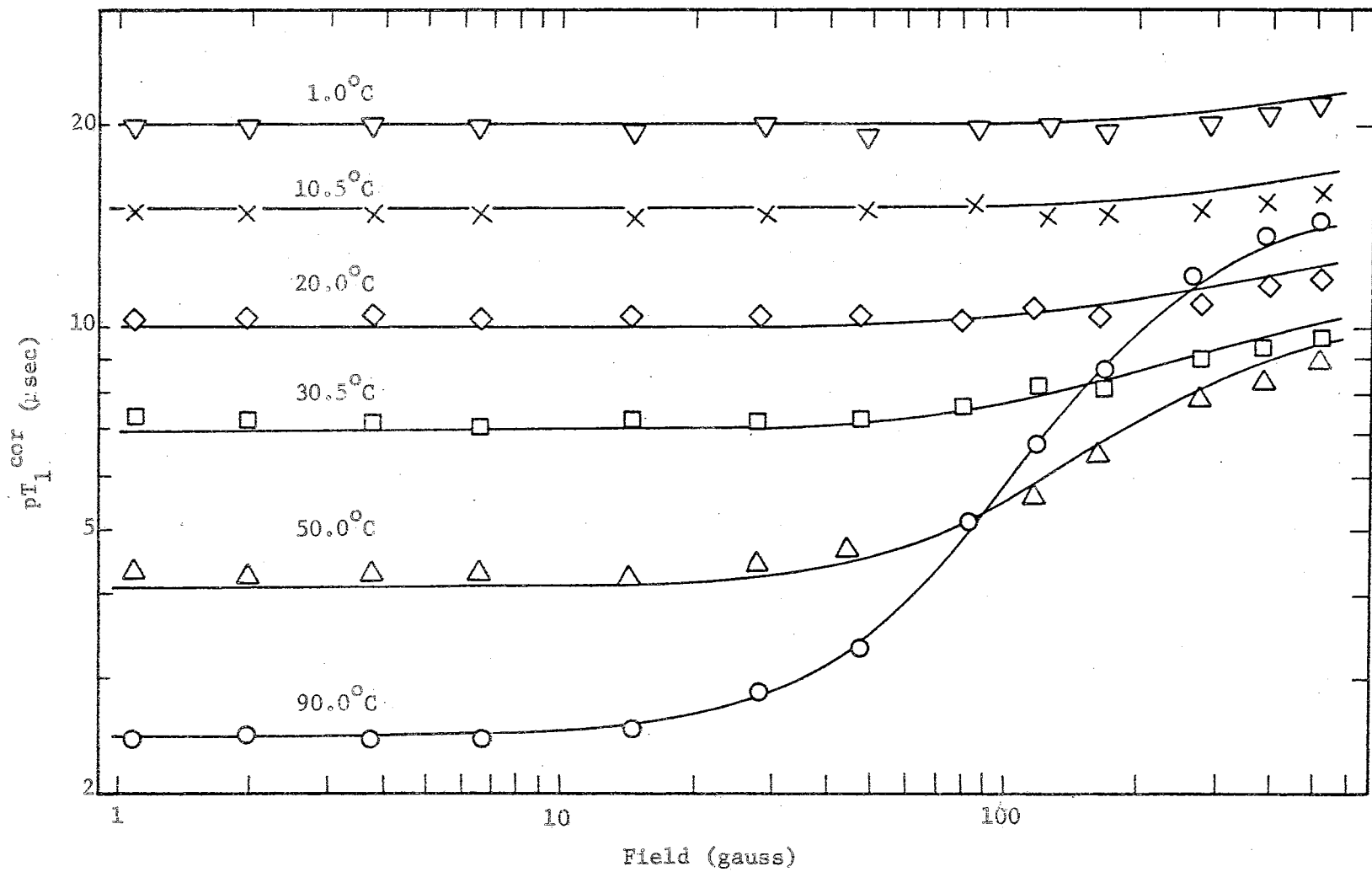


Figure 17: Field Dependence of  $pT_1^{cor}$  in 0.10 M  $HClO_4$  Solutions of  $Cr(NO_3)_3$

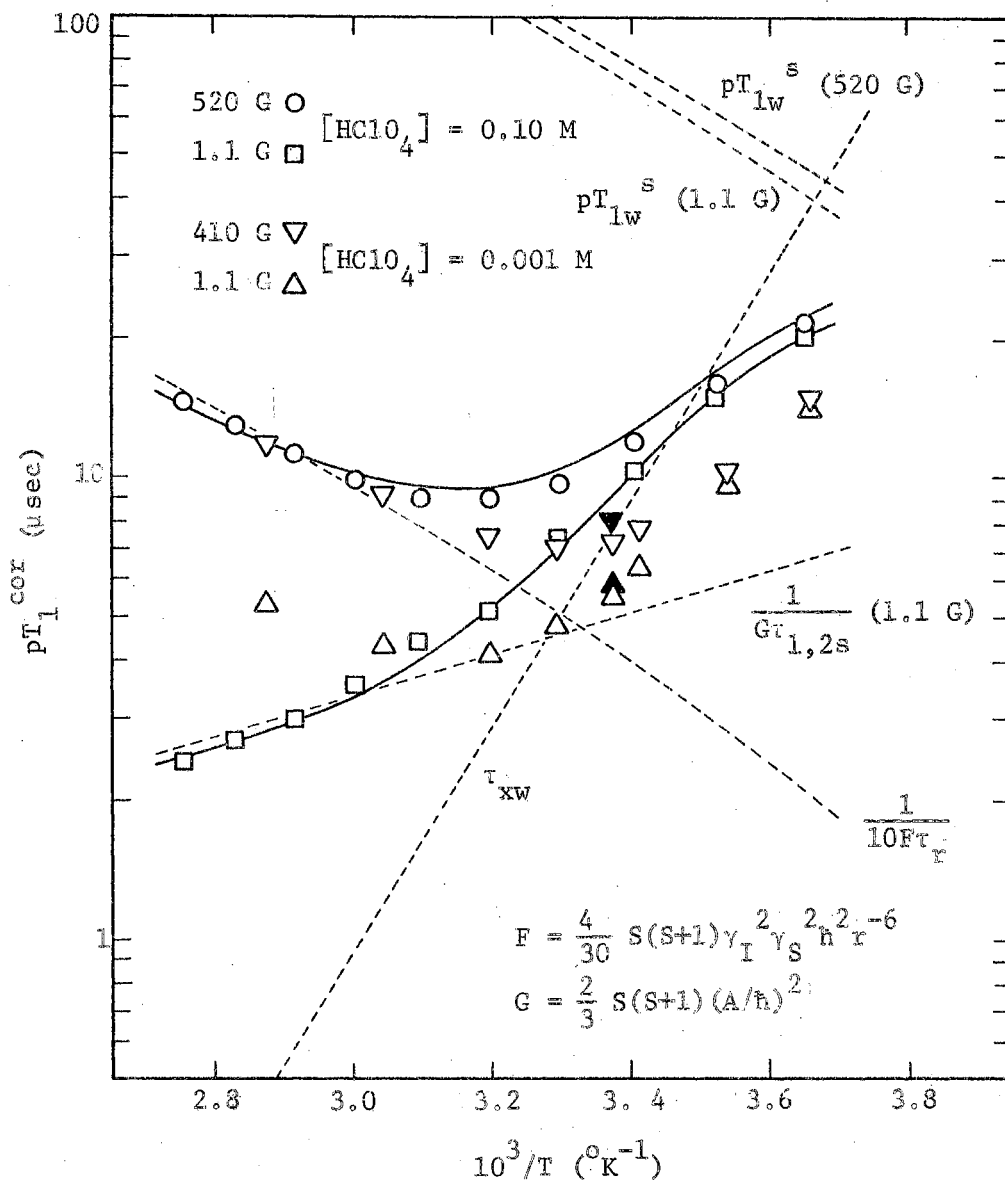


Figure 18. Temperature Dependence of  $pT_1^{\text{cor}}$  at Various Fields and Acid Concentrations. The Values  $\blacktriangle$  and  $\blacktriangledown$  were Measured After the Weakly Acidified Solution Had Been Heated to  $75^\circ\text{C}$ .  $[\text{Cr}(\text{NO}_3)_3] = 3.0 \times 10^{-4} \text{ M}$



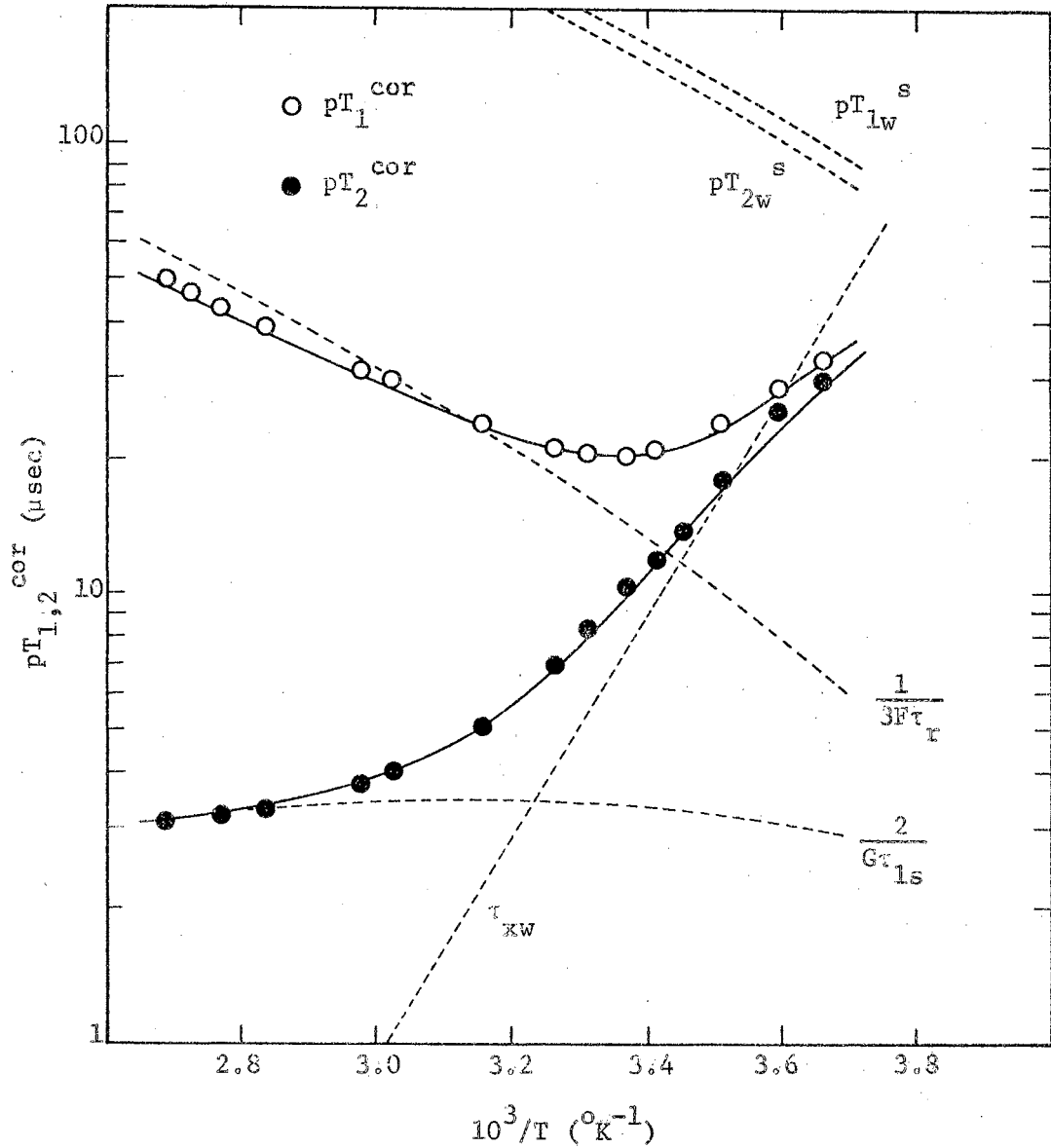


Figure 19. Temperature Dependence of  $pT_1^{cor}$  and  $pT_2^{cor}$  at 14 kG in 0.10 M  $\text{HClO}_4$  Solutions of  $\text{Cr}(\text{NO}_3)_3$

Morgan equation for  $\tau_{1s}$ , which is related to the asymmetry of the crystalline field around a  $\text{Cr}^{3+}$  ion. The value  $r = 2.74 \text{ \AA}$  obtained by Hausser and Noack<sup>7</sup> was used for the ion-proton distance in  $\text{Cr}(\text{H}_2\text{O})_6^{3+}$ . The same value was used for the closest distance of approach of a proton in the bulk to the ion spin since larger values gave slightly poorer fits to the data.

According to the Debye model<sup>26</sup>, the temperature dependence of the rotational correlation time can be computed from the expression

$$\tau_r = 4\pi\eta a^3/3kT \quad (20)$$

where  $\eta$  is the bulk viscosity of the solution at temperature  $T$ , and  $a$  is the radius of the coordinated paramagnetic ion. Exponential temperature dependences of the forms  $\tau_{xw} = \tau_{xw}^0 \exp(V_{xw}/RT)$  and  $\tau_v = \tau_v^0 \exp(V_v/RT)$  were assumed for  $\tau_{xw}$  and  $\tau_v$ . The solid curves through the data points in Figures 17-19 represent least squares fits of the theoretical equations to the experimental data, using as adjustable parameters the unknown quantities  $\tau_{xw}^0$ ,  $V_{xw}$ ,  $\tau_v^0$ ,  $V_v$ ,  $a$ ,  $C$ , and  $A$ . The non-linear least squares curve fitting procedure is outlined in Appendix A. All the parameters are determined unambiguously from the combination of field and temperature results and are presented in Table II. The remaining curves in Figures 18 and 19 result from the least squares curve fits and may be used to synthesize all the experimental data.

At low fields where  $\omega_s^2 \tau_v^2 \ll 1$ ,  $\tau_{1s}^{-1} = \tau_{2s}^{-1} = 5C\tau_v$  from Equation (B-5) of Appendix B. The slope of the line  $(G\tau_{1,2s})^{-1}$  in Figure 18 gives an activation energy for  $\tau_v$  of 2.1 kcal/mole. This compares

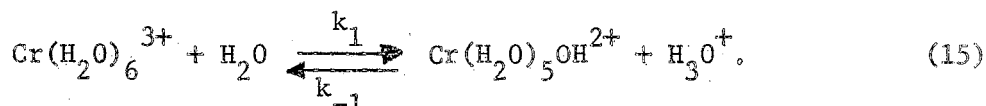
the ion and the bulk water. At high temperatures exchange is fast, and the solution relaxation rate is limited by the rate of relaxation in the ion hydration sphere. The observed proton relaxation time in a solution containing only  $\text{Cr}(\text{H}_2\text{O})_6^{3+}$  is given by the expression

$$(T_1^{\text{obs}})^{-1} = (T_{1w}^{\text{o}})^{-1} + (T_{1w}^{\text{s}})^{-1} + p(T_{1x} + \tau_{xw})^{-1} \quad (14)$$

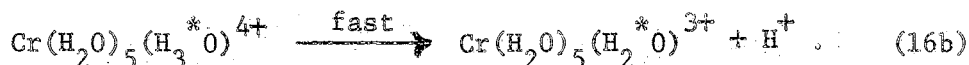
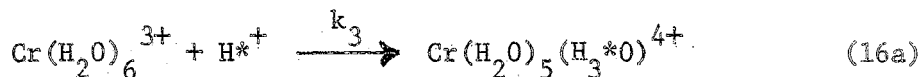
where the subscripts x and w refer to water of hydration in  $\text{Cr}(\text{H}_2\text{O})_6^{3+}$  and bulk water respectively. The quantity  $T_{1w}^{\text{s}}$  is the proton relaxation time in the bulk water due to dipolar interaction with the  $\text{Cr}^{3+}$  spins, and  $T_{1w}^{\text{o}}$  is the relaxation time due to other mechanisms in the solvent.

The latter quantity can be equated to the relaxation time in the solvent not containing paramagnetic ions, but otherwise under conditions identical to those of the studied solution. The time  $\tau_{xw}$  is the average lifetime of a proton in the hydration sphere of  $\text{Cr}(\text{H}_2\text{O})_6^{3+}$ , and p is the probability of finding a particular proton in  $\text{Cr}(\text{H}_2\text{O})_6^{3+}$ . A relation similar to Equation (14) is assumed to hold for  $T_2^{\text{obs}}$ , although in general there will also be transverse relaxation by the so-called " $\Delta\omega$ -effect"<sup>12</sup>. However, on the basis of the parameters derived herein, one can show that this relaxation mechanism is negligible in the case of  $\text{Cr}(\text{H}_2\text{O})_6^{3+}$  solutions up to 14 kG, which was the highest field studied. A more general expression for  $T_1^{\text{obs}}$ , valid for solutions containing  $\text{Cr}(\text{H}_2\text{O})_5\text{OH}^{2+}$  in addition to  $\text{Cr}(\text{H}_2\text{O})_6^{3+}$ , is given in Appendix B. Also reproduced there are theoretical expressions for  $T_{1x}$  and  $T_{1w}^{\text{s}}$  which will be used later in interpreting the experimental data.

Protons in  $\text{Cr}(\text{H}_2\text{O})_6^{3+}$  are known to exchange with the bulk water by transfer across hydrogen bonds rather than by exchange of whole water molecules. The latter have hydration lifetimes of the order of hours<sup>13</sup>. In intermediate acid concentrations the dominant exchange mechanism is believed to be the first acid hydrolysis reaction<sup>8,14</sup>



In highly acidified solutions there is an additional acid-catalyzed proton exchange reaction<sup>9,10</sup>, which is believed to occur via the mechanism



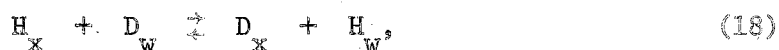
Reaction (16a) involves the protonation of one of the six coordinated water molecules of  $\text{Cr}(\text{H}_2\text{O})_6^{3+}$ , forming a coordinated  $\text{H}_3\text{O}^+$  in which the three protons are equivalent. This is assumed to be the rate determining step of the acid-catalyzed proton exchange reaction, and is followed by a rapid deprotonation with a probability of 2/3 that the proton transferred is not the proton originally accepted by the ion. In weakly acidified or non-acidified solutions complications arise due to formation of  $\text{Cr}(\text{H}_2\text{O})_5\text{OH}^{2+}$ , which is believed to have a pronounced effect on the observed relaxation rate due to its rapid rate of proton exchange with the bulk water<sup>8</sup>.

The effects of isotopic substitution of deuterons on the proton

relaxation times in aqueous solutions of  $\text{Cr}(\text{NO}_3)_3$  have been studied by Mazitov<sup>15</sup>. The observed increase in the proton relaxation times with deuteration was interpreted on the basis of an increase in the lifetime of protons in the primary hydration sphere of  $\text{Cr}^{3+}$ . It has been recently suggested that changes in proton relaxation times as the solvent is changed from  $\text{H}_2\text{O}$  to  $\text{D}_2\text{O}$  can also be expected on the basis of a change in the probability of finding a proton in the ion hydration sphere<sup>16</sup>. This arises due to the difference in vibrational zero-point energies of protons and deuterons, which can give rise to a proton fraction in the hydration sphere which differs from that in the bulk. In this case the observed relaxation time would be given by the equation

$$(\tau_1^{\text{obs}})^{-1} = (\tau_{1w}^{\text{c}})^{-1} + (\tau_{1w}^{\text{s}})^{-1} + p(\tau_{1x} + \tau_{xw})^{-1} [(1-K)\beta + K]^{-1} \quad (17)$$

where  $\beta$  is the fraction of protons in the solution. The constant  $K$  is the equilibrium constant for the exchange reaction



where  $K$  is assumed to be independent of  $\beta$ . Its temperature dependence is given by the relation  $K = \exp(\Delta S^\circ/R) \exp(-\Delta H^\circ/RT)$ , where  $\Delta S^\circ$  and  $\Delta H^\circ$  are the differences in entropy and enthalpy between the products and reactants in their standard states. Although not stated explicitly in the derivation in reference 16, Equation (17) holds only if the concentrations of the species  $\text{AH}_m\text{D}_{n-m}$ , where  $m = 0, 1, 2, \dots, n$ , are related by statistical factors alone<sup>17</sup>. This is a very good approximation for solvent water and should be expected to hold for coordinated water as well. This theory was in partial agreement with published experimental results,

but definitive conclusions were not possible on the basis of available data.

In the present study, measurements of the field and temperature dependence of proton spin relaxation times were undertaken on a 0.10 M  $\text{HClO}_4$  solution of  $\text{Cr}(\text{NO}_3)_3$  for the purpose of determining the rate constants of Reaction (15) and the relaxation parameters of the hexaquo species  $\text{Cr}(\text{H}_2\text{O})_6^{3+}$ . Proton spin relaxation times were measured in solutions containing up to 8.0 M  $\text{HClO}_4$  in order to determine the rate constant  $k_3$  of Reaction (16a). Measurements were made as a function of mole fraction of  $\text{D}_2\text{O}$  in order to determine the quantity  $K$  in Equation (17) and to study the effect of deuteration on the other parameters influencing proton spin relaxation. Measurements were also made on weakly acidified solutions of  $\text{H}_2\text{O}$  which contained appreciable quantities of the first hydrolysis product  $\text{Cr}(\text{H}_2\text{O})_5\text{OH}^{2+}$ . Its relaxation and exchange properties were examined and compared with those for  $\text{Cr}(\text{H}_2\text{O})_6^{3+}$ .

### Experimental

Measurements of proton  $T_1$  in the range from 1.1 to 520 gauss were made using the earth's field free precession technique. Measurements at 14 kG (60 MHz) were made using standard spin-echo NMR techniques<sup>18,19</sup>.

The sample temperature was controlled, in the earth's field technique, by pumping heated or cooled water around the sealed glass sample bottle. The tempering liquid was doped with  $\text{Mn}^{2+}$  ions so as to suppress its contribution to the NMR signal. At 14 kG the sample temperature was controlled by a regulated gas flow cryostat. Temperature stability

was approximately  $\pm 0.5$  C<sup>o</sup> with both systems.

The chromium solutions were prepared from reagent grade  $\text{Cr}(\text{NO}_3)_3$  and were acidified with  $\text{HClO}_4$ . All were prepared by dilution of the same master solution, which was 0.10 M in  $\text{HClO}_4$ . No measurable change could be detected between a freshly prepared master solution and one stored for over a year at room temperature.

Values of the viscosity of  $\text{H}_2\text{O}$  used in calculating rotational correlation times were taken from standard tables<sup>20</sup>; those for  $\text{D}_2\text{O}$  were calculated from  $\eta(\text{D}_2\text{O})/\eta(\text{H}_2\text{O})$  ratios taken from the data of Hardy and Cottrington<sup>21</sup> and Lewis and MacDonald<sup>22</sup>. Viscosities for mixtures of  $\text{H}_2\text{O}$  and  $\text{D}_2\text{O}$  were estimated by assuming a linear variation of viscosity with proton fraction<sup>22</sup>. For the calculation of  $T_{1w}^s$ , self-diffusion coefficients for  $\text{H}_2\text{O}$  were taken from the data of Simpson and Carr<sup>23</sup>. Self-diffusion coefficients for  $\text{Cr}^{3+}$  do not appear to have been measured and were approximated by the values for  $\text{La}^{3+}$ ,<sup>24</sup> which were calculated from conductivity data using the Nernst equation<sup>24</sup>. Errors introduced by this approximation are not serious since diffusion coefficients for the ions are less than 25% of those for water, and only the sum appears in the calculations. Self-diffusion coefficients for protons in mixtures of  $\text{H}_2\text{O}$  and  $\text{D}_2\text{O}$  have been measured by Douglass and McCall<sup>25</sup> at 25 C<sup>o</sup>. Values at other temperatures were calculated using the Stokes-Einstein equation

$$D(\beta, T) = kT/6\pi r(\beta) \eta(\beta, T).$$

Values of  $\eta(\beta, T)$  were known experimentally, and the  $\beta$ -dependence of the

Stokes-Einstein radius  $r$  could be calculated from the known variation of  $D$  and  $\eta$  with proton fraction at 25 °C. Self-diffusion coefficients for  $\text{Cr}^{3+}$  in deuterated solutions were calculated from the Stokes-Einstein equation by assuming that the ratios  $r(\beta)/r(\beta=1)$  were the same for  $\text{Cr}^{3+}$  as for  $\text{H}_2\text{O}$ .

## Results and Discussion

### Solutions of Moderate Acidity

The experimental field and temperature results for chromic ions in 0.10 M perchloric acid solution of water are shown in Figures 17-19. The observed proton relaxation times in the solution have been corrected for relaxation in water not containing paramagnetic ions using the relation

$$(T_1^{\text{cor}})^{-1} \equiv (T_1^{\text{obs}})^{-1} - (T_{1w}^{\text{o}})^{-1} \quad (19)$$

with a similar definition for  $T_2^{\text{cor}}$ . According to Equation (14),  $\rho T_1^{\text{cor}}$  should be independent of the concentration of paramagnetic ions, which was indeed found to be the case.

The experimental curves can be accounted for satisfactorily by using Equation (14) along with the standard theoretical expressions for  $T_{1x}$  and  $T_{1w}^{\text{s}}$  which are given in Appendix B. In all, the equations contain five unknown quantities which are to be determined by fitting the theoretical expressions to the experimental data. They are the proton lifetime  $\tau_{\text{xw}}$ , the rotational correlation time  $\tau_r$  of the  $\text{Cr}(\text{H}_2\text{O})_6^{3+}$  complex, the correlation time for electron relaxation  $\tau_v$ , the scalar coupling constant  $A$ , and the constant  $C$  appearing in the Bloembergen-



This seems reasonable for a molecule like  $\text{CHCl}_3$ , in which the proton is not at the center of a molecule of spherical symmetry, and would lead to an activation energy  $\Delta E_{\text{inter}} < \Delta E_{\text{D}}$ . However, since  $\tau_{\text{rot}}$  is so short, it is unlikely that such a mechanism could account satisfactorily for the observed relaxation rate.

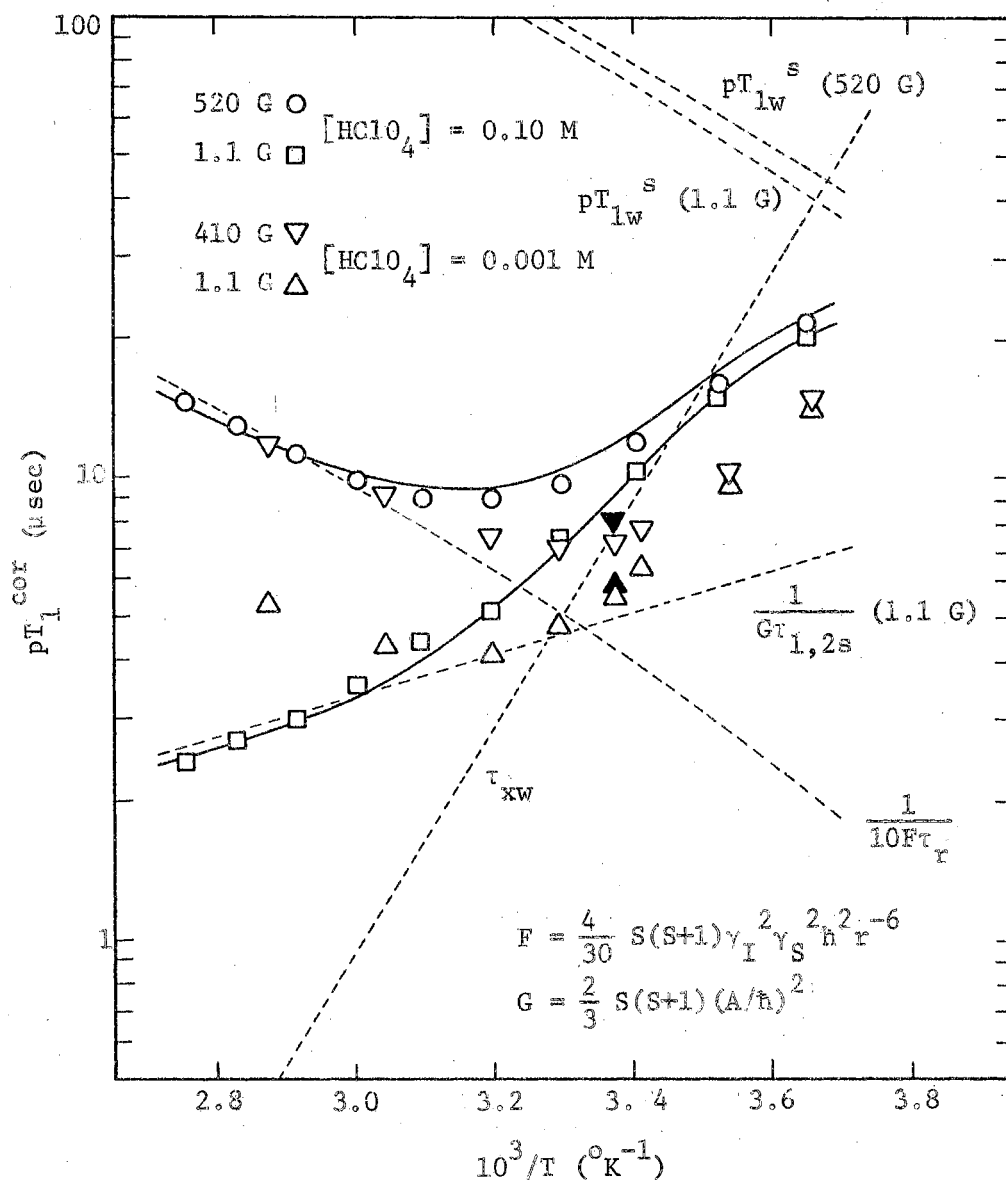


Figure 18. Temperature Dependence of  $pT_1^{cor}$  at Various Fields and Acid Concentrations. The Values ▲ and ▼ were Measured After the Weakly Acidified Solution Had Been Heated to  $75^\circ C$ .  $[Cr(NO_3)_3] = 3.0 \times 10^{-4} M$

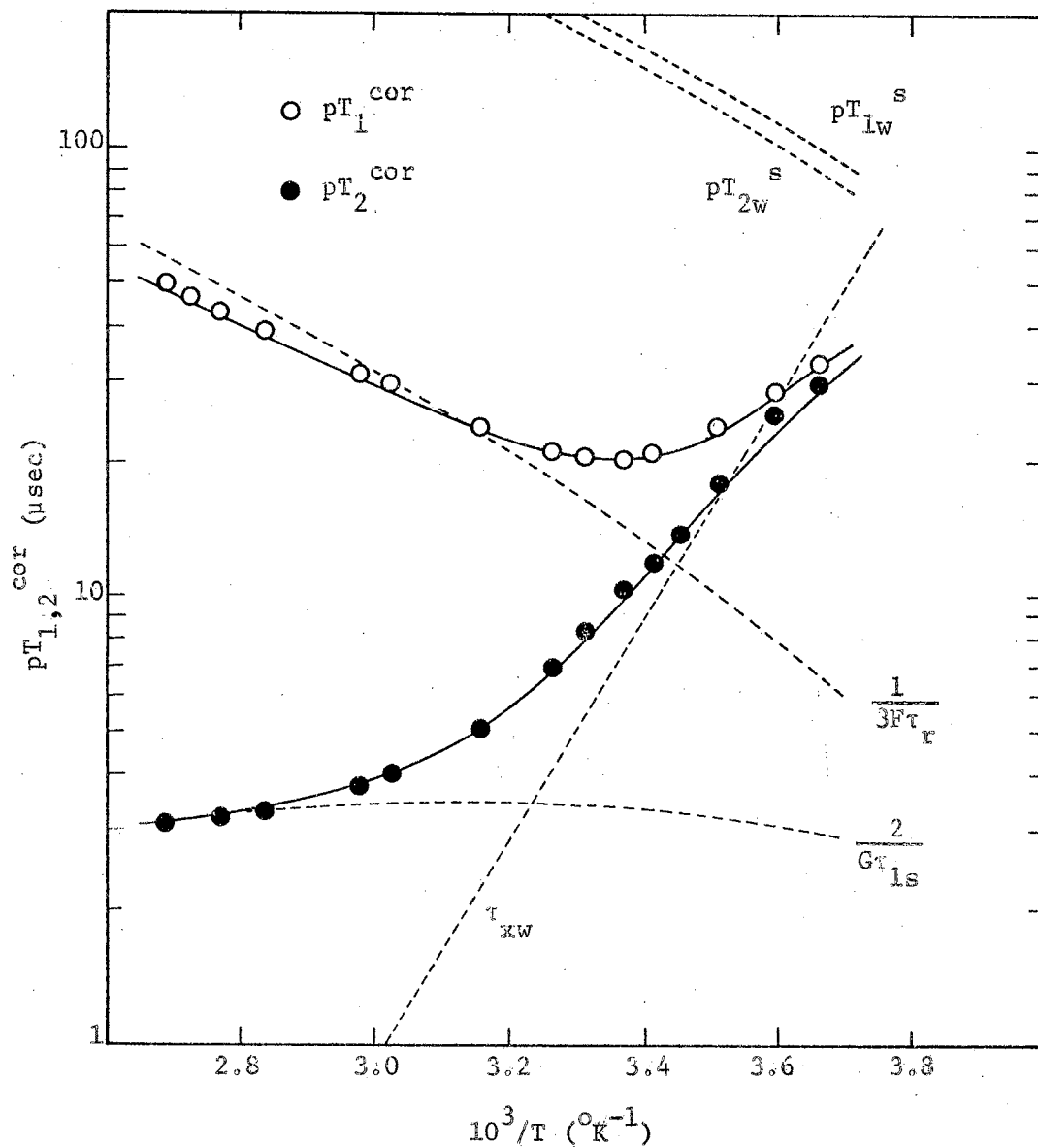


Figure 19. Temperature Dependence of  $pT_1^{cor}$  and  $pT_2^{cor}$  at 14 kG in 0.10 M  $HClO_4$  Solutions of  $Cr(NO_3)_3$

Morgan equation for  $\tau_{1s}$ , which is related to the asymmetry of the crystalline field around a  $\text{Cr}^{3+}$  ion. The value  $r = 2.74 \text{ \AA}$  obtained by Hausser and Noack<sup>7</sup> was used for the ion-proton distance in  $\text{Cr}(\text{H}_2\text{O})_6^{3+}$ . The same value was used for the closest distance of approach of a proton in the bulk to the ion spin since larger values gave slightly poorer fits to the data.

According to the Debye model<sup>26</sup>, the temperature dependence of the rotational correlation time can be computed from the expression

$$\tau_r = 4\pi\eta a^3/3kT \quad (20)$$

where  $\eta$  is the bulk viscosity of the solution at temperature  $T$ , and  $a$  is the radius of the coordinated paramagnetic ion. Exponential temperature dependences of the forms  $\tau_{xw} = \tau_{xw}^0 \exp(V_{xw}/RT)$  and  $\tau_v = \tau_v^0 \exp(V_v/RT)$  were assumed for  $\tau_{xw}$  and  $\tau_v$ . The solid curves through the data points in Figures 17-19 represent least squares fits of the theoretical equations to the experimental data, using as adjustable parameters the unknown quantities  $\tau_{xw}^0$ ,  $V_{xw}$ ,  $\tau_v^0$ ,  $V_v$ ,  $a$ ,  $C$ , and  $A$ . The non-linear least squares curve fitting procedure is outlined in Appendix A. All the parameters are determined unambiguously from the combination of field and temperature results and are presented in Table II. The remaining curves in Figures 18 and 19 result from the least squares curve fits and may be used to synthesize all the experimental data.

At low fields where  $\omega_s^2 \tau_v^2 \ll 1$ ,  $\tau_{1s}^{-1} = \tau_{2s}^{-1} = 5C\tau_v$  from Equation (B-5) of Appendix B. The slope of the line  $(G\tau_{1,2s})^{-1}$  in Figure 18 gives an activation energy for  $\tau_v$  of 2.1 kcal/mole. This compares

TABLE II  
PARAMETERS OBTAINED FROM THE LEAST SQUARES FIT OF THE  
EQUATIONS IN THE TEXT TO THE DATA IN FIGURES 17-19

---

---

$$\tau_{xw} = 4.1 \times 10^{-14} \exp(11.2/RT)$$

$$\tau_v = 9.3 \times 10^{-14} \exp(2.1/RT)$$

$$a = 4.4 \text{ \AA}^{\circ}$$

$$C = 1.3 \times 10^{20} \text{ sec}^{-2}$$

$$A/h = 2.1 \text{ MHz.}$$

---

favorably with the 2.4 kcal/mole from the ESR data of Hayes<sup>27</sup>. Using the parameters in Table II one calculates  $\tau_{1,2s} = 4.3 \times 10^{-10}$  sec in low fields and at 17.5 °C, which agrees within the experimental error with the value  $\tau_{2s} = 4.7 \times 10^{-10}$  sec obtained from ESR data by Sancier and Mills<sup>28</sup> at 15-20 °C and pH = 1. In high fields where  $\omega_s^2 \tau_v^2 \gg 1$ ,  $\tau_{1s}$  increases above its low field value, which causes a decrease in  $T_{2x}$  with increasing field. The quantity  $2(G\tau_{1s})^{-1}$  at 14 kG is plotted in Figure 19 for comparison with the low field values of  $(G\tau_{1,2s})^{-1}$  in Figure 18. At 25 °C  $\tau_v = 3.3 \times 10^{-12}$  sec, as compared with  $6.2 \times 10^{-12}$  sec obtained by Hausser and Noack<sup>7</sup>. Their values may be systematically too high since they also report  $\tau_v = 5.3 \times 10^{-12}$  sec for  $Mn^{2+}$ , as compared with  $\tau_v = 2.4 \times 10^{-12}$  sec reported by Bloembergen and Morgan<sup>1</sup>.

The value of the scalar coupling constant  $A/h = 2.1$  MHz is only slightly larger than the 2.0 MHz obtained by Luz and Shulman<sup>29</sup> from measurements of proton chemical shift, and by Bloembergen and Morgan<sup>1</sup> from proton relaxation data. The value  $\underline{a} = 4.4$  Å for the radius of the coordinated  $Cr^{3+}$  ion compares favorably with a Stokes radius of 4.1 Å obtained by Nightingale<sup>30</sup>. The Debye formula gives  $\tau_r = 7.7 \times 10^{-11}$  sec at 25 °C, which agrees with the  $8 \times 10^{-11}$  sec obtained by Bloembergen and Morgan<sup>1</sup>.

As is seen by the goodness of fit of the  $T_1^{cor}$  curve at 14 kG and at high temperature (Figure 19), the Debye formula predicts quite well the temperature dependence of the rotational correlation time  $\tau_r$ . An exponential temperature dependence  $\tau_r = \tau_r^0 \exp(V_r/RT)$  could have been assumed (which gives  $V_r = 4.2$  kcal/mole), but the Debye formula gives

an equally good fit with one less adjustable parameter.

The slope of the line  $\tau_{xw}$  in Figure 18 or 19 gives the activation energy for proton exchange  $V_{xw} = 11.2$  kcal/mole. This is greater than the 10 kcal/mole reported earlier<sup>1,15</sup> since previous authors have neglected the contribution of  $T_{1w}^S$  to the observed proton relaxation time. This error is particularly serious at 0 °C and in low fields where the contributions to proton relaxation in the primary hydration sphere of  $Cr^{3+}$  and in the bulk are approximately equal. The curves in Figure 19 are remarkably similar to those for  $VO^{2+}$ ,<sup>31</sup> in which it is also necessary to take into account relaxation outside the first hydration shell.

At 25 °C the lifetime  $\tau_{xw}$  for proton exchange leads to a forward rate constant for Reaction (15) of  $k_1 = 12/\tau_{xw} = 1.7 \times 10^6$  sec<sup>-1</sup>. Using this value and the value  $K_1 = k_1/k_{-1} = 1.4 \times 10^{-4}$  for the equilibrium constant of Reaction (15)<sup>32</sup>, one calculates for the reverse rate constant  $k_{-1} = 1.2 \times 10^{10}$  mole<sup>-1</sup> sec<sup>-1</sup>. The change in enthalpy for Reaction (15) has been measured by Postmus and King<sup>32</sup> who report a value of  $9.4 \pm 0.4$  kcal/mole for  $\Delta H^0$ . Thus one finds for the activation energy of the reverse rate constant  $V_{-1} = 11.2 - 9.4 = 1.8$  kcal/mole. Both the magnitude of  $k_{-1}$  and its activation energy are consistent with a diffusion-limited recombination process<sup>33</sup>.

### Highly Acidified Solutions

Measurements of the temperature dependence of proton  $T_1$  in highly acidified solutions of  $3.0 \times 10^{-4}$  M  $Cr(NO_3)_3$  are shown in Figure 20. In

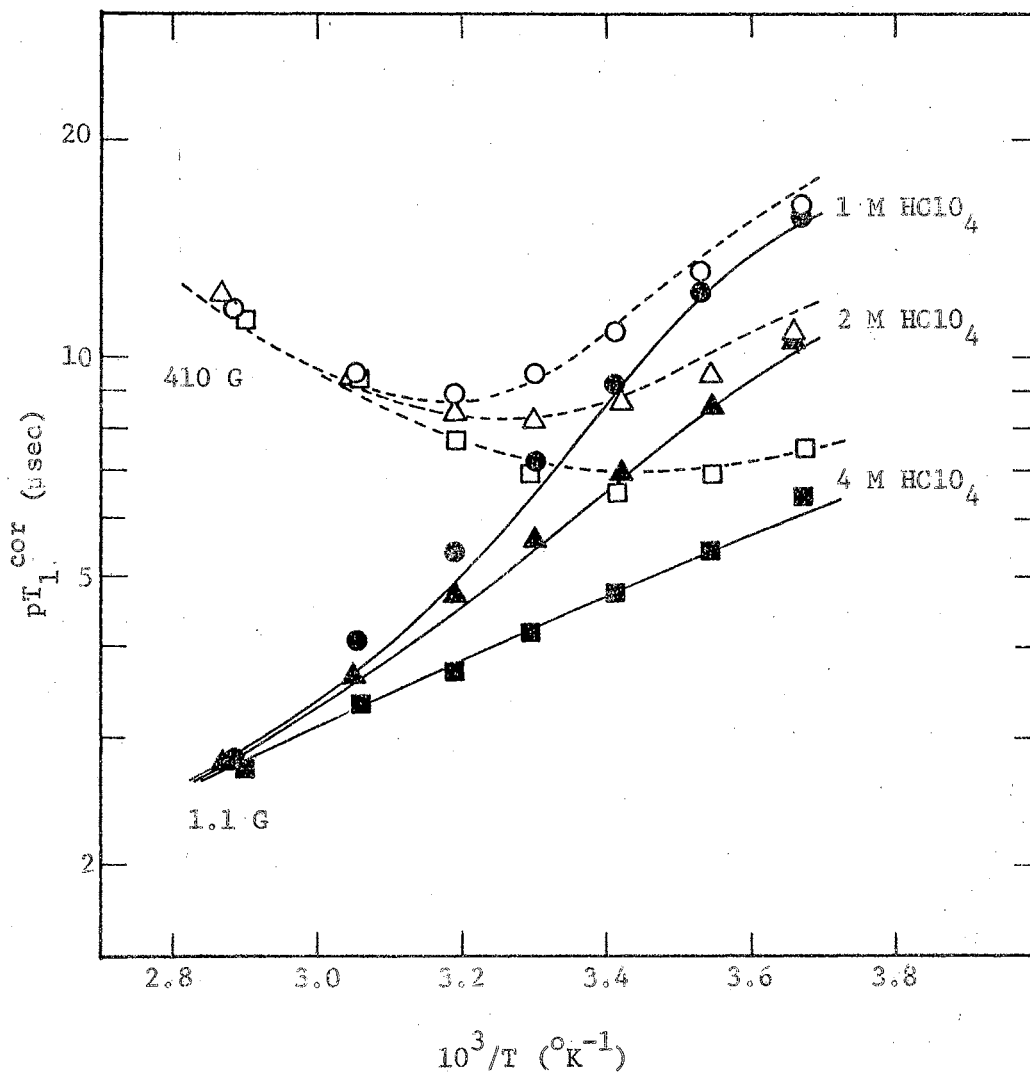


Figure 20. Temperature Dependence of  $pT_1^{cor}$  in Highly Acidified Solutions of  $\text{Cr}(\text{NO}_3)_3$



these highly acidified solutions, acid-catalyzed proton exchange between  $\text{Cr}(\text{H}_2\text{O})_6^{3+}$  and the bulk water becomes important<sup>9,10</sup>. This results in a decrease in the proton lifetime  $\tau_{xw}$  and a decrease in the observed proton relaxation times at low temperature. Acidification has no effect on  $T_{1x}$  for  $\text{Cr}(\text{H}_2\text{O})_6^{3+}$ , as evidenced by the data at high temperatures where the observed relaxation times are independent of the acid concentration up to 8.0 M  $\text{HClO}_4$ , which was the highest acid concentration studied. The results for this solution were virtually identical to those for the solution containing 4.0 M  $\text{HClO}_4$ . The fact that  $T_{1x}$  is independent of perchloric acid concentration is at odds with the results of Sancier and Mills<sup>28</sup>, who observed a decrease in spin intensity and linewidth of the ESR spectrum of  $\text{Cr}^{3+}$  in concentrated solutions of  $\text{HClO}_4$ . An increase in  $\tau_{1,2s}$  would result in a decrease in  $T_{1x}$ . (Appendix B).

The combination of the exchange processes (15) and (16) leads to the rate law

$$1/\tau_{xw} = k_1/12 + k_3 [\text{H}^+]/18. \quad (21)$$

A factor of 1/12 appears in the first term since whenever Reaction (15) occurs there is a probability of 1/12 that a particular proton originally in the hydration sphere of  $\text{Cr}(\text{H}_2\text{O})_6^{3+}$  will enter the water system.

A factor of 1/18 appears in the second term since in Reaction (16a) there is a probability of 1/6 that a particular proton will be on the water molecule which is protonated, and a probability of 1/3 that the proton in question will go into the water system in the rapid deprotonation step which follows. A more rigorous derivation, which also makes

explicit the approximations inherent in Equation (21), is given in Appendix C.

The rate constant  $k_3$  is a function of the acid concentration due to the change in ionic strength of the medium. Using absolute reaction rate theory one can write

$$k_3(H) = k_3(0) \frac{\gamma_{Cr^{3+}} \gamma_{H^+}}{\gamma_{Cr^{3+} \dots H^+}}$$

where  $k_3(H)$  is the rate constant at acid concentration  $H$ ,  $k_3(0)$  is the rate constant for infinite dilution, and  $\gamma_{Cr^{3+} \dots H^+}$  is the activity coefficient for the transition state of Reaction (16a). By assuming that  $\gamma_{Cr^{3+} \dots H^+} = \gamma_{Cr^{4+}}$  and calculating the activity coefficients using the Davies equation<sup>34</sup> one finds that  $k_3(0.1) = 4.7 k_3(0)$  for 0.1 M  $HClO_4$ , and  $k_3(1) = 8.2 k_3(0)$  for 1.0 M  $HClO_4$ . Hence, large changes in  $k_3$  with ionic strength are to be expected.

The curves in Figure 20 represent least squares fits of Equations (14) and (21) to the experimental data, assuming an exponential temperature dependence for the rate constant  $k_3$  of the form

$$k_3(H) = k_3(H)^0 \exp(-V_3/RT).$$

The activation energy  $V_3$  was assumed independent of ionic strength, which is equivalent to assuming that the activity coefficients are independent of temperature. The remaining quantities in Equations (14) and (21) were assumed to be the same as those found from fitting the 0.10 M  $HClO_4$  data in Figure 18 (Table II). The rate constant  $k_1$  was

assumed to be independent of the ionic strength<sup>10</sup> since for Reaction (15)

$$k_1 = k_1^{\circ} \frac{\gamma_{\text{Cr}^{3+}} \gamma_{\text{H}_2\text{O}}}{\gamma_{\text{Cr}^{3+} \cdot \cdot \cdot \text{H}_2\text{O}}} \approx k_1^{\circ}$$

The results of the curve fit are given in Table III.

TABLE III

RATE CONSTANTS FOR REACTION (16A) OBTAINED FROM DATA IN FIGURE 20

$\text{HClO}_4$	$\frac{1}{18} k_3$ at 0 °C	$V_3$
1.0 M	$1.8 \times 10^4 \text{ mole}^{-1} \text{ sec}^{-1}$	
2.0	$3.2 \times 10^4$	3.5 kcal/mole
4.0	$4.6 \times 10^4$	

Swift, et al.<sup>10</sup>, report a value for  $k_3$  of  $4.0 \times 10^4 \text{ mole}^{-1} \text{ sec}^{-1}$  at 10 °C in the range between 0.1 and 1.0 M  $\text{HClO}_4$ , with an activation energy near zero. Their analysis was based on the assumption that  $k_3$  was independent of ionic strength over this range and that  $\tau_{\text{xw}}$  could be approximated by  $pT_2^{\text{cor}}$  for temperatures less than 30 °C, which is a rather crude approximation, as seen from the curves in Figure 19.

#### Solutions of Low Acidity

Also shown in Figure 18 are results on a weakly acidified solution of  $\text{Cr}(\text{NO}_3)_3$  which contains, in addition to the hexahydrate  $\text{Cr}(\text{H}_2\text{O})_6^{3+}$ ,

some of the first hydrolysis product  $\text{Cr}(\text{H}_2\text{O})_5\text{OH}^{2+}$ . At low temperatures and low field (1.1 G) the effect of  $\text{CrOH}^{2+}$  is to shorten the observed relaxation time<sup>8</sup>, whereas at high temperatures the formation of  $\text{CrOH}^{2+}$  lengthens  $T_1^{\text{obs}}$ . At these high temperatures the proton lifetimes in both species are sufficiently short that the conditions  $\tau_{xw} \ll T_{1x}$  and  $\tau_{yw} \ll T_{1y}$  are fulfilled. Here the subscript y refers to the species  $\text{Cr}(\text{H}_2\text{O})_5\text{OH}^{2+}$ . Under these conditions the general expression for relaxation in the solution (Appendix B) reduces to

$$(T_1^{\text{obs}})^{-1} = (T_{1w}^{\text{o}})^{-1} + (T_{1w}^{\text{s}})^{-1} + (12x/2w)(T_{1x})^{-1} + (11y/2w)(T_{1y})^{-1} \quad (22)$$

where x and y are the molar concentrations of  $\text{Cr}^{3+}$  and  $\text{CrOH}^{2+}$  in the solution, and w is the molar concentration of solvent water. In this simple case the relaxation rate in the solution is the weighted average of the relaxation rates in the separate environments.

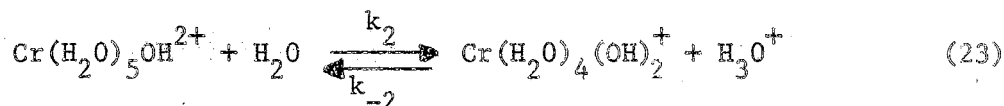
The fact that the presence of  $\text{CrOH}^{2+}$  at high temperatures lengthens  $T_1^{\text{obs}}$  at 1.1 gauss, whereas in fields greater than approximately 400 gauss there is almost no effect at all, suggests that the dipolar contribution to  $T_1$  is approximately the same for both species, but the scalar contribution is much less in  $\text{CrOH}^{2+}$  than in  $\text{Cr}^{3+}$  due to a shorter electron relaxation time  $\tau_{1,2s}$ , a smaller scalar coupling constant A, or both. In the 0.001 M  $\text{HClO}_4$  solution of  $3.0 \times 10^{-4}$  M  $\text{Cr}(\text{NO}_3)_3$  one estimates a value  $x/y = 0.46$  at 75 °C, using the value  $K_1 = 2.6 \times 10^{-3}$  for the equilibrium constant of Reaction (14). This value is for an ionic strength of  $2.4 \times 10^{-3}$  mole liter<sup>-1</sup>, and was calculated from the experi-

mental data of Postmus and King<sup>32</sup> at  $I = 0.034$  mole liter<sup>-1</sup>, using activity coefficients calculated from the Davies equation<sup>34</sup>. By using  $T_{1x} = 2.4$   $\mu$ sec and assuming that  $T_{1y}$  is identical to the dipolar contribution to  $T_{1x}$ , which is 12.2  $\mu$ sec at 75 °C (Figure 18), one calculates using Equation (22)  $pT_1^{\text{cor}} = 5.5$   $\mu$ sec at 1.1 gauss and 75 °C. This agrees well with the experimental value of 5.3  $\mu$ sec. A precise quantitative study is difficult since this solution exhibited thermal hysteresis effects similar to those observed by Brown, et al.<sup>6</sup> These effects occur at high temperatures and are attributed to the formation of polynuclear species which decompose very slowly when the sample is returned to room temperature<sup>11</sup>. However, the effect of polymerization on  $T_1$  was small compared to the effect of the presence of  $\text{CrOH}^{2+}$ , and the qualitative conclusions reached above remain unaltered.

The experimental data reported earlier<sup>8</sup> for  $(T_1^{\text{obs}})^{-1} - (T_{1w}^{\text{o}})^{-1}$  as a function of acidity of solutions of  $\text{Cr}(\text{NO}_3)_3$  have been refitted using Equation (B-1) of Appendix B. In the previous paper<sup>8</sup> the contribution of the quantity  $(T_{1w}^{\text{s}})^{-1}$  to the observed relaxation rate was neglected, which leads to considerable errors in the resulting parameters. If one uses the values  $(T_{1w}^{\text{s}})^{-1} = 0.74$  sec<sup>-1</sup>,  $T_{1x} = 3.7$   $\mu$ sec, and  $\tau_{\text{xw}} = 39$   $\mu$ sec, which were obtained in the present study at 380 gauss and 0.5 °C, then a least squares fit of the data of Manley and Pollak<sup>8</sup> using  $\tau_{\text{yw}}$  and  $T_{1y}$  as adjustable parameters yields the values  $T_{1y} = 7$   $\mu$ sec and  $\tau_{\text{yw}} = 1.3$   $\mu$ sec. In the calculations  $(T_{1w}^{\text{s}})^{-1}$  was assumed to be independent of the relative concentrations of  $\text{Cr}^{3+}$  and  $\text{CrOH}^{2+}$  in the solution.

Actually  $(T_{1w}^S)^{-1}$  could decrease slightly as the equilibrium shifts to the right in Reaction (15), due to a shorter electron relaxation time for  $\text{CrOH}^{2+}$ . However, this effect is masked by the increase in the third term of Equation (B-1) of Appendix B, which accompanies the formation of  $\text{CrOH}^{2+}$  at 0 °C. A shorter electron relaxation time for  $\text{CrOH}^{2+}$  could make  $T_{1y} > T_{1x}$  at 0 °C and 380 gauss since at low temperatures  $\tau_{1s}$  competes with  $\tau_r$  for the correlation time of the dipolar interaction. At high temperatures  $\tau_r \ll \tau_{1s}$  for both  $\text{Cr}^{3+}$  and  $\text{CrOH}^{2+}$ , which makes  $T_{1y} = T_{1x}$  in high fields, since  $\tau_r$  is expected to be approximately the same for both species.

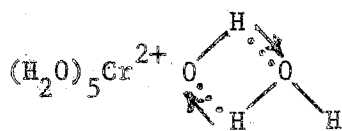
If it is assumed that species y exchanges protons with the bulk water via the second hydrolysis reaction



then  $k_2 = 10/\tau_{yw} = 7.7 \times 10^6 \text{ sec}^{-1}$ . Using the value  $K_2 = 2.5 \times 10^{-7}$  for the equilibrium constant of Reaction (23) at 0 °C,<sup>35</sup> one calculates  $k_{-2} = k_2/K_2 = 3.1 \times 10^{13} \text{ sec}^{-1}$ , which is about 300 times greater than the diffusion-limited recombination of  $\text{H}^+$  and  $\text{OH}^{-33}$ . Such a rate constant for diffusional encounter is impossibly high; hence, the proton exchange must occur by some additional reaction. A mechanism involving a collision between  $\text{Cr}(\text{H}_2\text{O})_5\text{OH}^{2+}$  and  $\text{OH}^-$  may be ruled out since it would also require an impossibly large reaction rate. An exchange reaction between  $\text{H}^+$  and coordinated water in  $\text{Cr}(\text{H}_2\text{O})_5\text{OH}^{2+}$  would require a rate constant of the order of  $10^{10} \text{ mole}^{-1} \text{ sec}^{-1}$  at  $10^{-3} \text{ M H}^+$ , which is not

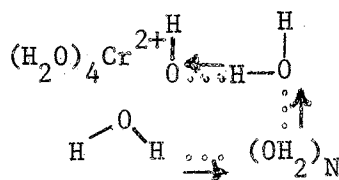
impossibly large. But rate constants for such acid-catalyzed proton exchange mechanisms are typically  $10^6 \text{ mole}^{-1} \text{ sec}^{-1}$  or less<sup>10</sup>. Furthermore, such a mechanism would give a  $\tau_{yw}$  which varied with solution acidity, contrary to what is observed. The short proton lifetimes cannot be due to rapid exchange of whole water molecules in  $\text{Cr}(\text{H}_2\text{O})_5\text{OH}^{2+}$  since Reaction (15) would provide a fast bridge for water molecules in  $\text{Cr}(\text{H}_2\text{O})_6^{3+}$  to enter the water system. In 1.0 M acid solutions at 0 °C lifetimes of water molecules in  $\text{Cr}(\text{H}_2\text{O})_6^{3+}$  would be of the order of milliseconds rather than days as experimentally observed<sup>13</sup>. It follows that the rapid proton exchange of  $\text{Cr}(\text{H}_2\text{O})_5\text{OH}^{2+}$  occurs via some mechanism involving proton jumps across hydrogen bonds to solvent water molecules.

It could be suggested that the rapid rate of proton exchange of  $\text{CrOH}^{2+}$  compared to  $\text{Cr}^{3+}$  is due to a mechanism involving the coordinated  $\text{OH}^-$  alone. A possibility would be a four center concerted proton transfer involving a jump of the two protons in the directions shown.



Similar four center proton transfers have been postulated previously<sup>36</sup>,  
<sup>37</sup>. But such a mechanism would allow only one of the eleven protons in  $\text{Cr}(\text{H}_2\text{O})_5\text{OH}^{2+}$  to be exchangeable with the bulk, and the increase in proton relaxation rate with the formation of  $\text{CrOH}^{2+}$  could only be accounted for if  $\text{CrOH}^{2+}$  were a more strongly relaxing species than  $\text{Cr}^{3+}$ , which has been shown not to be the case. Four center proton transfer involving

coordinated water molecules is not important for  $\text{Cr}(\text{H}_2\text{O})_6^{3+}$ , and there is no reason to assume that it would be an effective mechanism for  $\text{Cr}(\text{H}_2\text{O})_5\text{OH}^{2+}$  either. The most logical mechanism seems to be a concerted proton transfer reaction of the form



in which a coordinated water molecule is connected via a Grotthuss chain to the coordinated  $\text{OH}^-$  ion. The water molecules at the ends of the chain act as either acid or base catalysts, and transfer occurs via a counterclockwise jump of the protons through the chain in the directions indicated. The  $\text{OH}^-$  "diffuses" throughout the hydration sphere, which insures that all eleven protons are exchangeable with the bulk. Similar mechanisms have been proposed<sup>38,39</sup> to account for the rapid rates of other reactions, e.g., the mutarotation of glucose, which are both acid- and base-catalyzed. Such concerted mechanisms are not diffusion limited and are favored since they avoid the solvation and desolvation of any charged intermediates.

#### Isotope Effects in Moderately Acidified Solutions

Measurements at 14 kG on  $\text{Cr}(\text{NO}_3)_3$  samples of varying volume fractions of  $\text{H}_2\text{O}$  and  $\text{D}_2\text{O}$  are presented in Figure 21. The temperature dependence of proton  $T_1$  and  $T_2$  for a 20%  $\text{H}_2\text{O}$ -80%  $\text{D}_2\text{O}$  sample ( $\beta = 0.2$ ) are given in Figure 22. All the samples were uniformly made 0.10 M in  $\text{HClO}_4$ .



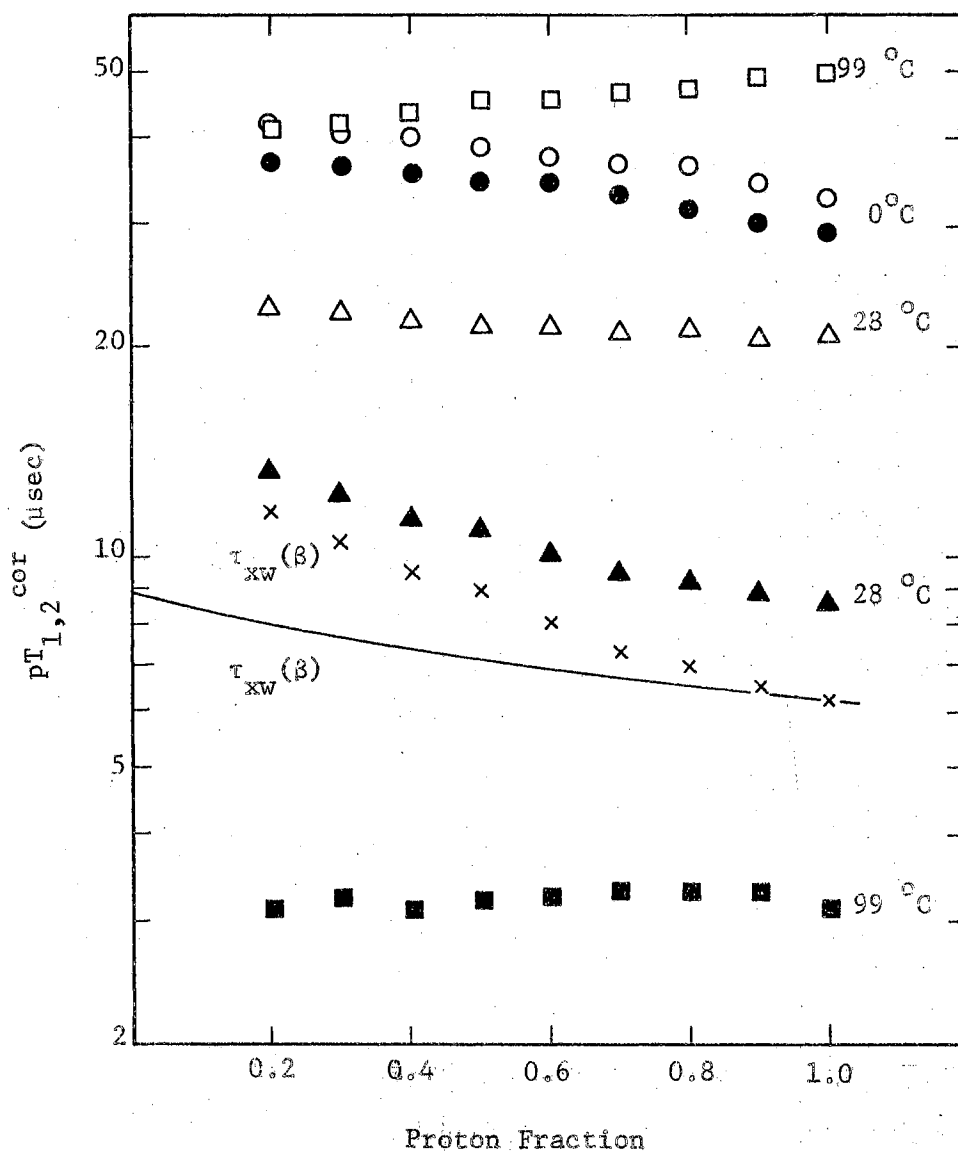


Figure 21. Proton Relaxation Times  $pT_{1,2}^{cor}$  at 14 kG in 0.10 M  $\text{HClO}_4$  Solutions of  $\text{Cr}(\text{NO}_3)_3$  of Varying Proton Fraction  $\beta$

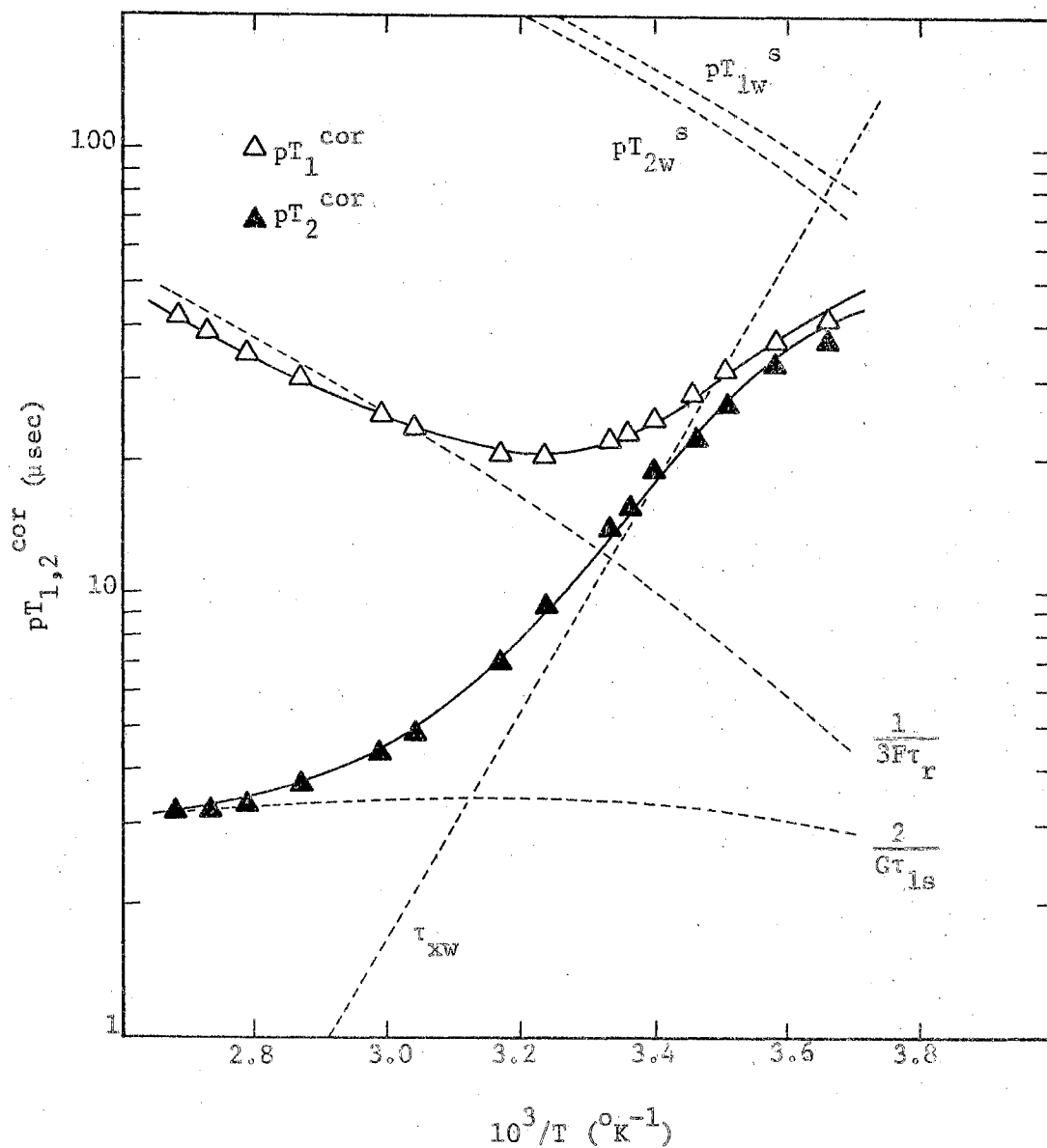


Figure 22. Temperature Dependence of Proton Relaxation Times  $pT_{1,2}^{cor}$  at 14 kG in 0.10 M  $\text{HClO}_4$  Solutions of  $\text{Cr}(\text{NO}_3)_3$  Containing 80%  $\text{D}_2\text{O}$ -20%  $\text{H}_2\text{O}$  ( $\beta = 0.2$ )

An interesting empirical result from Figures 19 and 22 is that the proton relaxation measurements at  $\beta = 1.0$  and  $\beta = 0.2$  can be made to coincide by a shift in the temperature scale by an amount  $10^3/T = 0.12 \text{ }^\circ\text{K}^{-1}$ , which corresponds to a temperature shift of approximately  $11 \text{ }^\circ\text{C}$  near room temperature. This fact suggests that the water structure around  $\text{Cr}^{3+}$ , and therefore the structure difference between  $\text{H}_2\text{O}$  and  $\text{D}_2\text{O}$ , remains constant over an extended range of temperature. A similar result was noted by Baker<sup>40</sup>, who observed that the viscosity of heavy water equals that of light water at a temperature  $8.5 \text{ }^\circ\text{C}$  less, from  $15 \text{ }^\circ\text{C}$  to the highest temperature studied,  $35 \text{ }^\circ\text{C}$ .

At low temperatures where  $\tau_{xw} \gg T_{1x}, T_{2x}$ , both  $pT_1^{\text{cor}}$  and  $pT_2^{\text{cor}}$  increase with decreasing proton fraction  $\beta$ . From Equation (17) this could be due either to an increase in the term in brackets with decreasing  $\beta$  (i.e.,  $K > 1$ ), an increase in  $\tau_{xw}$ , or both. The relaxation time  $T_{1w}^s$  contributes significantly to  $T_1^{\text{cor}}$  at  $0 \text{ }^\circ\text{C}$ , but it gives an isotope effect in the opposite direction due to the decrease in self-diffusion coefficients of the solvent protons with partial deuteration. Near  $100 \text{ }^\circ\text{C}$  where  $\tau_{xw} \ll T_{2x}, T_2^{\text{cor}}$  is independent of proton fraction to within  $\pm 3\%$ . This requires  $K = 1.00 \pm 0.03$ . Using this value and the equation  $K = \exp(-\Delta G^\circ/RT)$ , one obtains  $\Delta G^\circ = \Delta H^\circ - T\Delta S^\circ = 0 \pm 22$  cal/mole at  $100 \text{ }^\circ\text{C}$ . If, as is usually the case<sup>41</sup>, the main cause of any deviation from  $K = 1$  in Reaction (18) is a difference in vibrational zero-point energies between the products and the reactants, then  $\Delta G^\circ \approx \Delta H^\circ$ , and one calculates  $K = 1.00 \pm 0.04$  at  $0 \text{ }^\circ\text{C}$ . Thus, it is expected that most of the isotope effect near  $0 \text{ }^\circ\text{C}$  must be due to a change in  $\tau_{xw}$  with changing proton fraction. In any case, the data cannot be fitted

satisfactorily by assuming deviations from  $K = 1$  are alone responsible for the isotope effect at  $0^\circ\text{C}$ , regardless of what assumptions are made regarding the relative magnitudes of  $\Delta H^\circ$  and  $\Delta S^\circ$  for Reaction (18).

The linear decrease in  $T_1^{\text{cor}}$  at high temperatures with decreasing  $\beta$  correlates qualitatively with the linear increase in viscosity as the solvent is changed from  $\text{H}_2\text{O}$  to  $\text{D}_2\text{O}$ .<sup>22</sup> This gives rise to a longer rotational correlation time in deuterated solutions and a decrease in  $T_{1x}$ . The absence of an isotope effect for  $T_{2x}$  implies that the correlation time  $\tau_v$  for electron relaxation does not change with proton fraction, and is further evidence that electron relaxation is not related to rotation of the hydrated  $\text{Cr}^{3+}$  complex<sup>1</sup>. By linear extrapolation of the  $T_1^{\text{cor}}$  curve at  $99^\circ\text{C}$  in Figure 21 to  $\beta = 0$ , one finds that the rotational correlation time increases by approximately 28% in going from  $\text{H}_2\text{O}$  to  $\text{D}_2\text{O}$ , whereas the solvent viscosity increases by only 16%.<sup>21</sup> In terms of the Debye model this would imply that deuteration is accompanied by an increase in the radius of the  $\text{Cr}^{3+}$  complex ion. The increase in  $\tau_r$  with decreasing proton fraction for  $\text{Cr}^{3+}$  is in marked contrast to  $\text{Mn}^{2+}$  ions, which have a rotational correlation time that is independent of the proton fraction, except near  $0^\circ\text{C}$  where the difference in viscosities of  $\text{H}_2\text{O}$  and  $\text{D}_2\text{O}$  is a maximum<sup>42</sup>. This is almost certainly linked to the stronger interaction of  $\text{Cr}^{3+}$  ions with the solvent as compared with  $\text{Mn}^{2+}$ . Lifetimes of water molecules in the primary hydration sphere of  $\text{Cr}^{3+}$  are of the order of hours<sup>13</sup> as compared with approximately  $10^{-8}$  sec for water molecules in  $\text{Mn}(\text{H}_2\text{O})_6^{2+}$ .<sup>12</sup> Evidence for strong hydrogen bonds between  $\text{Cr}(\text{H}_2\text{O})_6^{3+}$  and a secondary hydration sphere has been provided by

measurements on transverse relaxation times of the fluorine nuclei in  $\text{PF}_6^-$  in aqueous solutions of  $\text{Cr}(\text{H}_2\text{O})_6^{3+}$ . Despite its high positive charge,  $\text{Cr}(\text{H}_2\text{O})_6^{3+}$  showed only a small tendency to form secondary coordination sphere complexes with  $\text{PF}_6^-$ .<sup>43</sup> Furthermore, in spite of the smaller ionic radius of  $\text{Cr}^{3+}$ , its rotational correlation time in  $\text{H}_2\text{O}$  at 25 °C is  $8 \times 10^{-11}$  sec as compared with  $3 \times 10^{-11}$  sec for  $\text{Mn}^{2+}$  at the same temperature<sup>1</sup>. The "structure-making" property of  $\text{Cr}^{3+}$  gives rise to this long rotational correlation time since additional water molecules (the secondary coordination sphere) rotate with the  $\text{Cr}(\text{H}_2\text{O})_6^{3+}$  ion. Due to the large volume of the rotating complex, it is not surprising that the Debye formula, which was derived for rotation of macroscopic particles, holds much better for  $\text{Cr}^{3+}$  than for other ions not having a well-defined secondary coordination sphere. These considerations also provide the rationale for allowing for a larger Debye radius in the more strongly hydrogen-bonded deuterated solutions. The present situation is in accord with that in pure liquids, where rotational correlation times are satisfactorily accounted for by the Debye formula only in the case of liquids which are highly associated.

If, as suggested, there is a secondary coordination sphere which rotates with the  $\text{Cr}(\text{H}_2\text{O})_6^{3+}$  ion and exchanges protons rapidly with the bulk water, then Equation (14) should contain an additional term  $p'(T_{1x}')^{-1}$ , where  $p'$  is the probability of finding a proton in the secondary coordination shell, and  $T_{1x}'$  is the proton relaxation time in that environment. The correlation time for  $T_{1x}'$  is the rotational correlation time  $\tau_r$ , which is related to the bulk viscosity of the solvent

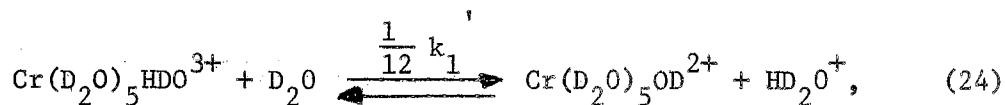
by the Debye formula. The quantity  $T_{1w}^s$  then becomes the relaxation time for protons outside the secondary coordination shell. Such a model introduces two additional unknown quantities, since the number of water molecules in the secondary coordination shell and the ion-proton distance are not known. In the present treatment  $p'(T_{1x}')^{-1}$  has been lumped in with  $(T_{1w}^s)^{-1}$  since this procedure gives a satisfactory fit to the data with fewer adjustable parameters.

The solid curves in Figure 22 for  $\beta = 0.2$  represent a least squares fit to the experimental data using as adjustable parameters the Debye radius  $\underline{a}$  and the activation energy  $V_{xw}$  for proton exchange. The constant  $K$  was assumed identical to unity over the whole temperature range, and the remaining parameters were assumed to be the same as those found from fitting the  $\beta = 1.0$  data (Table II). The values found were  $\underline{a} = 4.5$  Å and  $V_{xw} = 11.6$  kcal/mole at  $\beta = 0.2$ . The assumption of a constant  $\tau_{xw}^0$  is in accord with the model which will be introduced later to account for the isotope effect. However, an equally satisfactory fit can be obtained by making the opposite assumption of a constant activation energy and variable pre-exponential factor. The experimental data offers little information on this point due to the limited temperature range over which  $\tau_{xw}$  is the dominant factor influencing relaxation.

Finally there remains to be discussed the  $\beta$ -dependence of  $\tau_{xw}$ . At 28 °C the normalized relaxation time  $pT_2^{COR}$  is determined mainly by the rate of proton exchange between the primary hydration sphere of  $Cr^{3+}$  and the bulk water (Figures 19 and 22). Furthermore, since  $T_{2x}$  is almost

independent of  $\beta$  and  $pT_{2w}^s$  varies only slightly with  $\beta$ , the  $\beta$ -dependence of  $pT_2^{cor}$  at 28 °C in Figure 21 reflects primarily the  $\beta$ -dependence of  $\tau_{xw}$ . Semi-experimental values of  $\tau_{xw}$  vs.  $\beta$  at 28 °C have been extracted from the  $pT_2^{cor}$  data by using the  $T_2$  analogues of Equations (14) and (19) along with the values  $T_{2x} = 2.8 \mu\text{sec}$  and  $pT_{2w}^s = 170 \mu\text{sec}$ . The calculated  $\tau_{xw}$  values are given in Figure 21. Extrapolation to  $\beta = 0$  shows that the proton lifetime increases by approximately a factor of 2.3 as the solvent is changed from  $\text{H}_2\text{O}$  to  $\text{D}_2\text{O}$ .

Changes in proton lifetimes in the hydration sphere of  $\text{Cr}^{3+}$  with partial deuteration could be due to a difference between the rate constant  $k_1$  of Reaction (15) and the rate constants of reactions such as



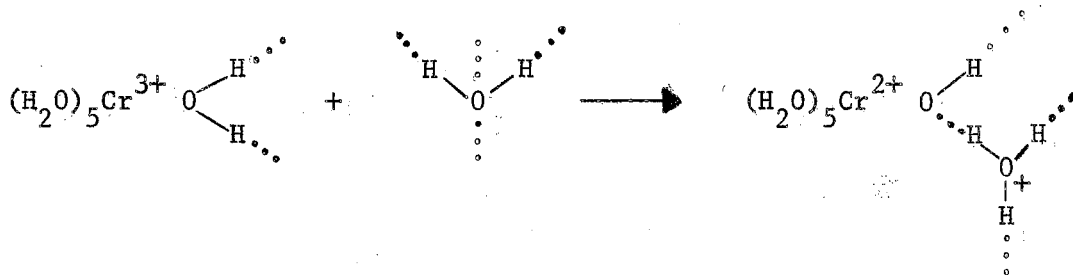
etc. In almost pure  $\text{D}_2\text{O}$  proton exchange with the bulk water occurs mainly by Reaction (24), whereas in pure  $\text{H}_2\text{O}$  the exchange is by Reaction (15). The ratio of the proton lifetimes in the two solvents is given by  $\tau(\text{D}_2\text{O})/\tau(\text{H}_2\text{O}) = k_1/k_1'$ . Differences between the rate constants  $k_1$  and  $k_1'$  (secondary isotope effects) can occur if the binding at proton sites other than the one being transferred changes in going from the initial to the transition state. Bunton and Shiner<sup>44</sup> have proposed a model for calculating secondary isotope effects which assumes that they arise mainly from the changes in zero-point energy, associated in turn principally with changes in hydrogen bond stretching frequencies in going from the initial to the transition state. In their model the

ratio of the rates in  $\text{H}_2\text{O}$  and  $\text{D}_2\text{O}$  is given by

$$\frac{k_1}{k_1^r} = \exp\left(\frac{\Sigma\nu_{\text{H}} - \Sigma\nu_{\text{H}}^\ddagger}{5.44 \text{ T}}\right) \quad (25)$$

where  $\Sigma\nu_{\text{H}}$  and  $\Sigma\nu_{\text{H}}^\ddagger$  are the sums of the hydrogen stretching frequencies ( $\text{cm}^{-1}$ ) in the initial and transition states respectively. The sum extends over all the isotopically substituted sites in the molecules.

Application of this theory requires assumptions concerning the nature of the transition state. For Reaction (15) the model



is assumed, where the dotted lines represent hydrogen bonds to solvent water molecules. The transition state consists of a hydronium ion hydrogen-bonded to a coordinated  $\text{OH}^-$  ion. This is the most reasonable assumption since the position of the proton in the state of highest potential energy, the transition state, should be nearer to the weaker base, and the coordinated  $\text{OH}^-$  ion is a much stronger base than a bulk water molecule. The frequencies  $3400 \text{ cm}^{-1}$  and  $2900 \text{ cm}^{-1}$  were used for the stretching frequencies of hydrogen-bonded water and hydronium ions. The stretching frequencies of protons bound to coordinated water molecules in  $\text{Cr}(\text{H}_2\text{O})_6^{3+}$  are not known, so the suggestion of Bunton and Shiner<sup>45</sup> was followed, and these frequencies were estimated using the equation

$$\nu (\text{cm}^{-1}) = 2937 + 28.8 \text{ pK}_a, \quad (26)$$



where  $K_a$  is the acid dissociation constant per proton of  $\text{Cr}(\text{H}_2\text{O})_6^{3+}$ .

Using the value  $K_a = 1.4 \times 10^{-4}/12$  at 25 °C,<sup>32</sup> one calculates from Equation (26) a value  $\nu = 3080 \text{ cm}^{-1}$ . For the stretching frequency of the proton on the coordinated  $\text{OH}^-$  ion in the transition state, a value of  $3500 \text{ cm}^{-1}$  is assumed, which is intermediate between the  $3600 \text{ cm}^{-1}$  frequency of free  $\text{OH}^-$  and the  $3400 \text{ cm}^{-1}$  frequency of free water. Thus, summing over all the protons except the one being transferred, one obtains

$$\Sigma \nu_{\text{H}} = 3080 + 4(3400) = 16,680 \text{ cm}^{-1} \quad (27a)$$

$$\Sigma \nu_{\text{H}}^{\ddagger} = 3500 + 2(2900) + 2(3400) = 16,100 \text{ cm}^{-1}. \quad (27b)$$

The two  $3400 \text{ cm}^{-1}$  frequencies are included in  $\Sigma \nu_{\text{H}}^{\ddagger}$  because two of the hydrogen bonds which were accepted by water molecules in the initial state are assumed to be accepted by solvent water molecules in the transition state (see Rule e of reference 45). Using Equations (27a) and (27b) in Equation (25) one obtains  $\tau(\text{D}_2\text{O})/\tau(\text{H}_2\text{O}) = 1.4$  at 25 °C, as compared with an observed value of approximately 2.3 (Figure 21). In the summations of Equations (27a) and (27b) the stretching frequencies of the protons on the five coordinated water molecules in the initial and transition states have been neglected. Actually one should expect a slight increase in stretching frequency according to Equation (26) due to a larger  $\text{p}K_a$  of  $\text{CrOH}^{2+}$ , which would lower  $\tau(\text{D}_2\text{O})/\tau(\text{H}_2\text{O})$ . However, the increase in stretching frequency is small and is probably offset by a decrease in librational frequencies of the water molecules of similar magnitude, so their effects have been neglected altogether.

In the range  $0 < \beta < 1$  other reactions besides (15) and (24) must

be considered in calculating proton lifetimes. Examples are proton jumps from  $\text{Cr}(\text{H}_2\text{O})_6^{3+}$  to HDO or  $\text{D}_2\text{O}$  molecules. By performing a calculation similar to that above for all possible such reactions and weighting each reaction rate by its probability of occurrence at a given value of  $\beta$ ,  $\tau(\beta)/\tau(\beta = 1)$  ratios were calculated at several values of  $\beta$ . The results are given in Figure 21, where  $\tau(\beta = 1) = 6.3 \mu\text{sec}$  at  $28^\circ\text{C}$  has been used as the reference value. The calculated  $\tau(\beta)$  curve is concave upward, in agreement with the curvature of the "experimental"  $\tau_{\text{xw}}$  values at  $28^\circ\text{C}$ .

Isotope effects on reaction rates can also occur due to the change in librational frequencies of adjacent solvent molecules in going from the initial to the transition state (solvent isotope effect). Reactions of solute molecules which are "structure-making" in the initial state (high solvent librational frequency), but "structure-breaking" in the transition state (low solvent librational frequency) can be expected to proceed more rapidly in  $\text{H}_2\text{O}$  than in  $\text{D}_2\text{O}$ <sup>47,48</sup>. Due to the strong "structure-making" character of  $\text{Cr}^{3+}$  one thus expects the proton transfer rate constants to decrease as the solvent is changed from  $\text{H}_2\text{O}$  to  $\text{D}_2\text{O}$ , which would serve to improve the agreement between the experimental and calculated isotope effects. The low frequency librations of the solvent have been shown to be responsible for the difference in solubilities of salts in  $\text{H}_2\text{O}$  and  $\text{D}_2\text{O}$ <sup>47</sup>. The effects are small compared to isotope effects on dissociations of oxygen acids and bases, however, so the solvent isotope effect has been neglected altogether.

Equation (25) can also be used to calculate the difference between the proton and deuteron lifetimes, or primary isotope effect, in the

same solvent<sup>46</sup>. In this case the summations include only the proton being transferred. If one assumes that the proton stretching frequency in the transition state is the same as that on a hydronium ion hydrogen-bonded to water, then  $\Sigma \nu_{\text{H}} - \Sigma \nu_{\text{H}}^{\ddagger} = 3080 - 2900 = 180 \text{ cm}^{-1}$ , and using Equation (25) one obtains  $\tau^{\text{D}}/\tau^{\text{H}} = 1.1$ . Deuteron lifetimes in the hydration sphere of  $\text{Cr}^{3+}$  have not been experimentally measured, but in solutions of vanadyl a ratio  $\tau^{\text{D}}/\tau^{\text{H}} = 1.3$  has been reported<sup>49</sup>, and one should expect a similar result for chromic solutions.

The agreement between the predicted and measured isotope effects is about as close as can be expected due to the approximations involved in the derivation of Equation (25) and the neglect of all but the stretching frequencies in the summations, as well as the uncertainties in estimating the stretching frequencies from Equation (26). The presence of large secondary and small primary isotope effects in the proton exchange is, however, correctly predicted by the theory, which lends support to the proposed model for the transition state.

#### Isotope Effects in Highly Acidified Solutions

Measurements of the temperature dependence of proton  $T_1$  and  $T_2$  in a 4.0 M  $\text{HClO}_4$  solution of  $\text{Cr}(\text{NO}_3)_3$  for proton fractions  $\beta = 1.0$  and  $\beta = 0.438$  are shown in Figure 23. The latter corresponds to the smallest proton fraction which can be obtained in 4.0 M solutions without using deuterated perchloric acid, which is not commercially available. The solid curves through the  $\beta = 1.0$  data were calculated using Equations (14) and (21) along with the parameters given in Tables II and III.

Deuteration causes an increase in proton lifetime and an increase

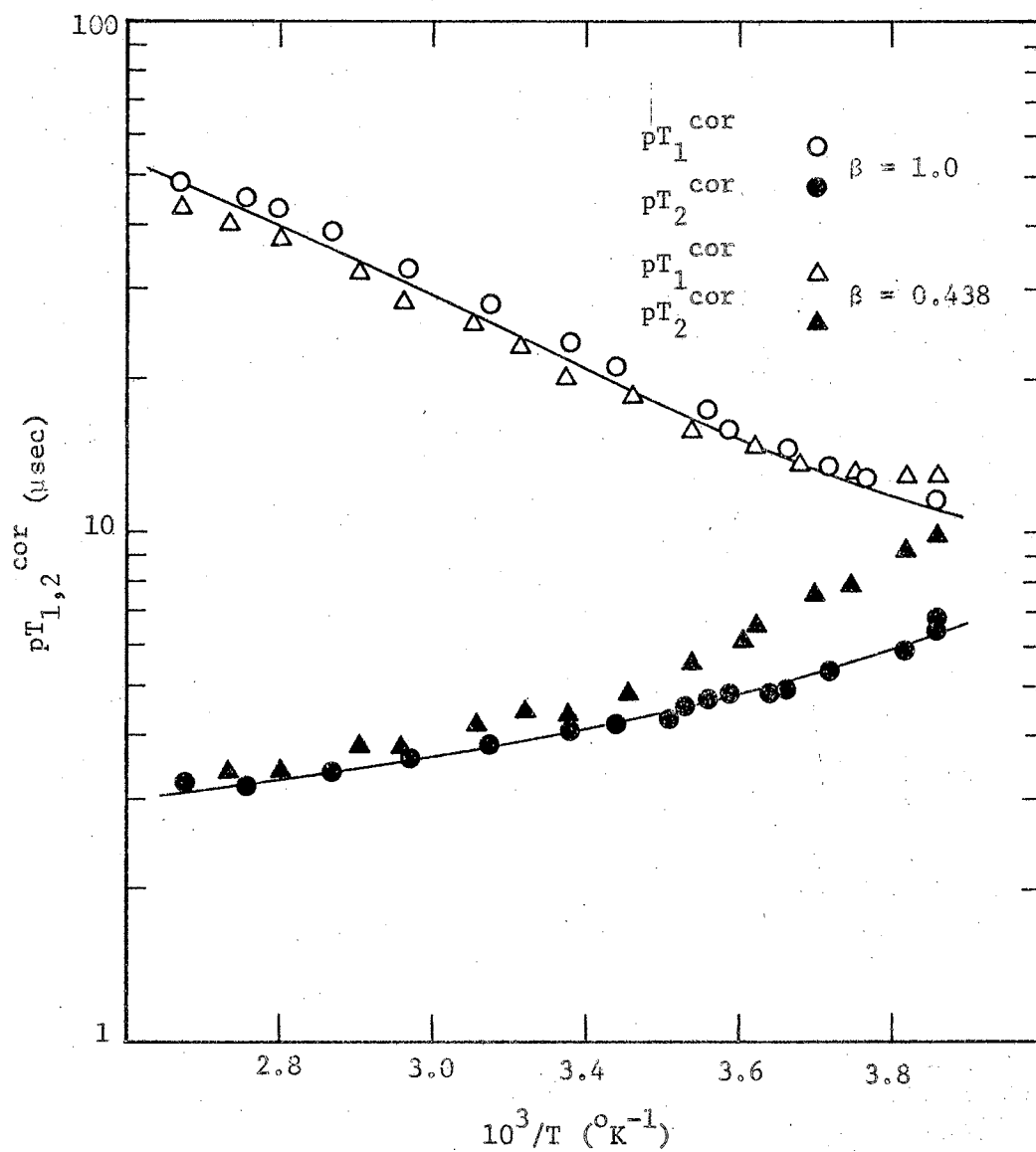
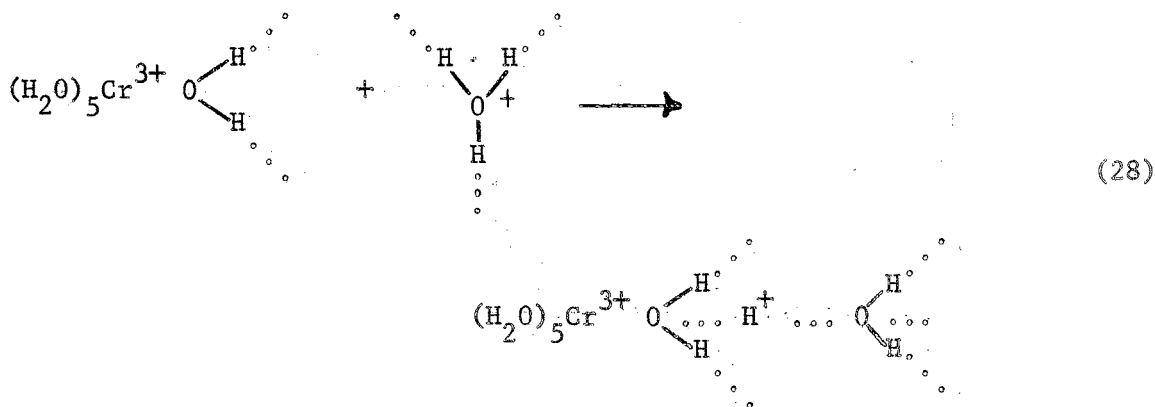


Figure 23. Temperature Dependence of Proton Relaxation Times  $pT_{1,2}^{cor}$  at 14 kG in 4.0 M  $HClO_4$  Solutions of  $Cr(NO_3)_3$  of Varying Proton Fraction  $\beta$

in  $pT_2^{\text{COR}}$ , as in the moderately acidified solutions (Figures 19 and 22). In the 4.0 M acid solution the acid-catalyzed exchange mechanism is dominant, which implies that the rate constant  $k_3$  for Reaction (16a) must decrease with deuteration. Calculation using the data in Figure 23 shows that  $k_3$  increases by a factor of approximately 1.9 in going from  $\beta = 1.0$  to  $\beta = 0.438$  at  $0^\circ\text{C}$ . Application of the Bunton-Shiner theory<sup>44-46</sup> to calculate the isotope effect for Reaction (16a) is complicated by the fact that both primary and secondary isotope effects must be considered, i.e., both the proton being transferred plus protons on all the water molecules in Reaction (16a) are replaced by deuterons as the solvent is changed from  $\text{H}_2\text{O}$  to  $\text{D}_2\text{O}$ .

If one assumes the free proton model<sup>46</sup> for the transition state of Reaction (16a),



then the loss of stretching frequency of the transferred proton in the transition state will give rise to a large primary isotope effect in the direction observed. It is convenient to separate the primary and secondary isotope effects in Reaction (28) for the purpose of calculation. For the primary isotope effect,

$$\Sigma \nu_{\text{H}} = 2900 \text{ cm}^{-1}$$

$$\Sigma \nu_{\text{H}}^{\ddagger} = 0,$$

and Equation (25) gives  $k_3(\text{H}_2\text{O})/k_3(\text{D}_2\text{O}) = 6.0$  at  $25^\circ\text{C}$ . For the secondary isotope effect,

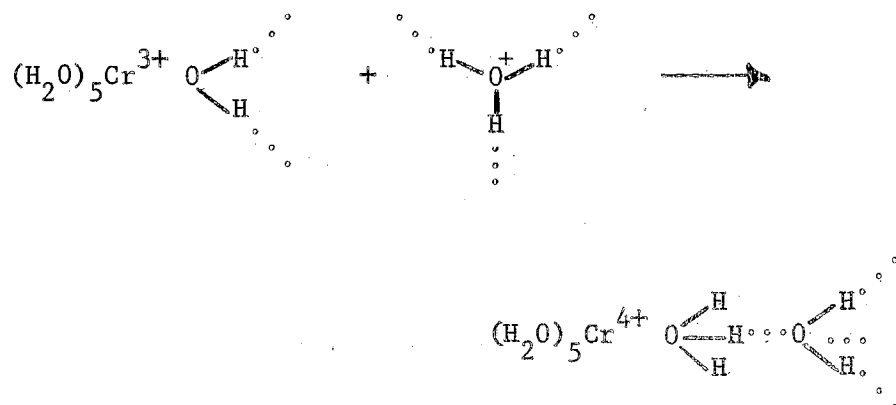
$$\Sigma \nu_{\text{H}} = 2(3080) + 2(2900) + 3600 = 15,560 \text{ cm}^{-1}$$

$$\Sigma \nu_{\text{H}}^{\ddagger} = 2(3080) + 3(3400) = 17,360 \text{ cm}^{-1},$$

and Equation (25) gives  $k_3(\text{H}_2\text{O})/k_3(\text{D}_2\text{O}) = 0.61$ . The  $3600 \text{ cm}^{-1}$  frequency is included in  $\Sigma \nu_{\text{H}}$  to account for the fact that the transition state, in this formulation, accepts one extra hydrogen bond from solvent water which, because of excess donors, was not accepted in the initial state. (see Rule d of reference 45). The product of the primary and secondary isotope effects gives  $k_3(\text{H}_2\text{O})/k_3(\text{D}_2\text{O}) = 3.7$  for the ratio of the rates in  $\text{H}_2\text{O}$  and  $\text{D}_2\text{O}$  at  $25^\circ\text{C}$ , in semi-quantitative agreement with the isotope effect observed.

The free proton model for the transition state should be expected to be a much better approximation for the acid-catalyzed proton exchange reaction than for Reaction (15), since the symmetry is much higher in the former case. The proton is being transferred between a coordinated and a solvent water molecule, whereas for Reaction (15) the proton transfer is between a solvent water molecule and a coordinated  $\text{OH}^-$  ion. The assumption that the proton is covalently bonded to the coordinated water molecule in the transition state would lead one to predict a small primary isotope effect, since the proton stretching frequency would be essentially conserved in the transition state. A small secondary isotope effect would likewise be expected since the changes in stretching fre-

quency for the remaining protons in the reaction



tend to cancel one another. Thus, as isotope effect of the magnitude observed could not reasonably be accounted for.

FOOTNOTES

- <sup>1</sup>N. Bloembergen and L. O. Morgan, J. Chem. Phys., 34, 842 (1961).
- <sup>2</sup>G. Laukien and J. Schlüter, Z. Physik, 146, 113 (1956).
- <sup>3</sup>R. Hausser and G. Laukien, Arch. Sci. (Geneva) 11, 252 (1958).
- <sup>4</sup>R. Hausser and G. Laukien, Z. Physik, 153, 394 (1959).
- <sup>5</sup>L. O. Morgan and A. W. Nolle, J. Chem. Phys., 31, 365 (1959).
- <sup>6</sup>T. H. Brown, R. A. Bernheim, and H. S. Gutowsky, J. Chem. Phys., 33, 1593 (1960).
- <sup>7</sup>R. Hausser and F. Noack, Z. Physik, 182, 93 (1964).
- <sup>8</sup>C. E. Manley and V. L. Pollak, J. Chem. Phys., 46, 2106 (1967).
- <sup>9</sup>T. J. Swift and T. A. Stephenson, Inorg. Chem., 5, 1100 (1966).
- <sup>10</sup>T. J. Swift, T. A. Stephenson, and G. R. Stein, J. Am. Chem. Soc., 89, 1611 (1967).
- <sup>11</sup>J. A. Laswick and R. A. Plane, J. Am. Chem. Soc., 81, 3564 (1959).
- <sup>12</sup>T. J. Swift and R. E. Connick, J. Chem. Phys., 37, 307 (1962).
- <sup>13</sup>J. P. Hunt and R. A. Plane, J. Am. Chem. Soc., 76, 5960 (1954).
- <sup>14</sup>R. G. Pearson, J. Palmer, M. M. Anderson, and A. L. Allred, Z. Elektrochem., 64, 110 (1960).
- <sup>15</sup>R. K. Mazitov, Dokl. Akad. Nauk SSSR, 156, 135 (1964).
- <sup>16</sup>V. L. Pollak and R. R. Slater, Z. Naturforsch., 22a, 2110 (1967).
- <sup>17</sup>A. E. Brodsky, Trans. Faraday Soc., 33, 1180 (1937).



- 18 H. Y. Carr and E. M. Purcell, *Phys. Rev.*, 94, 630 (1954).
- 19 S. Meiboom and D. Gill, *Rev. Sci. Instr.*, 29, 688 (1958).
- 20 E. W. Washburn, ed., International Critical Tables (McGraw-Hill, New York, 1926).
- 21 R. C. Hardy and R. L. Cottingham, *J. Chem. Phys.*, 17, 509 (1949).
- 22 G. N. Lewis and R. T. McDonald, *J. Am. Chem. Soc.*, 55, 4730 (1933).
- 23 J. H. Simpson and H. Y. Carr, *Phys. Rev.*, 111, 1201 (1958).
- 24 B. Ottar, Self-Diffusion and Fluidity in Liquids (Oslo University Press, Oslo, 1958), p. 118.
- 25 D. C. Douglass and D. W. McCall, *J. Chem. Phys.*, 31, 569 (1959).
- 26 N. Bloembergen, E. M. Purcell, and R. V. Pound, *Phys. Rev.*, 73, 679 (1948).
- 27 R. G. Hayes, Lawrence Radiation Laboratory Report UCRL-9873, Sept. 29, 1961.
- 28 K. M. Sancier and J. S. Mills, *J. Phys. Chem.*, 67, 1438 (1963).
- 29 Z. Luz and R. G. Shulman, *J. Chem. Phys.*, 43, 3750 (1965).
- 30 E. R. Nightingale, Jr., *J. Phys. Chem.*, 63, 1381 (1959).
- 31 K. Wüthrich and R. E. Connick, *Inorg. Chem.*, 7, 1377 (1968).
- 32 C. Postmus and E. L. King, *J. Phys. Chem.*, 59, 1208 (1955).
- 33 See, e.g., the chapter by M. Eigen, W. Kruse, G. Maass, and L. DeMaeyer in Progress in Reaction Kinetics, Vol. II, G. Porter, ed.
- 34 J. N. Butler, Ionic Equilibrium, A Mathematical Approach (Addison-Wesley Publishing Co., Inc., Reading, 1964), p. 437.
- 35 N. Bjerrum, *Z. Physik. Chem.*, 73, 724 (1910).
- 36 H. Kwart, L. P. Kuhn, and E. L. Bannister, *J. Am. Chem. Soc.*, 76,

5998 (1954).

<sup>37</sup>J. Hine, Physical Organic Chemistry (McGraw-Hill, New York, 1962), p. 112.

<sup>38</sup>C. G. Swain and J. F. Brown, *J. Am. Chem. Soc.*, 74, 2534 (1952).

<sup>39</sup>E. S. Gould, Mechanism and Structure in Organic Chemistry (Holt-Dryden, New York, 1959), p. 542.

<sup>40</sup>W. N. Baker, *J. Chem. Phys.*, 4, 294 (1936).

<sup>41</sup>See, e.g., Chap. XI, "Isotope Effects in Acid-Base Reactions" in R. P. Bell, The Proton in Chemistry (Cornell University Press, 1959).

<sup>42</sup>H. Sprinz, *Z. Naturforsch.*, 19a, 1243 (1964).

<sup>43</sup>T. R. Stengle and C. H. Langford, *J. Phys. Chem.*, 69, 3299 (1965).

<sup>44</sup>C. A. Bunton and V. J. Shiner, Jr., *J. Am. Chem. Soc.*, 83, 3207 (1961).

<sup>45</sup>*Ibid.*, p. 42.

<sup>46</sup>*Ibid.*, p. 3214.

<sup>47</sup>C. G. Swain and R. F. Bader, *Tetrahedron* 10, 182 (1960).

<sup>48</sup>*Ibid.*, p. 200.

<sup>49</sup>R. K. Mazitov and A. I. Rivkind, *Dokl. Akad. Nauk SSSR*, 166, 654 (1966).

## CHAPTER VII

### SUMMARY AND CONCLUSIONS

#### Instrumentation

A low-field NMR apparatus of the type that utilizes free precession in the earth's magnetic field has been designed and built. Its capabilities are as follows:

- (1) Nuclei accessible to measurement:  $H^1$  and  $F^{19}$ .
- (2) Range of measurable relaxation times  $T_2$ : 10 ms to 1 sec in a field of 0.5 G (earth's field).
- (3) Range of measurable relaxation times  $T_1$ : 50 ms and up, in fields ranging from 2 to 350 G.
- (4) Signal-to-noise ratio: 150:1 for a 450 ml water sample, at a bandwidth of 75 Hz.
- (5) Magnetic field (current) stability:  $\pm 1\%$ .
- (6) Timing interval stability:  $\pm 0.5\%$ .
- (7) Estimated accuracy of relaxation time measurements:  $\pm 3\%$ .

#### Chloroform

Measurements of the field and temperature dependence of proton spin-lattice relaxation times  $T_1$  in deoxygenated  $CHCl_3$  have been shown to yield the proton-chlorine scalar coupling constant and the chlorine quadrupole relaxation times. They also allow separation of the rotation-

al and translational motions of the  $\text{CHCl}_3$  molecules in the liquid. Activation energies for rotation and translation obtained from relaxation measurements are found to be smaller than the activation energies expected from the theory of Bloembergen, Purcell, and Pound. The failure of the BPP theory to correctly predict  $\Delta E_{\text{rot}}$  is well documented. But the discrepancy between  $\Delta E_{\text{tr}}$  and  $\Delta E_{\text{D}}$  found in this study for  $\text{CHCl}_3$ , and by others in  $\text{C}_6\text{H}_6$ , also raises a question about the adequacy of the BPP theory of relaxation by intermolecular dipolar interaction.

#### Solutions of Chromium (III)

The experimental proton spin relaxation results reported herein for moderately acidified aqueous solutions of  $\text{Cr}(\text{NO}_3)_3$  reflect the relaxation and exchange properties of  $\text{Cr}(\text{H}_2\text{O})_6^{3+}$  alone, free from the effects of hydrolysis products, or polymers which cause thermal hysteresis. At low temperatures the relaxation times are determined by the proton exchange rate and by the magnetic dipole interaction between the ion spin and protons outside the first hydration shell. In highly acidified solutions acid-catalyzed proton exchange becomes important, resulting in a decrease in proton lifetime with increasing acid concentration. The measurements on weakly acidified solutions confirm that  $\text{Cr}(\text{H}_2\text{O})_6^{3+}$  is a more strongly relaxing species than  $\text{Cr}(\text{H}_2\text{O})_5\text{OH}^{2+}$ , and that the latter undergoes much more rapid proton exchange with the bulk water. The rapid exchange is explained satisfactorily by assuming a homogeneous proton exchange mechanism involving the coordinated  $\text{OH}^-$  ion. A similar mechanism can be expected for the hydroxides of other metal ions, al-

though it is uncertain whether favorable cases could be found to demonstrate its effectiveness.

The increase in proton relaxation times with partial deuteration for moderately acidified solutions is due primarily to an increase in the lifetime of protons in the primary hydration sphere of  $\text{Cr}^{3+}$ , which is caused in turn by the greater basicity of  $\text{H}_2\text{O}$  as compared to  $\text{D}_2\text{O}$ . This result is in accord with other cases reported in the literature and may be explained on the basis of the theory of Bunton and Shiner. Studies on highly acidified solutions show that the rate constant for the acid-catalyzed proton exchange reaction decreases with deuteration. This result is also in agreement with the predictions of the Bunton-Shiner theory.

## A SELECTED BIBLIOGRAPHY

- Abragam, A., The Principles of Nuclear Magnetism (Oxford University Press, London, 1961), pp. 64, 65, 264-353.
- Benoit, H., J. Hennequin, and H. Ottavi, *Chim. Anal. (Paris)*, 44, 471 (1962).
- Blicharski, J., J. W. Hennel, K. Krynicki, J. Mikulski, T. Waluga, and G. Zapalski, *Arch. Sci. (Geneva)*, 13, 452 (1960).
- Bonera, G., and A. Rigamonti, *J. Chem. Phys.*, 42, 171 (1965).
- Bloembergen, N., and L. O. Morgan, *J. Chem. Phys.*, 34, 842 (1961).
- Bloembergen, N., E. M. Purcell, and R. V. Pound, *Phys. Rev.*, 73, 679 (1948).
- Brown, T. H., R. A. Bernheim, and H. S. Gutowsky, *J. Chem. Phys.*, 33, 1593 (1960).
- Bunton, C. A., and V. J. Shiner, Jr., *J. Am. Chem. Soc.*, 83, 42, 3207; 3214 (1961).
- Hausser, R., and G. Laukien, *Z. Physik*, 153, 394 (1959).
- Hausser, R., and F. Noack, *Z. Physik*, 182, 93 (1964).
- Laswick, J. A., and R. A. Plane, *J. Am. Chem. Soc.*, 81, 3564 (1959).
- Ligon, T. R., M.S. Thesis, Oklahoma State University, 1967 (unpublished).
- Manley, C. E., and V. L. Pollak, *J. Chem. Phys.*, 46, 2106 (1967).
- Mazitov, R. K., *Dokl. Akad. Nauk SSSR*, 156, 135 (1964).
- Mitchell, D. E., M.S. Thesis, Oklahoma State University, 1964 (unpublished).
- Morgan, L. O., and A. W. Nolle, *J. Chem. Phys.*, 31, 365 (1959).
- O'Reilly, D. E., and G. E. Schacher, *J. Chem. Phys.*, 39, 1768 (1963).
- Ottavi, H., *Compt. Rend.*, 252, 1439 (1961).
- Pollak, V. L., and R. R. Slater, *Z. Naturforsch.*, 22a, 2110 (1967).

Slichter, C. P., Principles of Magnetic Resonance (Harper and Row, New York, 1963), pp. 46, 84, 102, 135-42, 230.

Swift, T. J., and T. A. Stephenson, *Inorg. Chem.*, 5, 1100 (1966).

Swift, T. J., T. A. Stephenson, and G. R. Stein, *J. Am. Chem. Soc.*, 89, 1611 (1967).

Winter, J. M., *Compt. Rend.*, 249, 1346 (1959).

## APPENDIX A

### NON-LINEAR LEAST SQUARES CURVE FITTING PROCEDURE

The problem is to represent  $N$  experimental data points  $(y_i, x_i)$  with a functional relationship  $y = f(x, a_1, \dots, a_r)$  containing  $r$  unknown parameters  $a_1, a_2, \dots, a_r$ . The parameters  $a_r$  are chosen so as to minimize the sum of the squares of the deviations

$$S = \sum_{i=1}^N [f(x_i, a_1, \dots, a_r) - y_i]^2. \quad (\text{A-1})$$

The minimization condition is

$$\frac{\partial S}{\partial a_j} = 0 \quad j = 1, 2, \dots, r \quad (\text{A-2})$$

which is a set of  $r$  equations in the  $r$  unknown quantities  $a_j$ .

If the function  $y = f(x)$  is a polynomial in  $x$ , the normal equations (A-2) are linear in the unknown coefficients  $a_j$  and can be readily solved. If  $f(x)$  is not a polynomial in  $x$  the solution of the normal equations may prove difficult, and one may be obliged to seek an approximate solution by replacing  $f(x; a_1, \dots, a_r)$  by a function which is linear in the unknown parameters. This is accomplished by expanding  $f(x, a_1, \dots, a_r)$  in a Taylor's series in terms of  $a_j - \bar{a}_j \equiv \Delta a_j$ , where the  $\bar{a}_j$  are approximate values of the  $a_j$ . The expansion gives



$$f(x, a_1, \dots, a_r) = f(x, \overline{a_1}, \dots, \overline{a_r}) + \sum_{k=1}^r \frac{\partial f}{\partial a_k} \Delta a_k + \dots \quad (\text{A-3})$$

where

$$\frac{\partial f}{\partial a_k} = \left. \frac{\partial f}{\partial a_k} \right|_{x, \overline{a_1}, \dots, \overline{a_r}} \quad (\text{A-4})$$

Assuming the  $\overline{a_j}$  are chosen so that the  $\Delta a_j$  are small, the higher ordered terms in Equation (A-3) may be neglected, and the exact function  $f(x, a_1, \dots, a_r)$  replaced by the approximate function  $f(x, \Delta a_1, \dots, \Delta a_r)$  which is linear in the unknown parameters  $\Delta a_j$ . The normal equations

$$\frac{\partial S}{\partial (\Delta a_j)} = 0 \quad j = 1, 2, \dots, r \quad (\text{A-5})$$

become

$$\sum_{i=1}^N \sum_{k=1}^r \frac{\partial f}{\partial a_j} \frac{\partial f}{\partial a_k} \Delta a_k = \sum_{i=1}^N [y_i - f(x_i, \overline{a_1}, \dots, \overline{a_r})] \frac{\partial f}{\partial a_j} \quad j=1, 2, \dots, r \quad (\text{A-6})$$

These are  $r$  simultaneous linear equations in the  $r$  unknown quantities  $\Delta a_j$ , which can be easily solved. One then calculates the  $a_j$ 's using

$$a_j = \overline{a_j} + \Delta a_j \quad j = 1, 2, \dots, r \quad (\text{A-7})$$

In the event that the values  $\overline{a_j}$  are not close approximations to the  $a_j$ , the calculated  $\Delta a_j$  may be large enough that the higher ordered terms in Equation (A-3) are not negligible. The calculations may have to be repeated using for the new  $\overline{a_j}$  the value of  $a_j$  obtained from Equation (A-7). Experience shows that  $\Delta a_j$  converges rapidly toward zero for well-

behaved systems. Difficulties are sometimes encountered when the value of the function  $f(x, a_1, \dots, a_r)$  is relatively insensitive to one or more of the parameters  $a_j$ , in which case the  $\Delta a_j$  may oscillate or even diverge.

APPENDIX B

THEORETICAL EXPRESSIONS FOR PROTON SPIN  
RELAXATION TIMES IN CHROMIC SOLUTIONS

It has been recently shown<sup>1</sup> that in chromic solutions in the range of pH where the system is adequately described by the single equilibrium constant  $K_1 = k_1/k_{-1}$  of Reaction (15)<sup>2</sup>, the observed relaxation time is given by

$$(T_1^{\text{obs}})^{-1} = (T_{1w}^o)^{-1} + (T_{1w}^s)^{-1} + \left\{ \frac{12x}{2w} \left[ \frac{1}{12} \tau_{yw} + \frac{11}{12} \frac{\tau_{yw}}{\tau_{xw}} T_{1x} \right. \right. \\ \left. \left. + \left( 1 + \frac{x}{y} \frac{\tau_{yw}}{\tau_{xw}} T_{1y} \right) \right] + \frac{11y}{2w} (T_{1x} + \frac{1}{12} \tau_{xw}) \right\} D^{-1} \quad (\text{B-1})$$

where

$$D = (T_{1x} + \frac{1}{12} \tau_{xw}) (T_{1y} + \tau_{yw}) + \frac{x}{y} \frac{\tau_{yw}}{\tau_{xw}} (T_{1x} + \tau_{xw}) T_{1y}$$

and the subscripts x, y, and w refer to the species  $\text{Cr}(\text{H}_2\text{O})_6^{3+}$ ,  $\text{Cr}(\text{H}_2\text{O})_5\text{OH}^{2+}$ , and the bulk water respectively. The quantities x, y, and w are the molar concentrations of the various species in the solution;  $\tau_{jw}$  is the average lifetime of a proton in the species j before transfer to the bulk water; and  $T_{1j}$  is the proton relaxation time in environment j. The quantity  $(T_{1w}^s)^{-1}$  is the relaxation rate in the bulk water due to dipolar interaction with the spins S and is proportional to the number

of ion spins per unit volume;  $(T_{1w}^0)^{-1}$  is the relaxation rate due to other mechanisms in the bulk water, and can be equated to the relaxation rate in the solvent not containing paramagnetic ions, but otherwise under conditions identical to those of the studied solution. The proton lifetime  $\tau_{xw}$  is related to the forward rate constant of Reaction (15) by the equation  $\tau_{xw} = 12/k_1$ .<sup>2</sup> The quantity  $\tau_{yw}$  is included to allow for transfer of protons from the species  $y = Cr(H_2O)_5OH^{2+}$  to the water system. Such transfer is assumed to occur without the formation of appreciable quantities of other species in solution. As the solution acidity is increased  $y$  approaches zero, and  $x$  approaches  $m$ , the total analytical concentration of chromium in the solution. Equation (B-1) then reduces to Equation (14) of the text, where  $p = 12m/2w$  is the probability of finding a proton in the hydration sphere of  $Cr^{3+}$ .

The relaxation times  $T_{1x}$  and  $T_{2x}$  of protons in  $Cr(H_2O)_6^{3+}$  are given to a good approximation by the equations<sup>3</sup>

$$\frac{1}{T_{1x}} = \frac{4}{30} \frac{S(S+1)\gamma_I^2 \gamma_S^2 \hbar^2}{r^6} \left[ 3\tau_c + \frac{7\tau_c}{1 + \omega_s^2 \tau_c^2} \right] + \frac{2}{3} \frac{S(S+1)A^2}{\hbar^2} \left[ \frac{\tau_{2s}}{1 + \omega_s^2 \tau_{2s}^2} \right] \quad (B-2)$$

and

$$\frac{1}{T_{2x}} = \frac{4}{60} \frac{S(S+1)\gamma_I^2 \gamma_S^2 \hbar^2}{r^6} \left[ 7\tau_c + \frac{13\tau_c}{1 + \omega_s^2 \tau_c^2} \right] + \frac{1}{3} \frac{S(S+1)A^2}{\hbar^2} \left[ \tau_{1s} + \frac{\tau_{2s}}{1 + \omega_s^2 \tau_{2s}^2} \right] \quad (B-3)$$

where

$$\tau_c^{-1} = \tau_r^{-1} + \tau_{1s}^{-1} \quad (B-4)$$

In the above equations I and S refer to proton and electron spins respectively,  $\omega_s$  is the electron precession frequency;  $\gamma_I$  and  $\gamma_S$ , the proton and electron gyromagnetic ratios; r, the ion-proton internuclear distance; A, the scalar coupling constant;  $\tau_r$ , the rotational correlation time; and  $\tau_{1s}$  and  $\tau_{2s}$ , the longitudinal and transverse electron relaxation times. Bloembergen and Morgan<sup>3</sup> have derived an approximate equation for  $\tau_{1s}$  based on the assumption that relaxation occurs by modulation of the quadratic crystalline field splitting by collisions with water molecules outside the complex. The resulting equation was

$$\frac{1}{\tau_{1s}} = C \left[ \frac{\tau_v}{1 + \omega_s^2 \tau_v^2} + \frac{4\tau_v}{1 + 4\omega_s^2 \tau_v^2} \right] \quad (\text{B-5})$$

where  $\tau_v$  is the characteristic correlation time for the relaxation, and C is a constant for the hydrated complex. In high fields where  $\omega_s^2 \tau_v^2 \gg 1$  one expects  $\tau_{2s} < \tau_{1s}$ , but in such high fields the terms involving  $\tau_{2s}$  in Equations (B-2) and (B-3) are negligible.

Theoretical equations for  $T_{1,2w}^s$  have been derived by Pfeifer<sup>4</sup>.

His model includes modulation of the dipolar interaction by translational diffusion as well as by relaxation of the ion spin. With the usual approximations  $\omega_l \ll \omega_s$  and  $\omega_l^2 \tau_{1s}^2 \ll 1$ , these equations reduce to

$$\frac{1}{T_{1w}^s} = \frac{\gamma_I^2 \gamma_S^2 \hbar^2 S(S+1)}{2} \left[ 3J(0) + 7J(\omega_s) \right] \quad (\text{B-6})$$

and

$$\frac{1}{T_{2w}^s} = \frac{\gamma_I^2 \gamma_S^2 \hbar^2 S(S+1)}{4} \left[ 7 J(0) + 13 J(\omega_s) \right] \quad (\text{B-7})$$

The term  $J(\omega)$  is the spectral density function at the frequency  $\omega$  and is given by the integral

$$J(\omega) = \frac{16\pi N \tau_{1s}}{15d^3} \int_0^\infty B_{3/2}^2(\rho d) \frac{1 + D\rho^2 \tau_{1s}}{(1 + D\rho^2 \tau_{1s})^2 + \omega^2 \tau_{1s}^2} \frac{d\rho}{\rho} \quad (\text{B-8})$$

where  $N$  is the number of paramagnetic ions per unit volume;  $d$  is the average closest distance of approach between a proton in the bulk and spin  $S$ ;  $B_{3/2}$ , the Bessel function of order  $3/2$ ; and  $D = D_I + D_S$ , the self-diffusion coefficient of the bulk protons plus that of the spins  $S$ . Equation (B-8) can be integrated in closed form. The result, given by Equation (33) of Pfeifer's paper<sup>4</sup>, was used to calculate  $T_{1w}^s$  and  $T_{2w}^s$ .

#### FOOTNOTES

<sup>1</sup>C. E. Manley and V. L. Pollak, J. Chem. Phys., 46, 2106 (1967).

<sup>2</sup>Note that the rate constant  $k_1$  of this paper corresponds to  $k_1 w$  of reference 1.

<sup>3</sup>N. Bloembergen and L. O. Morgan, J. Chem. Phys., 34, 842 (1961).

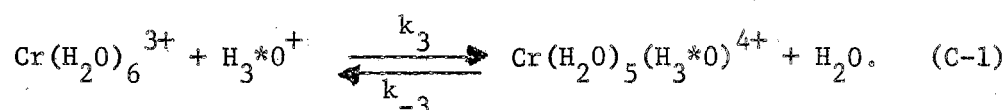
<sup>4</sup>H. Pfeifer, Ann. Physik, 7, 1 (1961).

APPENDIX C

SOLUTION OF THE BLOCH-McCONNELL EQUATIONS FOR

THE  $\text{Cr}(\text{H}_2\text{O})_6^{3+}$ - $\text{Cr}(\text{H}_2\text{O})_5(\text{H}_3\text{O})^{4+}$ - $\text{H}_2\text{O}$  SYSTEM

In an earlier paper<sup>1</sup> exchange Reaction (15) was discussed, and it was shown using McConnell's modification of the Bloch equations<sup>2</sup> that the relaxation time was described by an equation of the form of Equation (14) only in the limit of high acid concentration where the equilibrium concentration of  $\text{CrOH}^{2+}$  could be neglected. A similar analysis is now included for the reaction



The species  $\text{Cr}(\text{H}_2\text{O})_6^{3+}$  is assumed to exchange protons independently with the solvent via Reaction (15) with a lifetime  $\tau_{\text{xw}} = 12/k_1$ . In the range of high acid concentrations of interest here the species  $\text{CrOH}^{2+}$  can be neglected due to its short lifetime.

According to this exchange model, protons can exist in essentially four different environments: (1) in the bulk water  $w$ , (2) on water molecules  $x$  in  $\text{Cr}(\text{H}_2\text{O})_6^{3+}$ , (3) on one of the five water molecules  $z$  in  $\text{Cr}(\text{H}_2\text{O})_5(\text{H}_3\text{O})^{4+}$ , or (4) on the bound hydronium ion  $h$ . Letting  $y =$

$$[\text{Cr}(\text{H}_2\text{O})_5(\text{H}_3\text{O})^{4+}], \quad x = [\text{Cr}(\text{H}_2\text{O})_6^{3+}], \quad p = [\text{H}_3\text{O}^+], \quad \text{and} \quad w = [\text{H}_2\text{O}] + \frac{3}{2}[\text{H}_3\text{O}^+],$$



the Bloch-McConnell equations for this system become

$$\frac{dM_x}{dt} = \frac{M_{ox} - M_x}{T_{1x}} - M_x \left[ \frac{1}{\tau_{xz}} + \frac{1}{\tau_{xw}} + \frac{1}{\tau_{xh}} \right] + \frac{M_z}{\tau_{zx}} + \frac{M_h}{\tau_{hx}} + \frac{M_w}{\tau_{wx}}$$

$$\frac{dM_z}{dt} = \frac{M_{oz} - M_z}{T_{1z}} - \frac{M_z}{\tau_{zx}} + \frac{M_x}{\tau_{xz}}$$

(C-2)

$$\frac{dM_h}{dt} = \frac{M_{oh} - M_h}{T_{1h}} - M_h \left[ \frac{1}{\tau_{hx}} + \frac{1}{\tau_{hw}} \right] - \frac{M_x}{\tau_{xh}} + \frac{M_w}{\tau_{wh}}$$

$$\frac{dM_w}{dt} = \frac{M_{ow} - M_w}{T_{1w}} - M_w \left[ \frac{1}{\tau_{wx}} + \frac{1}{\tau_{wh}} \right] + \frac{M_x}{\tau_{xw}} + \frac{M_h}{\tau_{hw}}$$

One can express the  $\tau_{ij}$  in terms of the rate constants of reaction (C-1)

and obtain

$$\tau_{zx}^{-1} = k_{-3}$$

$$\tau_{xz}^{-1} = \frac{10}{12} k_3 p = \frac{10}{12} \frac{y}{x} k_{-3}$$

$$\tau_{xh}^{-1} = \frac{2}{12} k_3 p = \frac{2}{12} \frac{y}{x} k_{-3}$$

(C-3)

$$\tau_{hx}^{-1} = \frac{2}{3} k_{-3}$$

$$\tau_{hw}^{-1} = \frac{1}{3} k_{-3}$$

$$\tau_{wh}^{-1} = \frac{3y}{2w} \tau_{hw}^{-1} = \frac{y}{2w} k_{-3}$$

$$\tau_{wx}^{-1} = \frac{12x}{2w} \tau_{xw}^{-1}$$

The rate constant  $k_3$  has been eliminated from Equations (C-3) by making

use of the equilibrium constant expression  $K = k_3/k_{-3} = y/xp$ . The last

two equations in (C-3) arise from considerations of detailed balance.

The Equations (C-3) were substituted into Equations (C-2) and the resulting system of simultaneous differential equations solved under the usual assumption that the terms  $dM_z/dt$ ,  $dM_x/dt$ , and  $dM_h/dt$  could be neglected compared to the other terms, an approximation valid for dilute solutions. The result is an exponential decay of  $M_w$  toward  $M_{ow}$  with time constant

$$\frac{1}{T_1} = \frac{1}{T_{1w}} + \left\{ \frac{6x}{w} (T_{1z} + \tau_{zx}) (T_{1h} + \tau_{zx}) + \frac{y}{2w} \left[ 10(T_{1h} + \frac{13}{10} \tau_{zx}) + (T_{1z} + \tau_{zx}) \tau_{xw} \right. \right. \\ \left. \left. + \frac{2T_{1h}}{3} (T_{1z} + \tau_{zx}) \frac{\tau_{xw}}{\tau_{zx}} + 3T_{1z} T_{1x} + \frac{y}{6x} \frac{\tau_{xw}}{\tau_{zx}} (T_{1z} + \frac{10}{3} T_{1h} + 6\tau_{zx}) T_{1x} \right] \right\} D^{-1} \quad (C-4)$$

where

$$D = (T_{1x} + \tau_{xw}) (T_{1h} + \tau_{zx}) (T_{1z} + \tau_{zx}) + \frac{y}{18x} T_{1x} \tau_{xw} \left[ (T_{1h} + 3\tau_{zx}) \frac{T_{1z}}{\tau_{zx}} + 16 (T_{1h} + \frac{9}{8} \tau_{zx}) \right].$$

To simplify this cumbersome expression the reasonable assumption is made that  $T_{1z} = T_{1h} \gtrsim T_{1x}$ . It is further assumed that the rate constant  $k_{-3}$  is large so that the lifetime  $\tau_{zx} (= 1/k_{-3})$  and the ratio  $y/x = k_3 p/k_{-3}$  are small enough to satisfy the conditions

$$\tau_{zx} \ll T_{1z}, T_{1h}$$

$$\frac{y}{x} \ll 1, 12T_{1x} \tau_{xw}^{-1}, (108\tau_{zx} \tau_{xw}^{-1})^{1/2}. \quad (C-5)$$

Equation (C-4) then reduces to

$$\frac{1}{T_1} = \frac{1}{T_{1w}} + \frac{P}{T_{1x} + \tau_x}$$

where  $p = 6x/w$  and

$$\frac{1}{\tau_x} = \frac{1}{\tau_{xw}} + \frac{1}{18} \frac{y}{x} \frac{1}{\tau_{zx}} = \frac{1}{12} k_1 + \frac{1}{18} k_3 [\text{H}_3\text{O}^+]$$

From the parameters given in Table III it can be shown that the conditions in (C-5) are fulfilled in 4.0 M acid solutions, provided only that the rate constant  $k_{-3}$  satisfies the requirement  $k_{-3} \geq 10^8 \text{ mole}^{-1} \text{ sec}^{-1}$ .  $k_{-3}$  is probably much faster than this and should be expected to approach the diffusion limited rate  $10^{10} \text{ mole}^{-1} \text{ sec}^{-1}$  found for the proton transfer between unbound  $\text{H}_3\text{O}^+$  and  $\text{H}_2\text{O}$ .

FOOTNOTES

- <sup>1</sup>C. E. Manley and V. L. Pollak, J. Chem. Phys., 46, 2106 (1967).
- <sup>2</sup>H. M. McConnell, J. Chem. Phys., 28, 430 (1958).

VITA

Billy Frank Melton

Candidate for the Degree of  
Doctor of Philosophy

Thesis: PROTON SPIN RELAXATION IN LIQUID  $\text{CHCl}_3$  AND IN  $\text{H}_2\text{O}-\text{D}_2\text{O}$  SOLUTIONS OF CHROMIUM (III)

Major Field: Physics

Biographical:

Personal Data: Born in Tulsa, Oklahoma, August 13, 1942, the son of William F. and Ollie Melton.

Education: Graduated from Union High School, Broken Arrow, Oklahoma, in May, 1960; received the Bachelor of Science degree from Oklahoma State University in May, 1964, with a major in Physics; completed requirements for the degree of Doctor of Philosophy in May, 1970.

Professional Experience: NSF Cooperative Graduate Fellow, 1964-66; NASA Trainee, 1966-69; member of Sigma Pi Sigma.